Application of nanocoatings produced by electrostatic layer-by-layer self-assembling to improve the physicochemical properties of drugs and excipients

Schalk J. Strydom

Thesis submitted for the degree Doctor of Philosophy in Pharmaceutics at the Potchefstroom campus of North-West University

Promoter : Prof. M.M. de Villiers

Co-promoter : Prof. W. Liebenberg

September 2014

TABLE OF CONTENTS

Acknowledgements

This study was not without its fair share of challenges, and I would like to take this opportunity to thank the following people without whom this study would not have been possible:

- Firstly I would like to thank my family including my parents (Willie and Corrie) and my siblings (Alwyn and Carla). Words cannot express my appreciation for your continued support and encouragement throughout this process and in my life, even though I might not always express it.
- Prof. Wilna and Prof. Melgardt, thank you for always being willing to help and motivate me, especially when I wanted to give up. Above all, thank you for your friendship. Our journey together started with some challenges, but we have managed to beat the odds. I am sure that we will forever be connected to one another. Also, thank you for the once-in-a-lifetime opportunities and financial support throughout this process. Having you in my life has changed my future for the better.
- Nicole Stieger and Marique Aucamp, thank you for your help and friendship. You have been far too kind to me and I did not deserve any of it. I am humbled by your generosity.
- The fellow graduate students that I had the pleasure of working with, including Thomas Diezi, Nicole Rockich Winston and Howard Chen. You're friendship made it all worthwhile. It was "amAYzing", thank you.
- Thank you to the collaborating researchers Warren Rose, Daniel Otto, Yuri Lvov and Lian Yu, for your assistance and expertise.
- The Schools of Pharmacy at the North-West University – Potchefstroom Campus and the University of Wisconsin – Madison, thank you to all the faculty and staff that helped to make this project a reality and for granting me this opportunity.
- My "North American family", including Bonnie Fingerhut and the rest of the Fingerhut family, as well as Idy de Villiers. Thank you Bonnie for picking me out of the crowd at the airport with my wrapped luggage and for taking me under your wing. Also, thank you for exposing me to life in North America and for exposing my palate to the wonderful flavours of ice cream that Wisconsin has to offer. I am truly blessed to have you in my life.
- To all my friends in South Africa, the USA and Canada, thank you for your support and friendship. A special thank you to Jennifer Hart (Lamont) for showing me that I am good enough.

"Beauty is about being comfortable in your own skin. It's about knowing and accepting who you are"

Ellen DeGeneres

Abstract

Layer-by-layer (LbL) is a self-assembly technique, proven to be a simplified method for the modification of material surfaces. The LbL multilayers are formed due to electrostatic attraction between opposite charged polymers. Substrates which can be utilised using this technique include dyes, enzymes, drugs and cells. In this study which comprise of three separate LbL studies, 1) compactible cellulose was nanocoated by means of LbL, 2) poly(amidoamine) dendrimer mediated synthesis of silver sulfadiazine nanoparticles and 3) four poorly water soluble drugs were nanocoated, i.e. furosemide, isoxyl, rifampicin, paclitaxel.

In the first study Kraft softwood fibers was nanocoated using the LbL technique. This technique turned non-flowing, non-compacting cellulose into powders with positive tabletting properties which can be used in direct compression in the tabletting process. The cellulose microfibers which were coated with four PSS/PVP bilayers, display the best compaction properties. One of the major advantages of nanocoating is that the process adds less than 1% to the weight of the fibres. This process proved to be environmental friendly due to the type of materials used and the quantity.

In the second study silver sulfadiazine (limited aqueous solubility) was used to synthesize highly soluble AgSD nanoparticles. In this particular study the nanoparticles were stabilized against crystal growth by LbL coating. PAMAM dendrimers were used to coat the particles. The dendrimers served as solubility enhancer for this poorly water soluble antibiotic. This study illustrated that nanotechnology based dosage forms can be create and that PAMAM dendrimers were crucial to the success of this dosage form.

In the third study, a LbL nanocoat of chitosan and chondroitin sulfate was self-assembled step-wise onto drug nanoparticles. Furosemide, isoxyl, rifampin and paclitaxel were chosen to prepare these nanoparticles. All four of them display poor water solubility properties. Although the nanocoating reduced the dissolution proportional to the coat thickness, it still dissolved faster than the commercially available micronized powders of the drugs. Also this LbL nanocoating stabilizes the small particles against crystal growth and aggregation in suspension. The release patterns of the drugs were superior to that of the raw materials. This study proved that LbL coating can improve the performance of poorly water soluble drugs.

Uittreksel

Die tegniek van Laag-vir-Laag (LvL) bedekking is ŉ bewese metode om die oppervlaktes van materiale te verander. Hierdie tegniek behels die vorming van veelvuldige lae rondom ŉ deeltjie deur middel van elektrostatiese aantrekkingskrag tussen polimere met teenoorgestelde ladings. Substrate waarop hierdie tegniek toegepas kan word sluit in: kleurstowwe, ensieme, geneesmiddels en selle. Hierdie studie bestaan uit drie afsonderlike LvL studies naamlik; (1) die nanobedekking van saampersbare sellulose deur middel van LvL bedekking; (2) die sintese van silwersulfadiasien nanodeeltjies deur middel van die gebruik van ŉ poli-(amiedo-amien) dendrimeer en (3) die nanobedekking van vier swak wateroplosbare geneesmiddels, naamlik; furosemied, isoksiel, rifampisien en paklitaksel.

Tydens die eerste studie is die LvL tegniek gebruik vir die nanobedekking van Kraft sagtehout vesels. Die bedekking het tot gevolg gehad dat die vloei-eienskappe, en swak saampersbaarheid van die sellulose verbeter is. Hierdie verbeterde eienskappe het tot gevolg dat die sellulose suksesvol getabletteer kan word deur middel van direkte samepersing. Sellulose mikrovesels wat bedek is met vier dubbel lae bestaande uit PSS en PVP (polistireensulfonaat en polivinielpirrolidoon), het die beste saampersbaarheid getoon. Een van die grootste voordele van hierdie bedekkingsproses is dat daar minder as 1% tot die gewig van die vesels toegevoeg word. Verder nog is hierdie proses omgewingsvriendelik as gevolg van die hoeveelheid en tipe materiale wat gebruik word.

In die tweede studie was silwersulfadiasien (beperkte wateroplosbaarheid) gebruik om uiters wateroplosbare silwer-SD nanodeeltjies te sintetiseer. In hierdie spesifieke studie was die nanodeeltjies gestabiliseer met LvL bedekking om sodoende kristalgroei te beperk. PAMAM-dendrimere was gebruik vir die bedekkingsproses. Die dendrimere het gedien as oplosbaarheidsbevorderaars vir die swak wateroplosbare antibiotika. Hierdie studie het bewys dat doseervorme gebaseer op nanotegnologie vervaardig kan word en dat PAMAM-dendrimere noodsaaklik is vir die sukses van die doseervorm.

Die derde studie het ŉ stapsgewyse LvL nanobedekking van geneesmiddel nanodeeltjies behels. In hierdie studie was kitosan en kondroïtiensulfaat gebruik as bedekkers. Furosemied, isoksiel, rifampisien en paklitaksel was die gekose geneesmiddels. Al vier hierdie geneesmiddels toon eienskappe van swak wateroplosbaarheid. Die nanobedekking het tot gevolg gehad dat die dissolusie, eweredig aan die dikte van die bedekkingslaag, verlaag het. Nogtans het die geneesmiddels vinniger opgelos in vergelyking met die

gemikroniseerde poeiers van die geneesmiddels wat kommersieel beskikbaar is. Verder nog stabiliseer die LvL nanobedekking die klein deeltjies en voorkom dat kristalgroei en aggregasie in suspensie plaasvind. Geneesmiddelvrystelling was verbeter wanneer dit vergelyk word met die kommersiële grondstowwe. Hierdie studie het bewys dat LvL nanobedekking die wateroplosbaarheid van geneesmiddels kan verbeter.

Preface

The article format has been chosen for this PhD study. Chapter 1 of the thesis is an introduction to layer-by-layer technology. Chapter 2 describes the nano-coating of softwood fibers. In Chapter 3 highly soluble AgSD nanoparticles were synthesized and in chapter 4 poor water soluble drugs were nanocoated to improve their water solubility.

All the chapters were already published in leading pharmaceutical journals, i.e. Advanced Drug Delivery Reviews; International Journal of Pharmaceutics; Nanomedicine: Nanotechnology, Biology and Medicine and Powder Technology.

The composition of the thesis will then be:

Chapter 1 - Introductory chapter – "Introduction to nanocoatings produced by layer-by layer (LbL) self-assembly" *Advanced Drug Delivery Reviews, 63:701-715.*

Chapter 2 - Preparation and characterization of directly compactible layer-by-layer nanocoated cellulose. *International journal of pharmaceutics, 404:57-65.*

Chapter 3 - Poly(amidoamine) Dendrimer-mediated synthesis and stabilization of silver sulfonamide nanoparticles with increased antibacterial activity. *Nanomedicine: Nanotechnology, biology and medicine, 9:85-93.*

Chapter 4 - Self-assembled macromolecular nanocoatings to stabilize and control drug release from nanoparticles. *Powder Technology, 256:470-476.*

Chapter 5 - Concluding remarks

Annexure - Other research publications.

CHAPTER 1

This chapter was submitted to Advanced Drug Delivery Reviews.

Melgardt M. de Villiers, Daniel P. Otto, Schalk J. Strydom, and Yuri M. Lvov. 2011. Introduction to nanocoatings produced by layer-by-layer (LbL) self-assembly.

IMPACT FACTOR: 15.431

INSTRUCTIONS TO AUTHORS (SUMMARY)

The aim of the Journal is to provide a forum for the critical analysis of advanced drug and gene delivery systems and their applications in human and veterinary medicine. Theme issues are commissioned by one of the Executive Editors or the Editor-in-Chief. The Journal does not publish stand-alone manuscripts. If you wish to submit a theme issue topic for consideration, please contact one of the editors. Please note that manuscripts should be submitted within the timescales indicated by the Theme Editor. The deadlines that are set must be adhered too as the publication schedule of the journal is extremely strict. Authors are encouraged to submit video material or animation sequences to support and enhance your scientific research. For more information please see the paragraph on video data below.

Article structure

General arrangements of papers: Reviews should be divided into sections, each headed by a caption (abstract, introduction, review-specific subtitles, conclusions, references). The sections should be numbered 1, 1.1, 1.1.1 etc. for major sections and subsections, respectively. *A table of contents* specifying the sections and subsections should be supplied.

Title

Concise and informative. Titles are often used in information-retrieval systems. Avoid abbreviations and formulae where possible.

Author names and affiliations

Where the family name may be ambiguous (e.g., a double name), please indicate this clearly. Present the authors' affiliation addresses (where the actual work was done) below the names. Indicate all affiliations with a lower-case superscript letter immediately after the author's name and in front of the appropriate address. Provide the full postal address of each affiliation, including the country name and, if available, the e-mail address of each author.

Corresponding author

Clearly indicate who will handle correspondence at all stages of refereeing and publication, also post-publication. Ensure that phone numbers (with country and area code) are provided in addition to the e-mail address and the complete postal address. Contact details must be kept up to date by the corresponding author**.**

Abstract

A concise and factual abstract is required. The abstract should state briefly the purpose of the research, the principal results and major conclusions. An abstract is often presented separately from the article, so it must be able to stand alone. For this reason, References should be avoided, but if essential, then cite the author(s) and year(s). Also, non-standard or uncommon abbreviations should be avoided, but if essential they must be defined at their first mention in the abstract itself. The abstract should usually be less than 150 words.

Graphical abstract

A Graphical abstract is mandatory for this journal. It should summarize the contents of the article in a concise, pictorial form designed to capture the attention of a wide readership online. Authors must provide images that clearly represent the work described in the article. Graphical abstracts should be submitted as a separate file in the online submission system. Image size: please provide an image with a minimum of 531 × 1328 pixels (h × w) or proportionally more. The image should be readable at a size of 5 × 13 cm using a regular screen resolution of 96 dpi. Preferred file types: TIFF, EPS, PDF or MS Office files.

Keywords

A maximum of 6 to 10 keywords or short phrases (not already used in the title) should be provided immediately after the abstract.

Abbreviations

Define abbreviations that are not standard in this field in a footnote to be placed on the first page of the article. Such abbreviations that are unavoidable in the abstract must be defined at their first mention there, as well as in the footnote. Ensure consistency of abbreviations throughout the article.

Acknowledgements

Collate acknowledgements in a separate section at the end of the article before the references and do not, therefore, include them on the title page, as a footnote to the title or otherwise. List here those individuals who provided help during the research (e.g., providing language help, writing assistance or proof reading the article, etc.).

Nomenclature and units

Follow internationally accepted rules and conventions: use the international system of units (SI). If other quantities are mentioned, give their equivalent in SI. You are urged to consult IUB: Biochemical Nomenclature and Related Documents: http://www.chem.qmw.ac.uk/iubmb/ for further information.

Figure captions

Ensure that each illustration has a caption. Supply captions separately, not attached to the figure. A caption should comprise a brief title (**not** on the figure itself) and a description of the illustration. Keep text in the illustrations themselves to a minimum but explain all symbols and abbreviations used.

Tables

Number tables consecutively in accordance with their appearance in the text. Place footnotes to tables below the table body and indicate them with superscript lowercase letters. Avoid vertical rules. Be sparing in the use of tables and ensure that the data presented in tables do not duplicate results described elsewhere in the article.

References

Citation in text Please ensure that every reference cited in the text is also present in the reference list (and vice versa). Any references cited in the abstract must be given in full. Unpublished results and personal communications are not recommended in the reference list, but may be mentioned in the text. If these references are included in the reference list they should follow the standard reference style of the journal and should include a substitution of the publication date with either 'Unpublished results' or 'Personal communication'. Citation of a reference as 'in press' implies that the item has been accepted for publication.

Reference links Increased discoverability of research and high quality peer review are ensured by online links to the sources cited. In order to allow us to create links to abstracting and indexing services, such as Scopus, CrossRef and PubMed, please ensure that data

provided in the references are correct. Please note that incorrect surnames, journal/book titles, publication year and pagination may prevent link creation. When copying references, please be careful as they may already contain errors. Use of the DOI is encouraged.

Web references As a minimum, the full URL should be given and the date when the reference was last accessed. Any further information, if known (DOI, author names, dates, reference to a source publication, etc.), should also be given. Web references can be listed separately (e.g., after the reference list) under a different heading if desired, or can be included in the reference list.

References in a special issue Please ensure that the words 'this issue' are added to any references in the list (and any citations in the text) to other articles in the same Special Issue.

Reference management software This journal has standard templates available in key reference management packages EndNote (http://www.endnote.com/support/enstyles.asp) and Reference Manager (http://refman.com/support/rmstyles.asp). Using plug-ins to wordprocessing packages, authors only need to select the appropriate journal template when preparing their article and the list of references and citations to these will be formatted according to the journal style which is described below.

Reference formatting There are no strict requirements on reference formatting at submission. References can be in any style or format as long as the style is consistent. Where applicable, author(s) name(s), journal title/book title, chapter title/article title, year of publication, volume number/book chapter and the pagination must be present. Use of DOI is highly encouraged. The reference style used by the journal will be applied to the accepted article by Elsevier at the proof stage. Note that missing data will be highlighted at proof stage for the author to correct. If you do wish to format the references yourself they should be arranged according to the following examples:

Reference style *Text:* Indicate references by number(s) in square brackets in line with the text. The actual authors can be referred to, but the reference number(s) must always be given.

Advanced Drug Delivery Reviews

Introduction to nanocoatings produced by layer-by-layer (LbL) self-assembly (2011)

Melgardt M. de Villiers,[1] Daniel P. Otto[2], Schalk J. Strydom,[1,2] and Yuri M. Lvov[3]*

1 School of Pharmacy, University of Wisconsin-Madison, Madison, Wisconsin 53705-2222, USA

2 Unit for Drug Research and Development, Faculty of Health Sciences, North-West University, Potchefstroom, 2520, South Africa

3. Institute for Micromanufacturing and Biomedical Engineering Program, Louisiana Tech University, Ruston, LA 717272, USA

*To whom correspondence should be addressed.

School of Pharmacy, University of Wisconsin-Madison, 777 Highland Avenue, Madison, WI 53705-2222, USA. Phone: +1 608 890 0732. Fax: +1 608 262 5345. E-mail: mmdevilliers@pharmacy.wisc.edu.

Graphical abstract

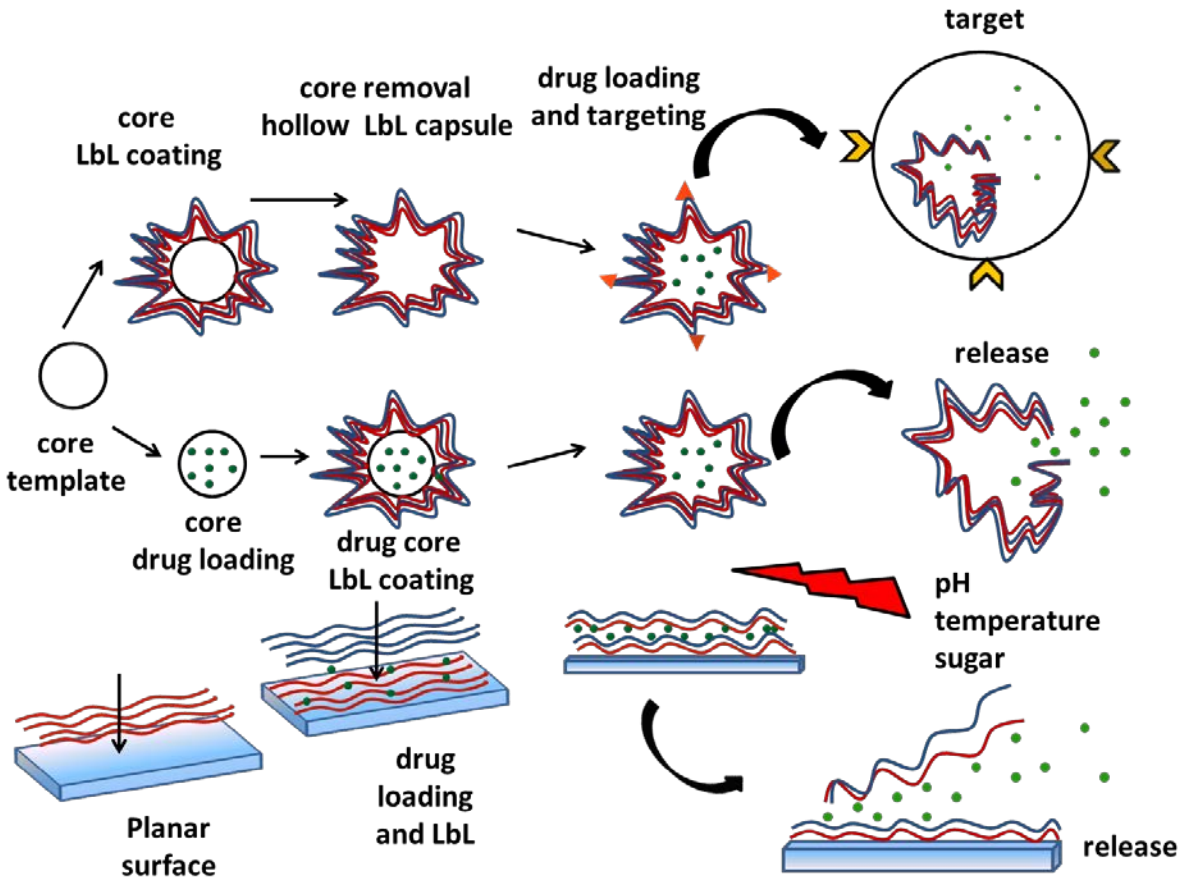

Abstract

Studies on the adsorption of oppositely charged colloidal particles ultimately resulted in multilayered polyelectrolyte self-assembly. The inception of layer-by-layer constructed particles facilitated the production of multifunctional, stimuli-responsive carrier systems. An array of synthetic and natural polyelectrolytes, metal oxides and clay nanoparticles is available for the construction of multilayered nanocoats on a multitude of substrates or removable cores. Numerous substrates can be encapsulated utilizing this technique including dyes, enzymes, drugs and cells. Furthermore, the outer surface of the particles presents and ideal platform that can be functionalized with targeting molecules or catalysts. Some processing parameters determining the properties of these successive self-assembly constructs are the surface charge density, coating material concentration, rinsing and drying steps, temperature and ionic strength of the medium. Additionally, the simplicity of the layer-by-layer assembly technique and the availability of established characterization methods, render these constructs extremely versatile in applications of sensing, encapsulation and target- and trigger-responsive drug delivery.

Keywords

Layer-by-Layer, Nanocoating, Self-assembly, Polyelectrolyte, Adsorption

1. Historical perspective on layer-by-layer self-assembly

Novel materials have always been sought and the employment of surface modification at the molecular level realized this goal. Surface modification resulted in a multitude of new properties that were previously not associated with the native material. These changes include modifications of the electrical, optical, magnetic, physicochemical and biological properties of the material in question. As consequence, several disciplines of natural science have experienced the impact of surface modifications, changing the fundamental properties of materials at the building-block-level. The historical evolution of self-assembly will, therefore, be discussed.

The development of surface science resulted from the ancient superstitious belief that pouring oil on water can calm the ripples caused by wind. This ancient believe was scientifically addressed by Franklin [1] and Rayleigh and his peers [2-4] followed by seminal work by Langmuir to finally realize monomolecular surface coating of solid substrates [5-7]. Blodgett expanded the Langmuir film technique to produce multilayer coatings known as the Langmuir-Blodgett (LB) technique [8-11].

The group of Kuhn [12-13] then explored the possibility to adsorb different oppositely charged dyes with the LB technique, discovering the potential of layer thickness and energy transfer. The LB-technique was however difficult and limited to only certain colloids. Iler [14] however observed that oppositely charged colloids could be alternately assembled onto glass substrates and work by Nicolau and colleagues illustrated successive layering of substrates with oppositely charged metal ions to produce polycrystalline coatings [15,16] and successive polymerizations steps in situ to produce alternating polymer coats onto a substrate [17,18].

The work of Iler and Nicolau probably inspired the seminal breakthrough made by the group of Decher, who used synthetic polyelectrolytes i.e. polymers with ionizable surface groups to form polyions that were successively layered onto a substrate by electrostatic interaction [19]. This method is robust, simple, does not require sophisticated equipment and precise stoichiometry, nor does it rely on complicated chemical reactions to deposit successive layers. Layer-by-layer self-assembly (LbL) is still seen as the true alternative to the LB technique.

Several characterization studies were undertaken on polyelectrolyte multilayers (PEM) in early to mid 1990s. The classic PEM characterization techniques were established using X-ray diffraction, UV-analysis [20,21] and gravimetric analysis by quartz crystal microbalance (QCM)

dissipation [22]. Novel coating colloids including proteins [22] and DNA [23] were also introduced.

Since the late 1990s, work has focused on development of multilayer composites based on interactions other than electrostatic interactions such as hydrogen bonding [24-27]. Controllable polymerization reactions also resulted in novel approaches to assemble layer-by-layer constructs through successive polymerization [28,29]. This development enabled LbL construction and applications in which organic, instead of aqueous working media could be employed.

Highly efficient covalent “click” chemistry was introduced modularly build or modify materials, providing an alluring alternative to a dispersion force assembly [30]. Figure 1 provides a timeline of the evolution of LbL modification techniques.

The layer-by-layer (LBL) self-assembly of multiple polyelectrolytes and other particles resulted in the production of multifunctional hybrid carrier systems [31-34] for dyes [35,36], sensors [37-39], enzymes [40,41], drugs [42-44], multiple components [45] and cells [46,47]. Additionally, nanocoated substrates provide a surface platform for the attachment of targeting molecules, i.e. folic acid [48–50], antibodies [51] or a variety of surface functional groups such as hydroxyl, carboxyl and thiol groups [52].

Moreover stimuli-responsive properties could be introduced by the inclusion of responsive materials in LbL constructs [34]. The following sections describe the robust nature of LbL self-assembly for the production of versatile carrier systems that comprise oppositely charged substances onto a substrate, resulting in a PEM-coated system [53,54]. In section 7, the LbL drug delivery technology will be featured.

~2000 BC	Babylonian sailors believe that the spreading of oil calms stormy seas and predicts health, prosperity etc and Chinese spread ink films on water
~1200 BC	Japanese spread ink films on water and deposit water-spread ink films on paper
~1000 BC	Greek sailors adopt the Babylonian belief that oil calms rough seas
429, 651 AD	Greek scholars and philosophers document the calming effect of oil on water ripples
1774	Benjamin Franklin records the first modern scientific account of calming water ripples with oil [1]
1890	Lord Rayleigh pours olive oil on water and measures the decrease of 'surface tension' at the water-oil interface [2]
1891	Agnes Pockels systematically observes a notable depression in surface tension when oil is compressed below a critical spreading area [3]
1899	Lord Rayleigh speculates on the findings of Pockels that oil molecules will be 'densely packed' when a certain compression limit is reached [4]
1917	Irving Langmuir proves Rayleigh's hypothesis and produces seminal work on monomolecular oil layer orientation (Langmuir films) [5]
1920	Langmuir transfers a monomolecular oil layer to a solid substrate to create the first monomolecular coating [6]
1935	Katharine Blodgett transfers successive monomolecular layers onto a solid substrate and the Langmuir-Blodgett (LB) film era is born [8]
1966	Iler studies electrostatic colloid self-assembly to produce multilayer coatings on surfaces, suggesting and alternative to the LB technique [14]
~1970	Kuhn et al. realizes the potential of multilayer manipulation and Förster- energy transfer, employing LB films [12,13]
1985-1989	Nicolau et al. study and establish polyion self-assembly and multilayer assembly by successive *in situ* polymerization of monomers [15-18]
1991	Decher introduces the first true alternative to LB modification by introduction of electrostatic polyelectrolyte self-assembly in a layer-by-layer (LbL) fashion [19]
1994, 1995	Lvov et al. uses proteins [22] to produce LbL assemblies and Sukhorukov et al. brings DNA [23] into play as a polyelectrolyte
1997	Rubner, Stockton et al. introduces hydrogen-bonded LbL assembly [24-27]
2000	Covalent bonding can now contribute to the assembly palette [28,29]
~2001	The first PEM deposited on a real drug, ibuprofen, is, reported [44]

Fig. 1. A timeline showing the evolution of LbL self-assembly.

2. Basic principles of the layer-by-layer technique

The formation of nanocoatings using LbL self-assembly technique distinguishes itself in its simplicity from other surface modification methods such as spin-coating, solution casting, thermal deposition, chemical self-assembly and the LB technique and will be discussed next.

2.1 Mechanism of self-assembly

The buildup of LbL mutlilayers is driven by the electrostatic attraction between the oppositely charged constituents [14]. However, hydrogen bonding [55-57], hydrophobic interactions [58] and van der Waals forces [59,60] may be exploited to assemble LbL systems or influence the stability, morphology and thickness of the films, particle/molecule depositions and permeation properties of the film [19,61,62].

Generally, LbL self-assembly proceeds as follows: (1) A charged substrate is immersed in a solution of an oppositely-charged colloid to adsorb the first monolayer, (2) a washing cycle follows to remove unbound material and preclude contamination of the subsequent oppositely-charged colloid, (3) in which the coated substrate is submerged to deposit a second layer and (4) the washing/coating cycle is repeated is formed [62] (Figure 2). Some LbL processes require no washing cycles thus shortens the duration of the assembly process [63].

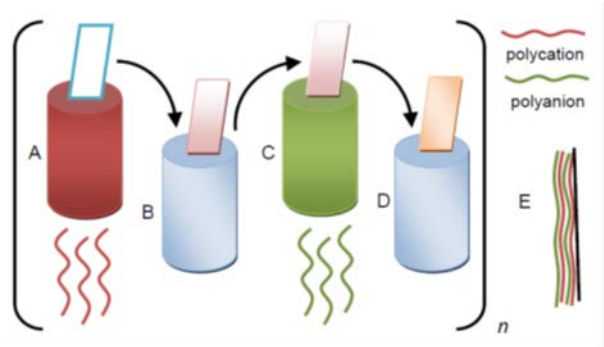

Fig. 2. A schematic illustration of the alternate adsorption of the polyelectrolyte species to produce a multilayered structure. (A) Dipping in a polycation (example) followed by (B) rinsing in a solvent for the polycation with (C) dipping in a polyanion and (D) rinsing in a solvent for the polyanion. The process is repeated *n* times to produce (E) the multilayered construct.

The polyelectrolytes or colloids, which exhibit a high linear surface charge density, are utilized in excess to prime the substrate. Therefore, a non-stoichiometric excess of charge is absorbed after each step relative to the preceding layer [53,64]. This surplus of charge provides the step-

wise mechanism for the reversal of the surface charge polarity, facilitating a favorable surface for the adsorption of the subsequent layer.

Techniques, not reliant on intermolecular forces, i.e. covalent or click chemistry were developed to produce stable [65,66] or biodegradable [67,68] multilayered structures. However, the principle of successive layering still applies.

The LbL self-assembly methods have advantages compared to the more conventional coating methods, including (1) the simplicity of the LbL process and equipment, (2) its suitability to coating most surfaces, (3) the availability of an abundance of natural and synthetic colloids, (4) the flexible application to objects with irregular shapes and sizes, (5) the formation of stabilizing coats and (6) control over the required multilayer thickness [69-71].

3. Coating materials and substrates

Several polyelectrolytes and nanoparticles can be utilized to form the ultrathin multilayer structures using the LbL self-assembly technique. Furthermore, several substrates can be coated with nanothin multilayers.

3.1 Polyelectrolytes

Polyelectrolytes are classified according to their origin. Standard synthetic polyelectrolytes include poly(styrene sulfonate) (PSS), poly(dimethyldiallylammonium chloride) (PDDA), poly(ethylenimine) (PEI), poly(N-isopropyl acrylamide (PNIPAM), poly(acrylic acid) (PAA), poly(methacrylic acid) (PMA), poly(vinyl sulfate) (PVS) and poly(allylamine) (PAH) [69].

Natural polyelectrolytes include nucleic acids [70], proteins [71] and polysaccharides [72] of which alginic acid, chondroitin sulfate [73], DNA [74] heparin, chitosan, cellulose sulfate, dextran sulfate and carboxymethylcellulose are most common [73-75].

3.2 Nanoparticles and nanoobjects

Nanoparticles utilized for LbL constructs are derived from stabilized colloidal dispersions of charged silica, charged poly(styrene) spheres, metal oxides [14], polyoxometalates [76,77] and conducting liquid crystalline polymers [78].

Positively and negatively charged platelets utilized for multilayer construction are derived from naturally-occurring clays such as hectorite, montmorillonite and saponite [79]. Charged liquid

crystalline polymers i.e. hydrotalcite were successfully assembled with these clay nanoobjects [78,79].

Dendrimers have also been successfully used to form PEMs, with poly(amidoamine) (PAMAM) dendrimers most commonly used [80,81].

Carrier systems can be functionalized with stimuli-responsive components that respond to temperature, pH and ionic strength [82,83]. The polymers/colloids used in the LbL technique can also be functionalized to alter its properties preceding LbL assembly.

3.3 Substrates

The prerequisite for successful LbL coating is the presence of a minimal surface charge, which is one of the few disadvantages of the technique. However, charged can be induced to still facilitate LbL [84]. Most commonly glass, quartz, silicon wafers, mica, gold-coated substrates are coated. The type of substrate that is encapsulated depends primarily on the colloids assembled into PEMs and analytical monitoring techniques for the coating steps [69].

Surface charge is not the only factor that may affect the multilayer adhesion. The surface texture could also affect the adhesion properties. Pretreatment of a substrate by annealing with sodium chloride smoothened the surface of the substrate, resulting in more intimate contact between the substrate and colloid to produce higher quality coats [85,86].

Furthermore, the coating elasticity, could also affect the surface adhesion of the coating layers to the substrate. The effect of the coating modulus is, however, ambiguous since some studies indicated an improvement in surface adhesion for elastic PAH-based coats [87,88] based on the morphology of the films and the polarity of the surface charge. However, a detrimental effect on coating interactions for highly elastic layers i.e. aminosilane-based PEMs adsorbed to glass was found [85]. The substrate might therefore require some pretreatment preceding the LbL assembly process to ensure its success.

4. Experimental parameters and LbL adsorption

The formation of polyelectrolyte multilayer self-assembly is usually reliant on the electrostatic adsorption between the substrate and subsequent layers [14,53]. A two-stage process is envisioned by which (1) an initial anchoring of the coating material to the surface is followed by

(2) a slow relaxation to form a densely-packed structure on the surface [89]. Some processing parameters that influence the adsorption steps of LbL assembly are briefly discussed.

4.1 Coating material concentration

Concentrated solutions are required for successful adsorption and to prevent colloid depletion during multistep LbL [53,62], to exceed the minimum threshold concentration for attachment and to reverse charge polarity for each adsorbed layer. The threshold is primarily dependent on solubility and charge density of the colloid. PSS, showed a critical concentration of 10-7 mol/L, whereas other polyions illustrated higher thresholds of 10-2 mol/L [90]. Above the threshold, concentration was irrelevant to adsorption, however, resulted in an exponential increase in the thickness of the monolayers [91,92].

4.2 Washing

As shown in Fig. 2, the LbL adsorption process includes a rinsing step, during which the coated substrate is washed in a good solvent for the polyelectrolyte to remove unbound polyelectrolytes and to prevent the cross-contamination of solutions [93].

Strong polyelectrolyte layers (with high surface charge density) are not significantly altered by rinsing of the LbL construct since the layer is secured by strong interactions. However, the weakly bound polyelectrolytes (low surface charge density) may be stripped off, limiting successful LbL assembly [94].

4.3 Drying

Successive dipping of the adsorbed films into the respective polyelectrolyte solutions ensures a moist environment, enhancing chain flexibility and ionization during the adsorption steps, therefore thinner and less dense films are generally formed due to a higher degree of multivalent adsorption [69].

Therefore, if a PEM is allowed to dry after each rinsing step, further film growth may be impeded due to the unfavorable rearrangement of the upper surface molecules as seen for PSS or by prevention suitable time scales to ensure polyvalent grip of the substrate [95,96].

Spontaneous drying under ambient conditions for PAH/PSS films produced more ordered films compared to those dried under nitrogen streaming, which showed large disordered regions and can thus influence film structure [97].

Different rates of drying are also dependent on the number of coated layers, especially the dehydration of the inner layers [98]. It is thus important to consider the impact of drying on the film if one/both of the colloids used in the PEM film is protein based since these could rearrange to prevent coating. Structural rearrangement can, therefore be controlled kinetically.

Conversely, LbL films assembled from synthetic polyelectrolytes such as poly(o-methoxyaniline), require a drying step for optimal film growth [99]. Temperature can affect drying rates and is therefore an important experimental parameter [69].

4.4 Ion concentration and pH of the medium

In the case of polyelectrolyte LbL self-assembly, electrostatic interactions between the alternating polyions result in film formation. Therefore, alterations in the electrostatic charge via ions or pH changes, will affect polyelectrolyte interaction and PEM growth [14,53,91].

PEM film thickness can increase exponentially or linearly with each step, with linear growth taking place when the polyelectrolytes in the solution interact exclusively with the outer layer of the multilayer film [100]. Generally, an increase in ionic concentration results in an increase in film thickness due to polyelectrolyte charge compensation resulting in more globular rather than extended polyelectrolyte structure [100-103]. However, with diffusion of the polyelectrolytes into the interior or if interactions between the adsorbing polyelectrolyte and interior takes place, the film thickness increases exponentially [100]. Salt ions affected the electrostatic charge between layers and consequently on layer thickness PSS/PDDA PEMs. With aid of dialysis, salt ions were leached from the media, producing thinner films from these polyelectrolytes compared to films produced without dialysis [103].

However, exceeding a certain threshold, an increase in salt concentration compensated all charge and the polyelectrolyte formed turbid, coagulated dispersions. No adhesion or successful multilayering could be achieved under these conditions [104,105].

Eq. (1) shows the ion exchange phenomenon regulating the adsorption step that can be manipulated by changing the pH or salt concentration in the polyelectrolyte solution [106]:

$$Pol^- M^+_{(m)} + Pol^+ A^-_{(aq)} \leftrightarrow Pol^- Pol^+_{(m)} + M^+_{(aq)} + A^-_{(aq)} \qquad (1)$$

where m and aq refer to molecules that are either associated with the substrate surface or which are dissolved respectively, Pol refers to charged polyelectrolyte segments whereas M and A are salt ions [106,107].

It is clear that an increase in the salt concentration in the polyelectrolyte solution(s) will force the adsorption step to slow down or cease altogether, unless the salt ions are removed e.g. dialysis [103] due to competitive binding between salt and polyelectrolyte ions for adsorption sites on the layer surface. Exceeding the critical salt concentration (csc) the adsorbed polyelectrolytes on the substrate surface may even be displaced by the salt ions [108].

A change in the pH of the solutions will alter the dissociation of the polyelectrolytes and ions, which will alter the successive adsorption steps [109,110]. Similarly to ion concentration, a change in pH value also resulted in a linear or exponential growth of film layers for weak polyelectrolytes dependent on a charge density mismatch under defined pH conditions [111].

Furthermore, a critical charge density was elaborated for selected polyelectrolytes coated in media containing a varying salt concentration. Below the threshold value, no growth in the multilayer construct was observed [112].

Monomolecular layer thickness of strong polyelectrolytes is amendable by adjusting the salt concentration in the respective solutions, whereas layers constructed from weak polyelectrolytes are more susceptible to the variation in the solution pH [113]. Thus the film thickness can be modified by adjusting the ionic strength and/or the pH of a specific polyelectrolyte solution [69].

4.5 Working medium

A number of studies have elaborated the effect of the working medium polarity on the efficiency of LbL assembly. Aqueous solutions of water-soluble polyelectrolytes are primarily used as coating materials and PSS and PAH count among the most studied [101]. However, the employment of non-aqueous systems have also been investigated with an azo-polyelectrolyte in N,N-dimethylformamide [114], PSS/PAH/formamide combinations, [115] and PSS/PAH/chloroform systems [116] all of which showed at least some extent of solvent polarity. Toluene could also be successfully utilized as an example of a non-polar solvent by addition of a surfactant to a suspension of carbon black or alumina particles [117].

The working medium should enable the polyelectrolyte or coating substance to ionize to some extent for water-soluble coating substances, since the major interaction between successive layers are electrostatic self-assembly. In non-polar solvents, the substances should be coated reliant on dispersion forces or hydrogen bonding. This enables the assembly of substances that might not ionize or only ionize under harsh conditions. The interactions that are responsible for PEM integrity can therefore be strengthened or compromised by the environmental conditions resulting in assembly/disassembly of the films. In Section 7, the importance of these conditions on drug delivery system assembly and disassembly will be reviewed.

4.6 Adsorption kinetics

The preceding sections briefly highlighted some of the experimental factors that could influence the adsorption of charged colloids onto a substrate. The factors all show some extent of time-dependence; therefore adsorption kinetics is the next topic.

PEM assembly is the result of the competitive interaction between polyelectrolytes, substrate and polyelectrolytes and the solvent which could in turn have interaction with both polyelectrolytes as well as the substrate [118].

Generally, the first step of adsorption onto a substrate is a fast, first-order process spanning a few seconds since several initial electrostatic anchoring sites are unsaturated on the substrate. The second, slower process could span minutes and reflects the rearrangement of the coated domains that were established by the first anchoring step. This two-step mechanism is best described as a Johnson–Mehl–Avrami biexponential saturation process [119]. During this second step, diffusion of additional polyelectrolyte chains might occur, resulting in additional domain growth.

The second growth step is diffusion-controlled since the level of coverage in the coated domain is saturated with time. Secondly, the duration of the conformational rearrangement of the initially-coated anchored coating material contributes to the slower rate of growth during the second adsorption step [103,119]. The rearrangement step results in the establishment of a brush-like polyelectrolyte conformation of the initially adsorbed chains, posing a barrier to further surface saturation [120-122]. Polyelectrolyte inter-chain interactions are responsible for this layer restructuring as was evidenced from surface tension and contact angle measurement on polymer-coated substrates [123].

Particle aspect ratio also affects adsorption kinetics. Hybrid multilayered films were produced by a combination of either montmorillonite (MMT) or laponite (LAP) particles with branched poly(ethylenimine) (BPEI). The thickness of both types of clay platelets approximates 1 nm, however MMT platelets showed an average lateral aspect of 200 nm, compared to approximately 25 nm for LAP. Additionally, MMT particles possess polydisperse aspect ratios ranging 200–1000 and that of a LAP approaches a uniform value of 27. The smaller LAP platelets could mover deeper into the uncoated voids left by the preceding layer than the larger MMT. MMT therefore, showed lesser dependency on the deposition of coating time. The LAP particles experienced the two-stage Johnson–Mehl–Avrami-type saturation process; however, the process could still be optimized with fairly quick coating exposure times. The smaller LAP clay particles required a slightly longer coating time to achieve the same film quality as that with the larger MMT particles [122].

The first step in the adsorption results in the adsorption of the most material to the surface [119] and will be the determining factor for a successful coat. It is not an absolute requirement that the surface of the substrate should be fully coated to produce a successful PEM, some material should be coated to prime the surface with charge. Therefore, the absorption kinetics should be optimized to ensure that the various experimental conditions as well as the exposure time to the coating solutions can successfully produce the self-assembled construct.

5. Layer-by-layer disassembly

In several cases, intact LbL constructed systems are required to remain stable in order to control the release of substances i.e. drugs [42,44] by posing a barrier to release with the possibility of variation of barrier permeability for water-soluble drugs and dyes substances under the influence of external stimuli such as changes in temperature or ultrasonic treatment [123].

The alternative approach to release the captured content in an LbL-assembled system relies on the disassembly of the vehicle. The disassembly can be affected by the complete destruction of the vehicle or a controlled or sustained erosion of the various layers of the construct, the latter posing several challenges due to the multitude of stabilizing interactions between adjacent layers [124].

Electrostatic screening with sodium chloride has been studied as an immediate disassembly trigger for multilayered capsules [125]. The salt concentrations needed to invoke disassembly

were often high and resulted in immediate, sometimes unwanted, release of the content [126]. Similarly, immediate release upon reaction to a change in pH could also be seen [127].

However, by incorporation of biodegradable polyelectrolytes, i.e. poly(ß-amino ester), and non-biodegradable polyelectrolytes in the multilayered structure, the slow and controlled disassembly under physiological conditions was achievable [133]. Similar controlled release effects was seen for the hydrolytically cleavable poly(ß-amino ester) with hydrophobic modification up to a certain critical point, after which rapid destabilization and release was observed [128]. Tailoring the polyelectrolyte of the polysaccharide chitosan by cross-linking to hyaluronan to enzymatic degradation also affected control over the degradation of the multilayered film [129]. The applications of LbL disassembly in drug delivery will be discussed later.

6. Characterization of LbL constructs

The combination of several techniques can be used to study the construction, disassembly or release of captured content from LbL PEMs. Some of the more common methods will be briefly discussed (Fig. 3).

6.1 Spectroscopic characterization

Multilayer growth can be monitored by UV–VIS spectroscopy that determines cumulative absorption attributed to stepwise deposition of UV-active colloids [130,131].

Ellipsometry determines the distance-dependent change in polarization of a light source as a function of reflection or transmission through a substance. Therefore, the multilayered film thickness can also be measured this way [132,133]. These methods are most commonly used to determine the layer thickness or adsorbed mass per layer during each step [66,119,134-136].

Cumulative visible light absorption is also used to determine PEM thickness. Additionally, substrate–polyelectrolyte interactions can be studied by the shifts in absorption maxima dependent on coating time. This shift was attributed to the interaction of a UV–chromophore that was also responsible for the surface adhesion [99] or for solvent–polyelectrolyte interactions [137].

PEM stability can be studied with confocal laser microscopy (CLSM), if fluorescently-labeled polyelectrolytes are assembled [138,139]. The method is limited to detectable particle size constraints [140]. Release of fluorescently-labeled substances from PEM capsules were also

studied with CLSM [141,142]. Multilayer thickness also scaled proportionally to the fluorescence intensity [142].

Infrared analysis can be used to determine the PEM moisture content. This could reveal useful information to study the structure of ionizing groups as well as the permeability of water-leachable substances [143] or PEM assembly in the presence of moisture [144,145].

Drug interactions with constituent PEM layers could be studied using Raman microscopy. It was found that methylene blue arranged as monomers or aggregates in different positions in gold-labeled polyelectrolyte chains. The interaction of the gold nanoparticles and anionic phospholipid was influenced by methylene blue aggregation and chain position, altering the gold particle clustering. Consequently, color changes in the surface-enhanced Raman scattering of the gold particles were observed [146].

Minute dioxin contamination could be by incorporation of Ag nanoparticle sensors in permeable LbL constructs of PDDA/PAA. These films were immersed in citrate solution and then Ag nanoparticles were trapped inside the porous film. Upon aggregation of these nanoparticles, due to complexation with dioxins, a marked increase in the electromagnetic fields between Ag particles were facilitated, amplifying the detected Raman signal [147].

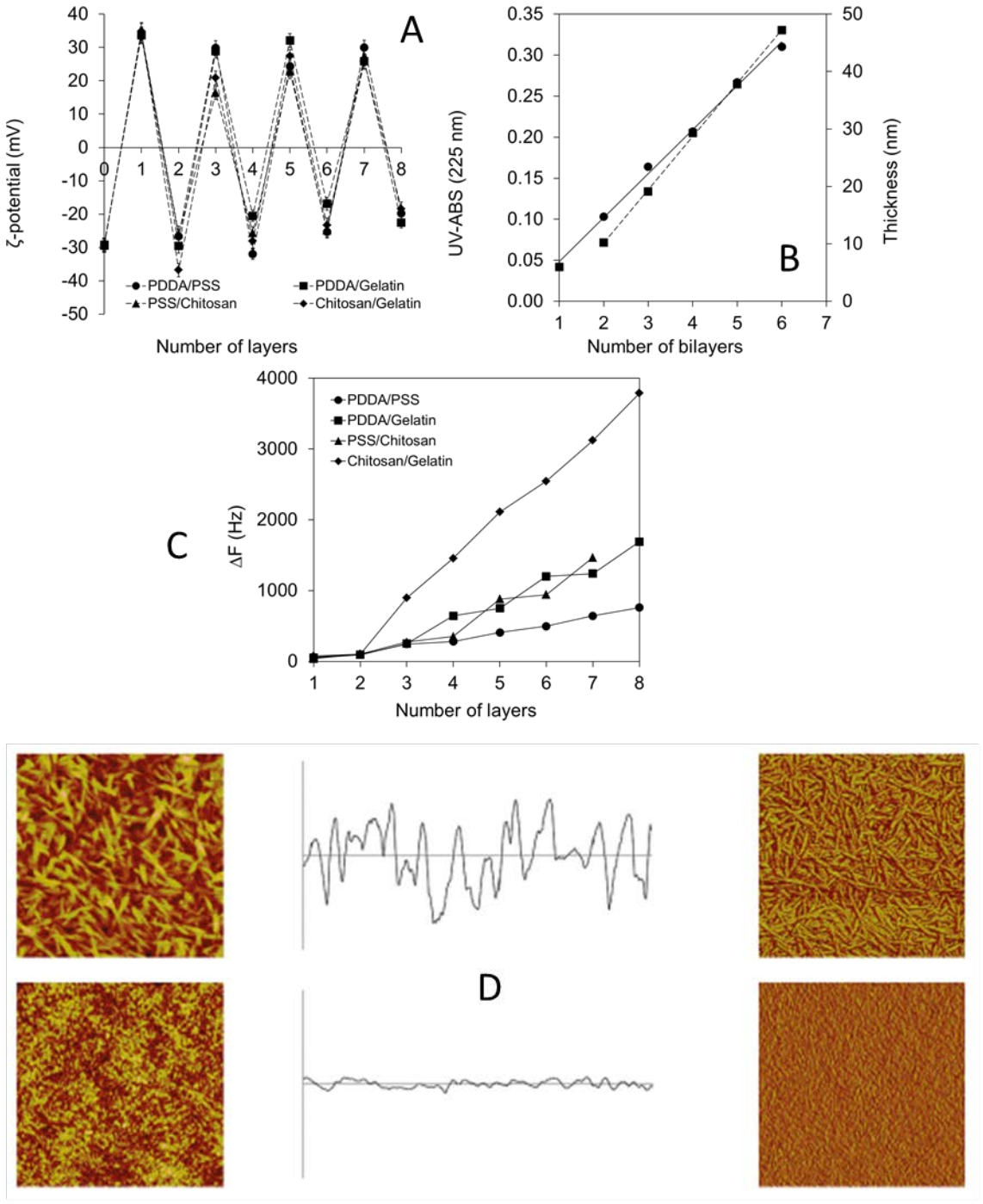

Fig. 3. Some of the most common characterization methods of LbL self-constructs (A) zeta potential measurements of alternately coated substrates, (B) UV and (C) QCM-D analysis of layer accumulation and thickness, (D) AFM analysis of a rough and smooth coated cellulose surface.

6.2 Structural characterization

Quartz crystal microbalance studies, relate vibration dissipation (QCM-D) as function of the step-wise amount of colloid adsorbed to a quartz crystal surface in real time. The dissipation values are converted by the Sauerbrey equation to the amount of material that was adsorbed per layer [148,149]. QCM-D should be used with caution if viscoelastic polyelectrolytes [88,150] are coated and where thicker layers are coated due to potential crystal vibration frequency compensation, resulting in erroneous interpretations of frequency shifts [151].

Electrophoretic particle mobility enables ζ-potential measurements of charged, therefore efficiently coated, surfaces to study charge reversal and colloidal stability [152].

The internal arrangement PEM structure can be determined by X-ray reflectivity [153,154] as seen for PAMAM dendrimers that were assembled in layers with sulfonated poly(aniline). The reflectogram intensities were converted to the thickness of the PAMAM layers. These layers were present in flat conformations or possibly interpenetrated with the poly(aniline) since the calculated thickness deviated from the expected thickness for globular conformations [155]. X-ray reflectivity also showed that hydrophobic substituents on PDDA produced globular structures due to a reduction in solubility. Thickness of the subsequent PDDA/clay PEMs was therefore proportional to medium hydrophobicity [156].

The surface texture and roughness of PEMs can be elucidated by atomic force microscopy (AFM) [106,177]. Water repellency could also be studied as a function of the number of silica layers that were assembled onto a glass surface [158]. AFM can aid studying the changes in wettability, contact angle and subsequently surface energy [159].

A comprehensive study was performed to study the effect of multilayer coating of PEI on cellulose substrates where AFM was employed to characterize the surface roughness of the coated cellulose substrates and ultimately the interaction of these surfaces with liquids [160]. The addition of a Hofmeister series of ions was studied with AFM to determine the effect on PSS/PDADMAC multilayer texture. It was observed that chaotropic anions destabilized/stripped some layers of a PSS/PDDA PEMs by charge screening [161], resulting in a higher surface roughness [162].

Spin relaxation NMR was also employed to study the hydration and dehydration properties of multilayers [98] or the mobility of polyionic multilayers [163]. It was proven that water mobility in a PAH/PSS LbL construct in solution was impaired when the polycation formed the outer layer [98], however in the solid state NMR analysis, the movement was indeed faster when PAH formed the outer layer, due to preferred association of water molecules with PSS. The effect of higher pH demonstrated bulkier conformations of PAH, allowing for more chain and water movement flexibility [164] which could influence drug delivery as seen in the next section.

Projected particle size and size distributions can be determined with dynamic light scattering (nanoparticles or smaller microparticles) or diffraction techniques (larger particles) [165].

These are some of the more common techniques that are currently used to confirm the self-assembly LbL process, as well as to characterize the final PEM structure and release properties of delivery systems.

7. The contribution of LbL self-assembly to drug delivery

7.1 Advantages of LbL-assembled multilayers

LbL self-assembly offers several advantages to other methods of encapsulation, coating or fixation of substances: (1) the wall thickness of capsules can be tailored in the nm–μm range, (2) several types of synthetic/natural colloids are available for LbL, (3) the location and sequence of the layers can be controlled, (4) surface labeling with targeting molecules is possible, (5) stabilization of submicron particles is possible [167], (6) LbL avoids the use of thermodynamically unstable mechanically-micronized particles [168,169] and (7) much lower amounts of colloids (~ 1%) is needed to produce a functional coating compared to a minimum of ~ 10% with conventional techniques.

7.2 Drug release

A major challenge in drug delivery is to produce controlled, sustained or triggered release systems for small encapsulated drug molecules. Fluorescein dye release from polyelectrolyte capsules showed that the number of layers determined the extent of diffusion resistance and encapsulated core dissolution, also relevant to drug delivery systems [170].

Tailored release systems minimize side-effects due to lower systemic drug concentrations, prolonged duration of drug action and protection of active ingredients in hostile physiological environments [171,172].

Another challenge of controlled-release drug delivery systems is curbing the fast initial release of drug. However, capturing procaine hydrochloride in nanoparticles smaller than 200 nm and depositing only a few layers of PAH/PSS, successfully eliminated burst release. The PEM prevented particle swelling; therefore, the particles were less permeable to drug diffusion, lengthening the release t1/2 from 30 min to 3 h [173].

A pulsatile release system was also developed by PSS/PAH layering of acrylate-based polymer microgel particles containing fluorescently-labeled dextran as a macromolecule model substance. These particles were cross-linked, however, these bonds were hydrolyzed in the release medium. Subsequently, the free dextran chains could absorb solvent, swell and upon a critical swelling value, rupture the PEM capsules to release a high concentration of dextran particles. By variation of PEM layering, acrylate-dextran composition and degree of cross-linking, the rupture of PEM capsules was rendered pH-responsive. Permeability to different molecular weight dextran model compounds could also be controlled due to difference in swelling capacity of the encapsulated particles [174].

Silk fibroin is a family of proteins with controllable levels of crystallinity that can be exploited to modulate the rate and extent of the release of drugs like paclitaxel and clopidogrel [175-177]. LbL with silk fibroin/gelatins alleviated burst release and facilitated tunable sustained release of trypan blue, inulin and BSA [178].

7.3 Encapsulated drugs

Chitosan, alginate, dextran sulfate and carboxymethylcellulose were used to capture ibuprofen, producing one of the first PEM drug delivery systems. The pH of the medium was optimized to prevent dissolution of ibuprofen, whilst ensuring optimum polyelectrolyte charge for assembly. Short release times were found, although the effect of the number of layers; therefore barrier thickness, on the rate of release was confirmed [44].

Furosemide microcrystals were nanoencapsulated by gelatin/PSS/PDDA multilayers. Release was prolonged by 50–300 times based on just 2 or 6 bilayers respectively which reached a

maximum thickness of ~ 155 nm, further suggesting LbL for sustained release applications [167].

Dextran, chitosan, alginate and poly(acrylic acid) as PEM colloids and vitamin E tocopherol poly(ethylene) glycol 1000 succinate as a crystal stabilizer was assembled to lower the extent naproxen release by ~ 50% compared to the uncoated crystals. A controlled zero-order release was also demonstrated for naproxen PEM capsules, achieving a release of 60–80% over 8 h [42].

Indomethacin microcrystals were coated with chitosan/alginate under various conditions. Raising the deposition temperature from 20 to 60 °C, produced thicker coats (16 or 32 nm respectively) due conformational compaction of the PEM which in turn prolonged drug release up to 2 h compared to less than 20 min for uncoated crystals [179].

Dexamethasone release was prolonged by PEMs comprising gelatin A/B layers of different thickness, combined with PSS/PDDA. Moreover, using sonication during LbL also deagglomerated and stabilized the micronized dexamethasone aggregates. Although small particles (0.5–5 μm) were obtained complete release could be prolonged to 2 h without burst release [180].

Doxorubicin was loaded into PAH/PSS capsules that were templated on sacrificial silica cores in media with low pH and low salt concentrations. Encapsulation of 90% was already achieved at pH 6.0 with even higher encapsulation at lower pH values due to lowering of electrostatic interactions between PAH/PSS with resultant higher permeability. Release of doxorubicin was subsequently also higher at low pH since doxorubicin–PSS interaction was at a minimum. Low salt ion concentrations slightly screened electrostatic interactions between colloids which therefore assumed a coiled, permeable conformation. The release t1/2 for all PEM capsules exceeded 14 h [181].

Doxorubicin and daunorubicin were loaded into carbonate cores doped with PSS. The cores were coated and upon dissolution, only the interior PSS layer remained with the assembled outer layers forming the PEM capsule. The interior PSS layer could selectively capture drug molecules in the capsule interior. Additional layering resulted in some loss of the internal PSS layer, lessening drug encapsulation. PEM capsules could however sustain drug release in a bimodal fashion by which the initial phase released 40–80% drug in the first 4 h depending on PEM composition [182].

Poorly water-soluble paclitaxel and tamoxifen aggregates were deagglomerated and stabilized as nanocolloids by sonication-assisted LbL with either PAH/PDDA as and PSS. The amine groups of surface-deposited PAH could also be covalently labeled with a tumor-specific antibody, resulting in a significant increase in target-specific drug delivery. Drug content in the carriers exceeded 85%, unprecedented by other carrier systems. Release spanned 2–10 h depending on the PEM architecture [183].

Ampicillin has a short biological half-life of < 1 h and its application could benefit from a sustained or controlled release formulation. The chitosan/alginate platform was exploited to form ampicillin-loaded beads which were then coated with the same polyelectrolytes. Cross-linking of multilayered beads with polyphosphate could sustain release of the antibiotic since only 20–30% release occurred within 24 h compared to uncoated beads that released > 70% in the first 4 h [184].

Tobramycin was assembled with dextran sulfate or PSS on a sacrificial ZnO core. Tobramycin loading in these PEM shells reached values of up to ~ 62% depending on the amount of bilayers. The release of tobramycin, using either dextran sulfate or PSS, into lachrymal fluid of rabbits attained values above the therapeutic concentration for over 6 h compared to the commercial product, which was already eliminated after 2 h. The PSS-based shells were more stable than the electrostatically-stabilized dextran sulfate shell due to hydrogen bonding of the phenyl rings of PSS could still stabilize the shells in the presence of counterions [185].

Rifampicin was encapsulated by hydrogen-bonded LbL assembly of PVP/PMA capsules on sacrificial silica template cores. Drug was preferentially encapsulated in the capsule interior and was enhanced at higher temperatures up to 40 °C. A sigmoidal release pattern was seen as function of pH with almost no release at low pH and a sudden release exceeding pH 6.8 (intestinal pH) when hydrogen-bonded layers were destabilized [186].

Ciprofloxacin was captured in PAH/PMA capsules templated on sacrificial $CaCO_3$ cores that were stabilized in PSS solution. PAH was thus the first coated layer on the anionic PSS-tagged core and a carbodiimide was used to cross-link the PEM layers for the desired duration. PSS formed the interior layer after core dissolution favoring drug encapsulation in the interior by adjustment of the medium pH to protonate ciprofloxacin. Release could be prolonged to 10 h with effective antibacterial action against E. coli still present after 25 h by which time the

unloaded control particles already showed a 900-fold increase in E. coli concentration of the inoculation dose [187].

Artemisinin, an antineoplastic drug, was encapsulated by chitosan, gelatin and alginate PEM capsules, with an encapsulation efficiency exceeding 90%. Four bilayers of gelatin/alginate lengthened the release half-life of the drug to 15 h compared to complete release for the same dose of uncoated crystals within 2.5 h. A six-layer chitosan/alginate PEM extended release to 20 h. The polymer:drug ratio for the 6-layer chitosan/alginate formulation was, remarkably efficient at 1:24. Ionic strength and type of polyelectrolyte significantly affected multilayer thickness and drug release rates [188].

A unique electrically-triggered drug delivery system was introduced for gentamicin an antibiotic with five amine groups which could be protonated at pH < pKa ~ 8.2. Prussian Blue was used as counter polyanion for gentamicin. Prussian Blue (PB), a conductive iron–cyanide complex becomes electrically neutral upon electrical current flow. Chitosan-PB layers were deposited onto a substrate, followed by PB-gentamicin layers of a desired sequence. A pulsatile release was illustrated as current flow was switched on and off, because the electrostatic interaction between PB and gentamicin was abolished. A period of controlled release was also demonstrated if current flow was maintained. One order of magnitude higher release could be shown for this triggered system compared to passive release systems [189].

7.4 Protein and peptide drug delivery

Acid-resistant, orally-administered insulin nanoparticles were produced by LbL with alginate and dextran sulfate preceding nucleation with calcium. These nucleated particles were coated with a poloxamer and stabilized with a chitosan layer before final coating with albumin. These PEM capsules released a high dose of insulin in alkaline media in the first 30 min with depletion of the vesicle in the next hour. A significant hypoglycaemic effect of 45% relative to basal plasma glucose concentration was maintained over a 24 h period for PEM nanoparticles, even though an oral bioavailability of only 13% could be illustrated. A subcutaneous insulin injection achieved a rapid, hypoglycaemic effect that dissipated relatively quickly. Conversely, the PEM system showed a sustained, clinically-relevant effect that could potentially prove more effective by avoidance of regular injections [190].

Insulin was encapsulated by consecutive layering of either Fe3+ or protamine as outerlayers onto dextran sulfate to produce gastric acid-resistant particles in the range of 2–3 μm. Loads of ~ 46% and encapsulation efficiency of ~ 70% could be achieved. PEM particles with just four bilayers produced a significant hypoglycaemic effect in test animals reaching 6 h, which was extended to 12 h by assembly of 10 bilayers, to only 2 h achieved with uncoated oral insulin [191].

Insulin was assembled with alginate by hydrogen bonding to construct PEM capsules around hydrocortisone cores. Immunosuppressive glucocorticoids commonly cause hyperglycemia; however, by release of insulin as a one of the PEM constituents, it could potentially control this side-effect. The exposure of the capsule to a phosphate buffered solution at pH 7.4 (0.01 M) slowly abolished the insulin–alginate hydrogen bonding interaction to slowly release insulin in addition to hydrocortisone. Insulin secondary structure was not affected during LbL, therefore holding great promise for in vivo applications [192].

Growth-promoting factors such as brain-derived neurotrophic factor (BDNF) are used to promote axonal regeneration for potential treatment of nerve tissue injuries. Biocompatible agarose scaffolds are mostly used to guide the growth of new axons. By employment of a protein model similar to BDNF i.e. lysozyme, hydrogen-bonded PAA/PEG/lysozyme PEMs were deposited onto agarose scaffolds. The exposure of proteins to harsh solvents normally used for simultaneous templating and drug loading of agarose scaffolds was thus avoided. Gradual degradation of the hydrogen-bonded film, released active protein over the period of one month. The PEM prevented detrimental contact between the agarose scaffold and growing neuronal cells illustrating a useful application of LbL in nerve regeneration promoted by delivery of therapeutic agents [193].

Glucose oxidase oxidizes glucose to produce gluconic acid and hydrogen peroxide. In turn, hydrogen peroxide can be converted to oxygen and water by catalase and this enzymatic synergy would, therefore, favor the constant oxidation of available glucose. Insulin was encapsulated in PEMs of glucose oxidase/catalase that were cross-linked to different extents. Exposure of these capsules to glucose activated the enzyme cascade, producing gluconic acid (and hydrogen peroxide) that lowered the pH in the PEM shell environment. Subsequent hydrolysis of the cross-linked bonds enhanced permeability and released insulin attaining 40% after 3 h incubation in

glucose solution before leveling off. Virtually no insulin was released in glucose-free control medium [194].

DNA vaccination results in the presentation of specific antigens on antigen-presenting cells i.e. dendritic cells that can then recognize foreign antibodies to trigger an immune response. PEM vaccine particles were prepared by LbL of a hydrolysable poly(ß-amino ester) and plasmid DNA (pDNA) onto poly(styrene) template cores. By changing the PEM outer layer from poly(ß-amino ester) to linear PEI, the particles were transported to the same extent into macrophages, however with PEI it seemed that the pDNA was also transported to the cytosol. Approximately 80% of the pDNA was released in the first 12 h whereas the remaining load was released over the next 60 h [195]. As illustrated for pDNA/poly(ß-aminoester) systems, the delivery is also physiologically relevant since the poly(ß-amino ester) can readily hydrolyse at pH ~ 7.0 at 37 °C [196].

A transdermal vaccination system was illustrated by an LbL construction of a poly(ß-amino ester) and/or the model protein antigen, ovalbumin (OVA) and the immunostimulatory DNA oligonucleotide, CpG. These films were coated onto a dermal delivery patch at an optimized pH of 6.0 and dried. Upon application of the films to stripped skin surface, the films rehydrated (pH ~ 7.4), resulting in disassembly of the hydrogen-bonded films with release of the active agents to be taken up by skin dendritic cells for antigen presentation and subsequent vaccination. Release could be extended from one to several days depending on the PEM compositions. The largest amount of OVA release takes place during the first 24 h and a maximum release period of 3 days could be achieved. CpG release was more gradual and could still be seen after 7 days [197].

7.5 Loaded object-based LbL drug delivery devices

Porous $CaCO_3$ microparticles were prepared by colloidal agglomeration and stabilized with PSS preceding loading of the cores in different solvents with ibuprofen. The washed, loaded cores were then layered with protamine sulfate/PSS. Depending on pH, layer composition and loading conditions, the bilayers could delay the release of ibuprofen; doubling the total release time from 220 to 420 min. The prolonged release was seen despite the fact that ibuprofen was now present in an amorphous, more soluble form compared to the crystalline uncoated particles [198].

The lumens of halloysite nanotubes were partially loaded with dexamethasone using an evacuation technique, yielding loads of approximately 7%. Loaded tubes were subsequently layered with PEI/PAH and other polyelectrolytes of various molecular weight. Coated tubes

produced superior release retardation compared to uncoated tubes, with medium to very high molecular weight polyelectrolytes showing 25–40% and uncoated tubes demonstrating 80% release over a 6 h period [199].

Mesoporous silica spheres were coated with PAH and PSS to produce PEM capsules for gentamicin. Drug loading was performed at pH 2.0 by incubation for a set period of followed by precipitation in the capsule interior at pH 8.0 due to a marked reduction in permeability of the PEM wall at pH 8.0. pH-triggered release was seen in low pH with 70% release over 12 h with capsule depletion at 30 h. Virtually no release in higher pH media was found due to low permeability of the PEM wall [200].

A carboxy-ß-cyclodextrin-analog (cCD) was utilized to host the anti-inflammatory drug piroxicam and then LbL coated with poly(l-glutamic acid) (PGA) and poly(l-lysine) (PLL). The poorly water-soluble piroxicam could be solubilised in high amounts in the cCD, however the release of piroxicam, as judged from the duration of suppression of inflammatory modulator expression, was markedly influenced by the PEM architecture [201].

The antitumor drug, risedronate, was complexed into a hybrid polyelectrolyte derivative of PLL that was grafted with a ß-cyclodextrin (ß-CD) to host the drug. The PLL-ß-CD polycation was then assembled with the PGA onto bone implants. These drug-loaded systems resulted in a 70% higher antitumor effect compared to unloaded complexes (that was slightly active due to cell penetration of ß-CD moieties). Additionally, the tumors seen with complexed drug were 60% smaller than for pure drug or placebo as monitored over an 18-day period. The loaded complexes also attained a drug concentration that was 2.3-fold larger than the minimum curative concentration over a period of 7 days [202].

A hybrid electrostatic PEM system was fabricated for the antibacterial substance, triclosan. A linear hydrophobic polymer, poly(propylene oxide) (PPO), was functionalized on both its terminals with generation 4.0 PAMAM dendrimers to provide a hydrophilic, ionizable amine-terminated corona. The PPO-PAMAM block copolymers formed micelles in water and the hydrophobic core encapsulated triclosan, whilst the outer polycationic corona could be coated by PAA to produce a delivery system containing ~ 35% triclosan. The release of triclosan significantly sustained with a release t1/2 of 77 h and a total release of 20 days, with efficient inhibition against *S. aureus*. Drug-free films produced no antibacterial effect [203].

Triclosan was captured in micelles based on biodegradable poly(ethylene oxide)-poly(ε-caprolactone) block copolymers (hydrogen bond acceptor) and assembled with PAA as hydrogen bond donor. The films were assembled at pH < 3.0 and disassembled at pH 7.4 to release the drug-loaded micelles. By cross-linking, the release of the micelles from the films could be controlled. Ultimately, cross-linked films achieved a maximum sustained release of 13 days compared to normally coated particles which showed only 90 min release. All the loaded systems proved effective against *S. aureus* [204] and again advocated the use of hydrogen bond assembled films for drug release under mild pH conditions, temperature-responsive systems under physiologically-relevant temperature as with polymers with low glass transition temperatures [205,206].

A number of studies have also reported the LbL coating of liposomes with PLL, PGA and hyaluronic acid to control the release of Ag+ ions with antibacterial action against E. coli [207] and control the release of fluorescent dyes from coated liposomes [208].

Ellagic acid, an antineoplastic phenolic compound, was captured in soybean lecithin liposomes and subsequently coated with chitosan/dextran sulfate. Loading reached 64% and encapsulation efficiency achieved 43%. Approximately 20% of the load was released during the first day from uncoated liposomes with slightly lower release for coated liposomes. By the third day uncoated formulations showed 50%, the two bilayer-liposomes ~ 30% and the four bilayer-liposomes ~ 20% release. From the third day onwards, prolonged release was seen with the uncoated liposomes showing > 80% cumulative release at 15 days, the two bilayer-liposomes achieved ~ 40% and the four bilayer-liposomes ~ 25% cumulative release. Temperature increases enhanced release for all liposomes, however the coated liposomes showed > 20% less release than uncoated carriers. An increase in pH from 3.0 to 7.0, with less destabilization of polyelectrolyte charge, reduced release for all liposomes, with coated carriers releasing less than uncoated liposomes [209].

7.6 Targeted delivery

Some of the most useful platforms to label the surface of LbL assembled carriers exploit specific interactions between (1) sugars and lectins such as concanavalin A to sensitize surfaces to sugars expressed on cell surfaces [210,211], (2) biotin and avidin for multilayering of specific antibodies [212] or sensitizing the surface to biotin-conjugates by deposition of an outer layer

containing avidin [213,214] and (3) labeling with virus proteins to fuse the carrier content with cells [215].

Folic acid labeling is commonly used against cancer tissues, overexpressing folate receptors compared to normal tissues. PLGA nanoparticles that were first coated with chitosan and alginate preceding covalent labeling with folic acid or PEG-modified folic acid illustrated tumor selectivity. The particles that were LbL coated, but not tagged with folic acid, showed virtually no uptake with the folate receptor expressing cell lines [50].

LbL carriers coated with A33 monoclonal antibody, could be successfully targeted to colorectal cancer tumors of which ~ 95% present the A33 antigen. The carrier particles were templated on sacrificial poly(styrene) cores of various sizes and comprised PSS, PAH, PEI and PAA among others. PEG-only terminated particles could avert the binding of antibody-free carriers to the antigen. However, the antibody-coated capsules were successfully targeted and delivered even when PEG was coated on top of the antibody [216].

Liver parenchymal cells were also successfully targeted. These cells express asialoglycoprotein receptors presenting lectins, proteins that recognize monosaccharides such as d-galactose [217]. Propranolol was loaded into $CaCO_3$-templated PEM capsules comprising PSS and a novel synthetic galactose-functionalized copolymer polycation. Loading was achieved selectively in the capsule interior due to good interaction between propranolol and the polycation. The galactose-labeled polycation illustrated excellent lectin affinity, implying potential liver targeting delivery systems [218].

Targeted gene delivery was successfully performed by coating biodegradable poly(d,l-lactic acid) films (as gene carrier). Poly(ethyleneimine), another commonly used gene vector, was modified to bear galactose moieties to target liver cell asialoglycoprotein receptors. A model plasmid DNA (pDNA) molecule served as the counter polyelectrolyte whilst also serving as a reporter gene. When the coated poly(lactic acid) particles attached to galactose recognizing cell lines, they were internalized and subsequently also released the pDNA in the surface layer. This pDNA, upon translation, resulted in heightened expression of β-galactodidase to produce a metabolite, o-nitrophenol which could be monitored to confirm LbL carrier delivery. Cell lines that are impervious to galactose did not report this increase in metabolism, implicating this system for targeted gene transfection as a therapeutic system [217].

7.7 Future outlook on LbL in drug delivery

The first ten years of LbL self-assembly laid the physicochemical foundation for the manufacturing of LbL constructs and the characterization thereof. During this period, different substances were also loaded into and released from these carriers dependent on PEM architecture and stimuli i.e. temperature, pH and changes in ion concentration.

Since the turn of the millennium, LbL drug delivery systems have been developed. The robust nature of the self-assembly process, the high encapsulation efficiency, targetability and biocompatibility of PEM drug delivery holds great potential controlled and targeted release of drugs and genes.

In future we can anticipate that the array of colloids utilized in LbL assembly will become more sophisticated due to improvements in organic and polymer synthesis. Polyelectrolytes might assume hybrid forms through functionalization of monomers with drug, gene or nucleic acid and other moieties preceding polymerization. These hybrid colloids will perform simultaneous roles as structural constituents, drug carriers/prodrugs and stimuli-sensitive release triggers. LbL stabilization will also to a larger extent to improve otherwise troublesome, unstable carriers such as liposomes or micelles.

PEM or colloidal shells will show more specific stimuli-responsiveness as was already shown for glucose-specific enzyme multilayer systems. It can be imagined that LbL reservoirs, containing therapeutic agents, could be implanted in patients with a genetic predisposition to a detrimental conditions. As soon as disease markers are encountered by these implanted LbL capsules, a therapeutic agent is released. Intense multidisciplinary cooperation is needed to develop these sensor mechanisms for specifically-triggered release.

The development of multi-agent delivery vaccines are also on the rise. These vaccines can be made very specific with LbL vesicles providing adequate storage and protection until activation is needed. Differently loaded LbL carriers could perhaps be included in a larger carrier and depending on the stimulus; reactants could be released from smaller entrapped vesicles that trigger the release of different agents from the larger carrier. Alternatively, a selectively permeable large carrier would control the exposure of encapsulated smaller vesicles to these triggers before releasing of therapeutic agents that diffuse through the PEM.

Long-term treatment with biodegradable PEM implants for low therapeutic index drugs i.e. corticosteroids or anti-cancer drugs could be useful in treatment of tumors. These implants could be situated close to/in the tumor, ensuring long-term sustained release of the drug. The same principle could probably be applied to deliver genes/DNA fragments to patients with metabolic defects to ensure long-term treatment.

Negative feedback release drug delivery systems with retained sensitivity and release potential should also be realized soon. A sensor system should, therefore be developed to stimulate, but also turn off, the release of therapeutic agent. Temperature and pH changes can already result in such releases based on conformational changes in certain polyelectrolytes; however sensors to specific disease markers or metabolites need to be developed.

Exotic targeting proligands could also be developed that will only on encountering certain signaling markers/enzymes be converted to the active ligand. These LbL particles could be administered without the release of drug, until the targeting proligand is activated, recognized by the target receptor and taken up into the cell with subsequent release.

Additionally, LbL delivery systems will become subject to clinical trials and especially pharmacokinetic and toxicological evaluations of these delivery systems will be seen. These tests will not only determine the safety of the therapeutic agent, but also study elimination of the actual carrier systems from the body.

LbL self-assembly systems therefore provide a very robust platform to create novel, hybrid or stabilized drug delivery systems for a myriad drugs and genes can be employed on various nano- to macroscopically-sized systems. Due to its technological ease and cost of preparation, avoidance of hazardous preparative chemicals, independence of precise stoichiometry, facilitation of controlled, triggered and target release, the technique should see significant growth in future as a leading drug delivery technology. Fig. 4 shows some of the applications of LbL drug delivery systems.

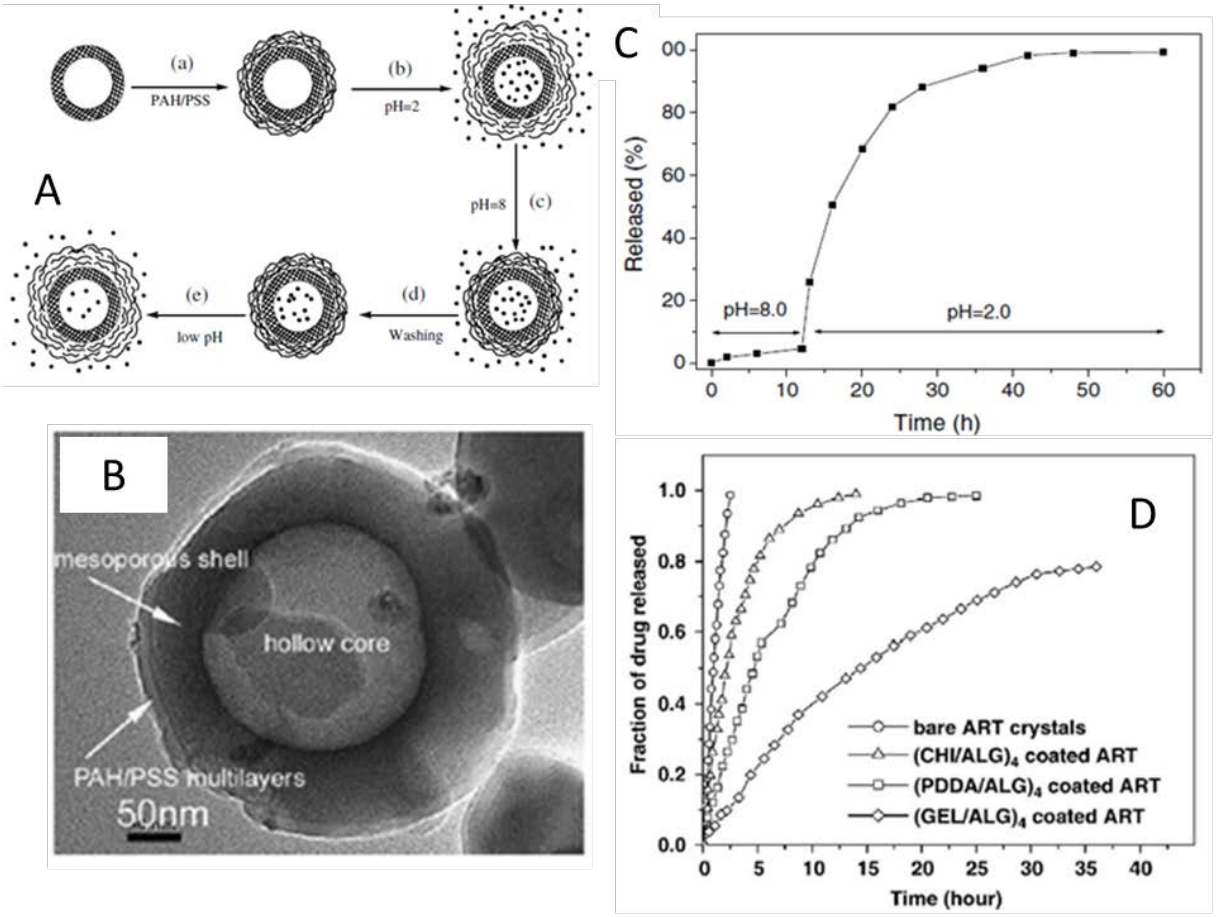

Fig 4. A schematic of (A) the LbL coating of silica cores with PSS/PAH and loading with gentamicin to produce (B) gentamicin PEM nanocapsules with (C) pH-dependent, prolonged release [203]. (D) The effect of different PEM architectures and number of bilayers on artemisinin sustained release [191].

8. Conclusions

The evolvement and simplicity of LbL construction provided a simple, robust platform, independent of precise stoichiometry, for the modification of material surfaces or the encapsulation of various substrates. The technique facilitated a ‘library’ approach to create novel carrier systems, especially in the field of drug delivery. A myriad of colloids can be used to create novel hybrid-coated materials by use of different intermolecular forces.

Multifunctionality of LbL systems can be introduced by the inclusion of different materials in the multilayers i.e. polyelectrolytes, metal oxides, clay nanoobjects and enzymes all of which could be rendered stimuli-responsive. Ultimately, the surface of these constructs can be labeled with

targeting molecules and reagents, enabling targeted and triggered delivery of the encapsulated substances or the activation of catalytic reactions under suitable conditions.

A sound knowledge of the historical evolution of LbL as well as the physicochemical basis which first characterized these systems was transferred to the field of drug delivery. This resulted in the development of some novel, highly efficient drug delivery systems and the foundation on which even more sophisticated delivery systems will be based in the near future.

9. References

[1] B. Franklin, W. Brownrigg, Farish, Of the stilling of waves by means of oil. Extracted from sundry letters between Benjamin Franklin, L.L.D. F.R.S. William Brownrigg, M.D. F.R.S. and the Reverend Mr. Farish, Philos. Trans. R. Soc. Lond. A 64 (1774) 445–460.

[2] L. Rayleigh, Measurement of the amount of oil necessary in the order to check the motions of camphor upon water, Proc. R. Soc. Lond. (1890) 364–367.

[3] A. Pockels, Surface tension, Nature (London) 43 (1891) 437–439.

[4] L. Rayleigh, XXXVI. Investigations in capillarity: the size of drops. The liberation of gas from supersaturated solutions. Colliding jets. The tension of contaminated water surfaces, Philos. Mag. 48 (1899) 321–337.

[5] I. Langmuir, The constitution and fundamental properties of solids and liquids. II. Liquid, J. Am. Chem. Soc. 39 (1917) 1848–1906.

[6] I. Langmuir, The mechanism of the surface phenomena of flotation, Trans. Faraday Soc. 15 (1920) 62–74.

[7] N.K. Adam, The properties and molecular structure of thin films of palmitic acid on water. Part I, Proc. R. Soc. Lond. A Math. Phys. Sci. 99 (1921) 336–351.

[8] K.B. Blodgett, Films built by depositing successive monomolecular layers on a solid surface, J. Am. Chem. Soc. 57 (1935) 1007–1022.

[9] I. Langmuir, V.J. Schaeffer, Activities of urease and pepsin monolayers, J. Am. Chem. Soc. 60 (1938) 1351–1360.

[10] K.B. Blodgett, I. Langmuir, Built-up films of barium stearate and their optical properties, Phys. Rev. 51 (1937) 964–982.

[11] J.A. Zasadzinski, R. Viswanathan, L. Madsen, J. Garnaes, D.K. Schwartz, Langmuir-Blodgett Films, Science 263 (1994) 1726–1733.

[12] H. Kuhn, Interaction of chromophores in monolayer assemblies, Pure Appl.Chem. 27 (1971) 421–438.

[13] H. Kuhn, D. Möbius, Systems of monomolecular layers—assembling and physicochemical behavior, Angew. Chem. Int. Ed. 10 (1971) 620–637.

[14] R.K. Iler, Multilayers of colloidal particles, J. Colloid Interface Sci. 21 (1966) 569–594.

[15] Y.F. Nicolau, Deposition of thin solid compound films by a successive ionic-layer adsorption and reaction process, Appl. Surf. Sci. 22–23 (1985) 1061–1074.

[16] Y.F. Nicolau, J.C. Menard, Solution growth of ZnS, CdS and Zn1−xCdxS thin films by the successive ionic-layer adsorption and reaction process, growth mechanism, J. Cryst. Growth 91 (1988) 128–142.

[17] Y.F. Nicolau, M. Nechtschein, Electronic Properties of Conjugated Polymers III, Springer, Heidelberg, 1989, p. 461.

[18] Y.F. Nicolau, S. Davied, F. Genoud, M. Nechtshein, J.P. Travers, Polyaniline, polypyrrole, poly(3-methylthiophene) and polybitiophene layer-by-layer deposited thin films, Synth. Met. 42 (1991) 1491–1494.

[19] G. Decher, J.D.Hong, J. Scmitt, Buildup of ultrathinmultilayer films by self-assembly process: III. Consecutively alternating adsorption of anionic and cationic polyelectrolytes on charged surfaces, Thin Solid Films 210/211 (1992) 831–835.

[20] B. Lehr, M. Seufert, G.Wenz, G. Decher, Fabrication of poly(p-phenylene vinylene) (PPV) nanoheterocomposite films via layer-by-layer adsorption, Supramol. Sci. 2 (1995) 199–207.

[21] Y. Lvov, G. Decher, H. Haas, H. Möhwald, A. Kalachev, X-ray analysis of ultrathin polymer films self-assembled onto substrates, Physics B (Amsterdam, Neth.) 198 (1994) 89–91.

[22] Y. Lvov, K. Ariga, I. Ichinose, T. Kunitake, Assembly of multicomponent protein films by means of electrostatic layer-by-layer adsorption, J. Am. Chem. Soc. 117 (1995) 6117–6123.

[23] G.B. Sukhorukov, H. Möhwald, G. Decher, Y.M. Lvov, Assembly of polyelectrolyte films by consecutively alternating adsorption of polynucleotides and polycations, Thin Solid Films 284–285 (1996) 220–223.

[24] W.B. Stockton, M.F. Rubner, Molecular-level processing of conjugated polymers. 4. Layer-by-layer manipulation of polyaniline via hydrogen-bonding interactions, Macromolecules 30 (1997) 2717–2725.

[25] L. Wang, Z. Wang, X. Zhang, J. Shen, L. Chi, H. Fuchs, A new approach for the fabrication of an alternating multilayer film of poly(4-vinylpyridine) and poly (acrylic acid) based on hydrogen bonding, Macromol. Rapid Commun. 18 (1997) 509–514.

[26] E. Hao, T. Lian, Buildup of polymer/Au nanoparticle multilayer thin films based on hydrogen bonding, Chem. Mater. 12 (2000) 3392–3396.

[27] L. Wang, Y. Fu, Z. Wang, Y. Fan, X. Zhang, Investigation into an alternating multilayer film of poly(4-vinylpyridine) and poly(acrylic acid) based on hydrogen, Langmuir 15 (1999) 1360–1363.

[28] P. Kohli, G.J. Blanchard, Applying polymer chemistry to interfaces: layer-by-layer and spontaneous growth of covalently bound multilayers, Langmuir 16 (2000) 4655–4661.

[29] T. Serizawa, K. Nanameki, K. Yamamoto, M. Akashi, Thermoresponsive ultrathin hydrogels prepared by sequential chemical reactions, Macromolecules 35 (2002) 2184–2189.

[30] H.C. Kolb, M.G. Finn, K.B. Sharpless, Click chemistry: diverse chemical function from a few good reactions, Angew. Chem. Int. Ed. 40 (2001) 2004–2021.

[31] G.B. Sukhorukov, H. Möhwald, Multifunctional cargo systems for biotechnology, Trends Biotechnol. 25 (2007) 93–98.

[32] L.E. van Vlerken, M.M. Amiji, Multi-functional polymeric nanoparticles for tumour-targeted drug delivery, Expert Opin. Drug Deliv. 3 (2006) 205–216.

[33] K.J. Loh, J. Kim, J.P. Lynch, N.W.S. Kam, N.A. Kotov, Multifunctional layer-by-layer carbon nanotube-polyelectrolyte thin films for strain and corrosion sensing, Smart Mater. Struct. 16 (2007) 429–438.

[34] B.G. de Geest, A.G. Skirtach, T.R.M. de Beer, G.B. Sukhorukov, L. Bracke, W.R.G. Baeyens, J. Demeester, S.C. de Smedt, Stimuli-responsive multilayered hybrid nanoparticles/polyelectrolyte capsules, Macromol. Rapid Commun. 28 (2007) 88–95.

[35] Z. Dai, A. Voigt, E. Donath, H. Möhwald, Novel encapsulated functional dye particles based on alternately adsorbed multilayers of active oppositely charged macromolecular species, Macromol. Rapid Commun. 22 (2001) 756–762.

[36] X. Wang, J. Fang, D. Wang, W. Zheng, Multilayer films consisted of azulene-based dye molecules and polyelectrolyte: preparation, characterization and photoluminescent property, Thin Solid Films. 517 (2009) 6497–6501.

[37] I. Galeska, T. Hickey, F. Moussy, D. Kreutzer, F. Papadimitrakopoulus, Characterization and biocompatibility studies of novel humic acids based films as membrane materials for an implantable glucose sensor, Biomacromolecules 2 (2001) 1249–1255.

[38] K.V. Gobi, F. Mizutani, Layer-by-layer construction of an active multilayer enzyme electrode applicable for direct amperometric determination of cholesterol, Sens. Actuators B 80 (2001) 272–277.

[39] D. Lee, T. Cui, Low-cost, transparent, and flexible single-walled carbon nanotube nanocomposite based ion-sensitive field-effect transistors for pH/glucose sensing, Biosens. Bioelectron. 25 (2010) 2259–2264.

[40] S.V. Rao, K.W. Anderson, L.G. Bachas, Controlled layer-by-layer immobilization of horseradish peroxidase, Biotechnol. Bioeng. 65 (1999) 389–396.

[41] C. Gao, X. Liu, J. Shen, H. Möhwald, Spontaneous deposition of horseradish peroxidise into polyelectrolyte multilayer capsules to improve its activity and stability, Chem. Commun. 17 (2002) 1928–1929.

[42] D.B. Shenoy, G.B. Sukhorukov, Engineered microcrystals for direct surface modification with layer-by-layer technique for optimized dissolution, Eur. J. Pharm. Biopharm. 58 (2004) 521–527.

[43] A.S. Zahr, M. de Villiers, M.V. Pishko, Encapsulation of drug nanoparticles in selfassembled macromolecular nanoshells, Langmuir 21 (2005) 403–410.

[44] X. Qiu, S. Leporatti, E. Dontah, Möhwald, Studies on the drug release properties of polysaccharide multilayers encapsulated inbuprofen microparticles, Langmuir (17) (2001) 5375–5380.

[45] K. Wood, H.F. Chuang, R.D. Batten, D.M. Lynn, P.T. Hammond, Controlling interlayer diffusion to achieve sustained multiagent delivery from layer-by-layer thin films, Proc. Natl. Acad. Sci. U. S. A. 103 (2006) 10207–10212.

[46] N.G. Veerabadran, P.L. Goli, S.S. Stewart-Clark, Y.M. Lvov, D.K. Mills, Nanoencapsulation of stem cells within polyelectrolyte multilayer shells, Macromol. Biosci. 7 (2007) 877–882.

[47] Y. Teramura, Y. Kaneda, H. Iwata, Islet-encapsulation in ultra-thin layer-by-layer membranes of poly(vinyl alcohol) anchored to poly(ethylene glycol)-lipids in the cell membrane, Biomaterials 28 (2007) 4818–4825.

[48] J. Zhou, G. Romero, E. Rojas, L.Ma, S.Moya, C. Gao, Layer by layer chitosan/alginate coatings on poly(lactide-co-glycolide) nanoparticles for antifouling protection and folic acid binding to achieve selective cell targeting, J. Colloid Interface Sci. 345 (2010) 241–247.

[49] K. Sato, Y. Imoto, J. Sugama, S. Seki, H. Inoue, T. Odagiri, T. Hoshi, J. Anzai, Sugar induced disintegration of layer-by-layer assemblies composed of concanavalin A and glycogen, Langmuir 21 (2005) 797–799.

[50] T. Hoshi, S. Akase, J. Anzai, Preparation of multilayer thin films containing avidin through sugar–lectin interactions and their binding properties, Langmuir 18 (2000) 7024–7028.

[51] A.S. Angelatos, B. Radt, F. Caruso, Light-responsive polyelectrolyte/gold nanoparticle microcapsules, J. Phys. Chem. B 109 (2005) 3071–3076.

[52] W. Chen, T.J. McCarthy, Layer-by-layer deposition: a tool for polymer surface modification, Macromolecules 30 (1997) 78–86.

[53] G. Decher, Fuzzy nanoassemblies: toward layered polymeric multicomposites, Science 277 (1997) 1232–1237.

[54] Y. Lvov, G. Decher, H. Möhwald, Assembly, structural characterization, and thermal behavior of layer-by-layer deposited ultrathin film of poly(vinyl sulfate) and poly(allylamine), Langmuir 9 (1993).

[55] S.L. Clark, P.T. Hammond, The role of secondary interactions in selective electrostatic multilayer deposition, Langmuir 16 (2000) 10206–10214.

[56] Y. Fu, S. Bai, S. Cui, D. Qiu, Z. Wang, X. Zhang, Hydrogen-bonding-directed layer-by-layer multilayer assembly: reconformation yielding microporous films, Macromolecules 35 (2002) 9451–9458.

[57] E. Kharlampieva, V. Kozlovskya, J. Tyutina, S.A. Sukhishvili, Hydrogen-bonded multilayers of thermoresponsive polymers, Macromolecules 38 (2005) 10523–10531.

[58] N.A. Kotov, Layer-by-layer self-assembly: the contribution of hydrophobic interactions, Nanostruct. Mater. 12 (1999) 789–796.

[59] M. Sano, A. Kamino, J. Okamura, S. Shinkai, Noncovalent self-assembly of carbon nanotubes for construction of “cages”, Nano Lett. 2 (2002) 531–533.

[60] M. Sato, M. Sano, van der Waals layer-by-layer construction of a carbon nanotube 2D network, Langmuir 21 (2005) 11490–11494.

[61] P.T. Hammond, Recent explorations in electrostatic multilayer thin film assembly, Curr. Opin. Colloid Interface Sci. 4 (2000) 430–442.

[62] Y. Lvov, K. Ariga, M. Onda, I. Ichinose, T. Kunitake, A careful examination of the adsorption step in the alternate layer-by-layer assembly of linear polyanion and polycation, Colloids Surf. A 146 (1999) 337–346.

[63] G. Bantchev, Z. Lu, Y. Lvov, Layer-by-layer nanoshell assembly on colloids through simplified washless process, J. Nanosci. Nanotechnol. 9 (2009) 396–403.

[64] C.J. Ochs, G.K. Such, Y. Yan, M.P. van Koeverden, F. Caruso, Biodegradable click capsules with engineered drug-loadedmultilayers, ACS Nano 4 (2010) 1653–1663.

[65] C.R. Kinnane, G.K. Such, G. Antequera-García, Y. Yan, S.J. Dodds, L.M. Liz-Marzan, F. Caruso, Low-fouling poly(N-vinyl pyrrolidone) capsules with engineered degradable properties, Biomacromolecules 10 (2009) 2839–2846.

[66] K. Ariga, Y. Lvov, T. Kunitake, Assembling alternate dye-polyion molecular films by electrostatic layer-by-layer adsorption, J. Am. Chem. Soc. 119 (1997) 2224–2231.

[67] D.M. Lynn, Layes of opportunity: nanostructured polymer assemblies for the delivery of macromolecular therapeutics, Soft Matter. 2 (2006) 269–273.

[68] A. Ulman, An Introduction to Ultrathin Films, from Langmuir–Blodgett to Self-Assembly, Academic Press, Boston, 1991, pp. 1–440.

[69] P. Bertrand, A. Jonas, A. Laschewsky, R. Legras, Ultrathin polymer coatings by complexation of polyelectrolytes at interfaces: suitable materials, structure and properties, Macromol. Rapid Commun. 21 (2000) 319–348.

[70] A.L. Becker, A.P.R. Johnston, F. Caruso, Peptide nucleic acid films and capsules: assembly and enzymatic degradation, Macromol. Biosci. 10 (2010) 488–495.

[71] A.P.R. Johnston, E.S. Read, F. Caruso, DNA multilayer films on planar and colloidal supports: sequential assembly of like-charged polyelectrolytes, Nano Lett. 5 (2005) 953–956.

[72] K. Cai, A. Rechtenbach, J. Hao, J. Bossert, K.D. Jandt, Polysaccharide-protein surface modification of titanium via a layer-by-layer technique: characterization and cell behaviour aspects, Biomaterials 26 (2005) 5960–5971.

[73] R. Dhamodharan, T.J. McCarthy, Adsorption of alginic acid and chondroitin sulfate-A to amine functionality introduced on polychlorotrifluoroethylene and glass surfaces, Macromolecules 32 (1999) 4106–4112.

[74] G. Decher, B. Lehr, K. Lowack, Y. Lvov, J. Schmitt, New nanocomposite films for biosensors: layer-by-layer adsorbed films of polyelectrolytes, proteins or DNA, Biosens. Bioelectron. 9 (1994) 677–684.

[75] A. Voigt, H. Lichtenfeld, G.B. Sukhorukov, H. Zastrow, E. Donath, H. Bäumler, H. Möhwald, Membrane filtration for microencapsulation and microcapsules fabrication by layer-by-layer polyelectrolyte adsorption, Ind. Eng. Chem. Res. 38 (1999) 4037–4043.

[76] F. Caruso, D.G. Kurth, D. Volkmer, M.J. Koop, A. Müller, Ultrathin molybdenum polyoxometalate–polyelectrolyte multilayer films, Langmuir 14 (1998) 3462–3465.

[77] F. Caruso, H. Möhwald, Preparation and characterization of ordered nanoparticle and polymer composite multilayers on colloids, Langmuir 15 (1999) 8276–8281.

[78] D. Cochin, M. Passmann, G. Wilbert, R. Zentel, E. Wischerhoff, A. Laschewsky, Layered nanostructures with LC-polymers, polyelectrolytes, and inorganics, Macromolecules 30 (1997) 4775–4779.

[79] B. vanDuffel, R.A. Schoonheydt, C.P.M.Grim, F.C.De Schryver,Multilayered clay films: atomic force microscopy study and modeling, Langmuir 15 (1999) 7520–7529.

[80] S. Watanabe, S.L. Regen, Dendrimers as building blocks for multilayer construction, J. Am. Chem. Soc. 116 (1994) 8855–8856.

[81] W. Tsukruk, F. Rindespacher, V.N. Bliznyuk, Self-assembled multilayer films from dendrimers, Langmuir 241 (1997) 2171–2176.

[82] S.A. Shukhsvili, Responsive polymer films and capsules via layer-by-layer assembly, Curr. Opin. Colloid Interface Sci. 10 (2005) 37–44.

[83] A.A. Antopov, G.B. Sukhorukov, Polyelectrolyte multilayer capsules with tunable permeability, Adv. Colloid Interface Sci. 111 (SI) (2004) 49–61.

[84] F. Caruso, W. Yang, D. Trau, R. Renneberg, Microencapsulation of uncharged low molecular weight organic materials by polyelectrolyte multilayer self-assembly, Langmuir 16 (2000) 8932–8936.

[85] A.J. Nolte, J.Y. Chung, M.L. Walker, C.M. Stafford, In situ adhesion measurements utilizing layer-by-layer functionalized surfaces, ACS Appl. Mater. Interfaces. 1 (2009) 373–380.

[86] A.J. Nolte, N. Takane, E. Hindman, W. Gaynor, M.F. Rubner, R.E. Cohen, Thin film thickness gradients and spatial patterning via salt etching of polyelectrolyte multilayers, Macromolecules 40 (2007) 5479–5486.

[87] H. Gong, J. Garcia-Turiel, K. Vasilev, O.I. Vinogradova, Interaction and adhesion properties of polyelectrolyte multilayers, Langmuir 21 (2005) 7545–7550.

[88] S.M. Notley, M. Eriksson, L. Wårberg, Visco-and adhesive properties of adsorbed polyelectrolyte multilayers determined in situ with QCM-D and AFM measurements, J. Colloid Interface Sci. 292 (2005) 29–37.

[89] M. Sano, Y. Lvov, T. Kunitake, Formation of ultrathin polymer layers on solid substrates by means of polymerization-induced epitaxy and alternate adsorption, Ann. Rev. Mater. Sci. 26 (1996) 153–187.

[90] T. Okubo, M. Suda, Absorption of polyelectrolytes on colloidal surfaces as studied by electrophoretic and dynamic light-scattering techniques, J. Colloid Interface Sci. 213 (1999) 565–571.

[91] D.L. Elbert, C.B.Herbert, J.A.Hubbell, Thin polymer layers formed by polyelectrolyte multilayer techniques on biological surfaces, Langmuir 15 (1999) 5355–5362.

[92] A. Szarpak, I. Pignot-Paintrand, C. Nicolas, C. Picart, R. Auzély-Velty, Multilayer assembly of hyaloronic acid/poly(allylamine): control of the buildup for the production of multilayer capsules, Langmuir 24 (2008) 9767–9774.

[93] N.G. Hoogeveen, M.A. Cohen Stuart, G.J. Fleer, Formation and stability of multilayers of polyelectrolytes, Langmuir 12 (1996) 3675–3681.

[94] M.R. Linford, M. Auch, H. Möhwald, Nonmonotonic effect of ionic strength on surface dye extraction during dye–polyelectrolyte multilayer formation, J. Am. Chem. Soc. 120 (1998) 178–182.

[95] D. Cochin, A. Laschewsky, Layer-by-layer self-assembly of hydrophobically modified polyelectrolytes, Macromol. Chem. Phys. 200 (1999) 609–615.

[96] A. Izquierdo, S.S. Ono, J.C. Voegel, P. Schaaf, G. Decher, Dipping versus spraying: exploring the deposition conditions for speeding up layer-by-layer assembly, Langmuir 21 (2005) 7558–7567.

[97] H.S. Silva, T.M. Uehara, K. Bergamaski, P.B. Miranda, Molecular ordering in layer-by-layer polyelectrolyte films studied by sum-frequency vibrational spectroscopy: the effects of drying process, J. Nanosci. Nanotechnol. 8 (2008) 3399–3405.

[98] B. Schwarz, M. Schönhoff, Surface potential driven swelling of polyelectrolyte multilayers, Langmuir 18 (2002) 2964–2966.

[99] M. Raposo, R.S. Pontes, L.H.C. Mattoso, O.N. Oliveira Jr., Kinetics of adsorption of poly(o-methoxyaniline) self-assembled films, Macromolecules 30 (1997) 6095–6101.

[100] N. Laugel, C. Betscha, M. Winterhalter, J.C. Voegel, P. Schaaf, V. Ball, Relationship between the growth regime of polyelectrolyte multilayers and the polyanion/polycation complexation enthalpy, J. Phys. Chem. B 110 (2006) 19443–19449.

[101] X. Arys, A. Jonas, B. Laguitton, R. Laschewsky, A. Wischerhoff, Structural studies on thin organic coatings built by repeated adsorption of polyelectrolytes, Prog. Org. Coat. 32 (1998) 108–118.

[102] L. Kolarik, D.N. Furlong, H. Joy, C. Struijk, R. Rowe, Building assemblies from high molecular weight polyelectrolytes, Langmuir 15 (1999) 8265–8275.

[103] E. Guzmán, H. Ritacco, J.E.F. Rubio, R.G. Rubio, F. Ortega, Salt-induced changes in the growth of polyelectrolyte layers of poly(diallyldimethylammonium chloride) and poly(4-styrene sulfonate of sodium), Soft Matter. 5 (2009) 2130–2142.

[104] S. Bharadwaj, R. Montazeri, D.T. Haynie, Direct determination of the thermodynamics of polyelectrolyte complexation and implications thereof for electrostatic layer-by-layer assembly of multilayer thin films, Langmuir 22 (2006) 6093–6101.

[105] C.C. Buron, C. Filiâtre, F. Membrey, C. Bainier, L. Buisson, D. Charraut, A. Foissy, Surface morphology and thickness of a multilayer film composed of strong and weak polyelectrolytes: effect of the number of adsorbed layers, concentration and type of salts, Thin Solid Films 517 (2009) 2611–2617.

[106] S.T. Dubas, J.B. Schlenoff, Factors controlling the growth of polyelectrolyte multilayers, Macromolecules 32 (1999) 8153–8160.

[107] H.H. Rmaile, J.B. Schlenoff, “Internal pKa's” in polyelectrolyte multilayers: coupling protons and salt, Langmuir 18 (2002) 8263–8265.

[108] H.G.M. van de Steeg, M.A.C. Stuart, A. de Keizer, B.H. Bijsterbosch, Polyelectrolyte adsorption: a subtle balance of forces, Langmuir 8 (1992) 2538–2546.

[109] L. Chang, X. Kong, F. Wang, L. Wang, J. Schen, Layer-by-layer assembly of poly(Nacryloyl-N′-propylpiperazine) and poly(acrylic acid): effect of pH and temperature, Thin Solid Films 516 (2008) 2125–2129.

[110] C. Gergely, S. Bahi, B. Szalontai, H. Flores, P. Schaaf, J.C. Voegel, F.J.G. Cuisinier, Human serum albumin self-assembly on weak polyelectrolyte multilayer films structurally modified by pH changes, Langmuir 20 (2004) 5575–5582.

[111] P. Bieker, M. Schönhoff, Linear and exponential growth regimes of multilayers of weak polyelectrolytes in dependence on pH, Macromolecules 43 (2010) 5052–5059.

[112] B. Schoeler, G. Kumaraswamy, F. Caruso, Investigation of the influence of polyelectrolyte charge density on the growth of multilayer thin films prepared by the layer-by-layer technique, Macromolecules 35 (2002) 889–897.

[113] S.S. Shiratori, M.F. Rubner, pH-dependent thickness behavior of sequentially adsorbed layers of weak polyelectrolytes, Macromolecules 33 (2000) 4213–4219.

[114] X. Tuo, D. Chen, H. Cheng, X. Wang, Fabricating water-insoluble polyelectrolyte into multilayers with layer-by-layer self-assembly, Polym. Bull. 54 (2005) 427–433.

[115] V.K. Kamineni, Y.M. Lvov, T.A. Dobbins, Layer-by-layer polyelectrolytes using formamide as the working medium, Langmuir 23 (2007) 7423–7427.

[116] S. Hirsjärvi, L. Peltonen, J. Hervonen, Layer-by-layer polyelectrolyte coating of low molecular weight poly(lactic acid) nanoparticles, Colloids Surf. A 49 (2006) 93–99.

[117] K.E. Tettey, M.Q. Yee, D. Lee, Layer-by-layer assembly of charged particles in nonpolar media, Langmuir 26 (2010) 9974–9980.

[118] M. Raposo, O.N. Oliveira, Adsorption mechanisms in layer-by-layer films, Braz. J. Phys. 28 (1998) 392–404.

[119] M. Ferreira, M.F. Rubner, Molecular-level processing of conjugated polymers. 1. Layer-by-layer manipulation of conjugated polyions, Macromolecules 28 (1995) 7107–7114.

[120] H. Motschmann, M. Stamm, Adsorption kinetics of block copolymers from a good solvent: a two-stage process, Macromolecules 24 (1991) 3681–3688.

[121] H. Haidara, L. Vonna, J. Schultz, Kinetics and thermodynamics of surfactant adsorption at model interfaces: evidence of structural transitions in the adsorbed films, Langmuir 12 (1996) 3351–3355.

[122] Y.H. Yang, F.A. Malek, J.C. Grunlan, Influence of the deposition time on layer-by-layer growth of clay-based thin films, Ind. Eng. Chem. Res. 49 (2010) 8501–8509.

[123] W. Song, Q. He, H. Möhwald, Y. Yang, J. Li, Smart polyelectrolyte microcapsules as carriers for water-soluble small molecular drug, J. Control. Release 139 (2009) 160–166.

[124] S. Sukhishvilli, S. Granick, Layered, erasable, ultrathin polymer films, J. Am. Chem. Soc. 122 (2000) 9550–9551.

[125] C. Schüler, F. Caruso, Decomposable hollow biopolymer-based capsules, Biomacromolecules 2 (2001) 921–926.

[126] S.T. Dubas, T.R. Farhat, J.B. Schlenoff, Multiple membranes from “true” polyelectrolyte multilayers, J. Am. Chem. Soc. 123 (2001) 5368–5369.

[127] J. Cho, F. Caruso, Polymeric multilayer films comprising deconstructible hydrogen-bonded stacks confined between electrostatically assembled layers, Macromolecules 36 (2003) 2845–2851.

[128] E. Vázquez, D.M. Dewitt, P.T. Hammond, D.M. Lynn, Construciton of hydrolytically-degradable thin films via layer-by-layer deposition of degradable polyelectrolytes, J. Am. Chem. Soc. 124 (2002) 13992–13993.

[129] R.C. Smith, A. Leung, B.S. Kim, P.T. Hammond, Hydrophobic effects of the critical destabalization and release dynamic of degradable multilayer films, Chem. Mater. 21 (2009) 1108–1115.

[130] C. Picart, A. Schneider, O. Etienne, J. Mutterer, P. Schaaf, C. Egles, N. Jessel, J.C. Voegel, Controlled degradability of polysaccharide multilayer films in vitro and in vivo, Adv. Funct. Mater. 15 (2005) 1771–1780.

[131] G. Decher, J.D. Hong, J. Scmitt, Buildup of ultrathin multilayer films by selfassembly process: III. Consecutively alternating adsorption of anionic and cationic polyelectrolytes on charged surfaces, Thin Solid Films 210/211 (1992) 831–835.

[132] P. Kurt, D. Banerjee, R.E. Cohen, M.F. Rubner, Structural color via layer-by-layer deposition: layered nanoparticle arrays with near-UV and visible reflectivity bands, J. Mater. Chem. 19 (2009) 8920–8927.

[133] Y.T. Kim, R.W.Collins, K.Wedam, D.L. Allara, Real-time spectroscopic ellipsometry-in situ characterization of pyrrole electropolymerization, J. Electrochem. Soc. 138 (1991) 3266–3275.

[134] E. Langereis, S.B.S. Heil, H.C.M. Knoops, W. Keuning, M.C.M. van de Sanden, W.M. M. Kessels, In situ spectroscopic ellipsometry as versatile tool for studying atomic layer deposition, J. Phys. D: Appl. Phys. 42 (2009) 1–19, doi:10.1088/0022-3727/42/7/073001.

[135] I. Ichinose, K. Fujiyoshi, S. Mizuki, Y. Lvov, T. Kunitake, Layer-by-layer assembly of aqueous bilayer membranes on charged surfaces, Chem. Lett. 25 (1996) 257–258.

[136] J.J. Harris, M.L. Bruening, Electrochemical and in situ ellipsometric investigation of the permeability and stability of layered polyelectrolyte films, Langmuir 16 (2000) 2006–2013.

[137] A.C. Nieuwkerk, E.J.M. van Kan, A. Koudijs, A.T.M. Marcelis, E.J.R. Sudhölter, Polyelectrolytes carrying pendant (cyanobiphenylyl)oxy chromophores. Synthesis, behaviour in aqueous solution and interactions with surfactants, Langmuir 14 (1998) 5702–5711.

[138] I. Pastoriza-Santos, B. Schöler, F. Caruso, Core-shell colloids and hollow polyelectrolyte capsules om diazoresins, Adv. Funct. Mater. 11 (2001) 122–128.

[139] G.B. Sukhorukov, A.A. Antipov, A. Voigt, E. Donath, H. Möhwald, pH-controlled macromolecule encapsulation in and release from polyelectrolyte multilayer nanocapsules, Macromol. Rapid Commun. 22 (2001) 44–46.

[140] A.P.R. Johnston, A.N. Zelikin, L. Lee, F. Caruso, Approaches to quantifying and visualizing polyelectrolyte multilayer film formation, Anal. Chem. 78 (2006) 5913–5919.

[141] A.N. Zelikin, J.F. Quinn, F. Caruso, Disulfide cross-linked polymer capsules: en route to biodeconstructible systsems, Biomacromolecules 7 (2006) 27–30.

[142] K. Müller, J.F. Quinn, A.P.R. Jonhston, M. Becker, A. Greiner, F. Caruso, Polyelectrolyte funtionalization of electrospun fibers, Chem. Mater. 18 (2006) 2397–2403.

[143] T. Farhat, G. Yassin, S.T. Dubas, J.B. Schlenoff, Water and ion pairing in polyelectrolyte multilayers, Langmuir 15 (1999) 6621–6623.

[144] M. Müller, T. Rieser, K. Lunkwitz, S. Bergwald, J. Meier-Haack, D. Jenichen, An in situ ATR-FTIR study on polyelectrolyte multilayer assemblies on solid surfaces and their susceptibility to fouling, Macromol. Rapid Commun. 19 (1998) 333–336.

[145] M. Müller, T. Rieser, K. Lunkwitz, J. Meier-Haack, Polyelectrolyte complex layers: a promising concept for anti-fouling coatings verified by in-situ ATR-FTIR spectroscopy, Macromol. Rapid Commun. 20 (1999) 607–611.

[146] P.H.B. Aoki, P. Alessio, J.A. de Saja, C.J.L. Constantino, Incorporation of Ag nanoparticles into membrane mimetic systems composed by phospholipd layer-by-layer (LbL) films to achieve surface-enhanced Raman scattering as a tool in drug interaction studies, J. Raman Spectrosc. 41 (2010) 40–48S.

[147] S. Abalde-Cela, S. Ho, B. Rodrígez-González, M.A. Correa-Duarte, R.A. Álvarez-Pueblam, L.M. Öiz-Marzán, N.A. Kotov, Loading of exponentially grown LbL films with silver nanoparticles and their application to generalized SERS detection, Angew. Chem. Intl. Ed. 48 (2009) 5326–5329.

[148] K.A. Marx, Quartz crystal microbalance: a useful tool for studying thin polymer films and complex biomolecular systems at the solution-surface interface, Biomacromolecules 4 (2003) 1099–1120.

[149] D.T. Haynie, S. Balkundi, N. Palath, K. Chakravarthula, K. Dave, Polypeptide multilayer films: role of molecular structure and charge, Langmuir 20 (2004) 4539–4547.

[150] E. Donath, P. Kuzmin, A. Krabi, A. Voigt, Electrokinetics of structured interfaces with polymer depletion—a theoretical study, Colloid. Polym. Sci. 271 (1993) 930–939.

[151] B.D. Vogt, E.K. Lin, W.L. Wu, C.C. Wu, Effect of the film thickness on the validity of the Sauerbrey equation for hydrated polyelectrolyte films, J. Phys. Chem. B 108 (2004) 12685–12690.

[152] D. Lee, Z. Gemici, M.F. Rubner, R.E. Cohen, Multilayers of oppositely charged SiO_2 nanoparticles: effect of surface charge on multilayer assembly, Langmuir 23 (2007) 8833–8837.

[153] S. Erokhina, T. Berzina, L. Christofolini, V. Erokhin, C. Folli, O. Konovalov, I.G. Marino, M.P. Fontana, X-ray reflectivity measurements of layer-by-layer films at the solid/liquid interface, Langmuir 24 (2008) 12093–12096.

[154] M. Lütt, M.R. Fitzsimmons, D. Li, X-ray reflectivity study of self-assembled thin films of macrocycles and macromolecules, J. Phys. Chem. B 102 (1998) 400–405.

[155] C. Li, K. Mitamura, T. Imae, Electrostatic layer-by-layer assembly of poly(amidoamine) dendrimer/conducting sulfonated polyaniline: structure and properties of multilayer films, Macromolecules 36 (2003) 9957–9965.

[156] P.Y. Vuillaume, K. Glinel, A.M. Jonas, A. Laschewsky, Ordered polyelectrolyte "multilayers". 6. Effect of molecular parameters on the formation of hybrid multilayers based on poly(diallylammonium) salts and exfoliated clay, Chem. Mater. 15 (2003) 3625–3631.

[157] X. Arys, A. Laschewsky, A.M. Jonas, Ordered polyelectrolyte "multilayers". 1. Mechanisms of growth and structure formation: a comparison with classical fuzzy "multilayers", Macromolecules 34 (2001) 3318–3330.

[158] S. Jindasuwan, O. Nimittrakoolchai, P. Sujaridworakun, S. Jinawath, S. Supothina, Surface characteristics of water-repellent polyelectrolyte multilayer films containing various silica contents, Thin Solid Films 517 (2009) 5001–5005.

[159] D. Yoo, S.S. Shiratori, M.F. Rubner, Controlling bilayer composition and surface wettability of sequentially adsorbed multilayers of weak polyelectrolytes, Macromolecules 31 (1998) 4309–4318.

[160] C. Aulin, S. Ahola, P. Josefsson, T. Nishino, Y. Hirose, M. Österberg, L. Wåberg, Nanoscale cellulose films with different crystallinities and mesostructures - their surface properties and interaction with water, Langmuir 25 (2009) 7675–7685.

[161] M. Salomäki, P. Tervasmäki, S. Areva, J. Kankare, The Hofmeister anion effect and the growth of polyelectrolyte multilayers, Langmuir 20 (2004) 3679–3683.

[162] J. Irigoyen, S.E.Moya, J.J. Iturri, I. Llarena, O. Azzaroni, E. Donath, Specific ζ-potential response of layer-by-layer coated colloidal particles triggered by polyelectrolyte ion interactions, Langmuir 25 (2009) 3374–3380.

[163] R.N. Smith, L. Reven, C.J. Barrett, 13C solid-state NMR study of polyelectrolyte multilayers, Macromolecules 36 (2003) 1876–1881.

[164] R.N. Smith, M. McCormick, C.J. Barrett, L. Reven, H.W. Spiess, NMR studies of PAH/PSS polelectrolyte multilayers adsorbed onto silica, Macromolecules 37 (2004) 4830–4838.

[165] N. Pargaonkar, Y.M. Lvov, N. Li, J.H. Steenekamp, M.M. de Villiers, Controlled release of dexamthasone from microcapsules produced by polyelectrolyte layer-by-layer nanoassembly, Pharm. Res. 22 (2005) 826–835.

[166] S.J. Strydom, D.P. Otto, W. Liebenberg, Y.M. Lvov, M.M. de Villiers, Preparation and characterization of directly compactible layer-by-layer nanocoated cellulose, Int. J. Pharm. 404 (2011) 57–65.

[167] H. Ai, S.A. Jones, M.M. de Villiers, Y.M. Lvov, Nano-encapsulation of furosemide microcrystal for controlled release, J. Control. Release 86 (2003) 59–68.

[168] N. Rasenack, B.W. Müller, Dissolution rate enhancement by in situ micronization of poorly water-soluble drugs, Pharm. Res. 19 (2002) 1894–1900.

[169] N. Rasenack, B.W. Müller, Properties of ibuprofen crystallized under different conditions: a comparative study, Drug Dev. Ind. Pharm. 28 (2002) 1077–1089.

[170] A.A. Antipov, G.B. Sukhorukov, E. Donath, H. Möhwald, Sustained release properties of polyelectrolyte multilayer capsules, J. Phys. Chem. B 105 (2001) 2281–2284.

[171] K.E. Uhrich, S.M. Cannizzaro, R.S. Langer, K.M. Shakesheff, Polymeric systems for controlled drug release, Chem. Rev. 99 (1999) 3181–3198.

[172] L. Yang, P. Alexandridis, Physicochemical aspects of drug delivery and release from polymer-based colloids, Curr. Opin. Colloid Interface Sci. 5 (2000) 132–143.

[173] J.P.K. Tan, Q. Wang, K.C. Tam, Control of burst release from nanogels via layer by layer assembly, J. Control. Release 128 (2008) 248–254.

[174] B.G. de Geest, C. Déjugnat, E. Verhoefen, G.B. Sukhorukov, A.M. Jonas, J. Plain, J. Demeester, S.C. de Smedt, Layer-by-layer coating of degradable microgels for pulsed drug delivery, J. Control. Release 116 (2006) 159–169.

[175] X. Wang, X. Hu, A. Daley, O. Rabotyagova, P. Cebe, D.L. Kaplan, Nanolayer biomaterial coatings of silk fibroin for controlled release, J. Control. Release 121 (2007) 190–199.

[176] X. Wang, E. Weng, X. Hu, G.R. Castro, L.R. Meinela, X. Wang, C. Li, H. Merkle, D.L. Kaplan, Silk coatings on PLGA and alginate microspheres for protein delivery, Biomaterials 28 (2007) 4161–4169.

[177] X. Wang, X. Zhang, J. Castellot, I. Herman, M. Lafrati, D.L. Kaplan, Controlled release from multilayer silk biomaterial coatings to modulate vascular cell responses, Biomaterials 29 (2008) 894–903.

[178] B.B. Mandal, J.K. Mann, S.C. Kundu, Silk fibroin/gelatin multilayered films as model system for controlled drug release, J. Control. Release 37 (2009) 160–171.

[179] S. Ye, C. Wang, X. Liu, Z. Tong, Deposition temperature effect on release rate of indomethacin microcrystals of layer-by-layer assembled chitosan and alginate microlayer films, J. Control. Release 106 (2005) 319–328.

[180] N. Pargaonkar, Y.M. Lvov, N. Li, J.H. Steenekamp, M.M. de Villiers, Controlled release of dexamethasone from microcapsules produced by polyelectrolyte layer-by-layer nanoassembly, Pharm. Res. 22 (2005) 826–835.

[181] X. Yang, X. Han, Y. Zhu, (PAH/PSS)5 microcapsules templated on silica core: encapsulation of anticancer drug DOX and controlled release study, Colloids Surf. A 264 (2005) 49–54.

[182] Q. Zhao, S. Zhang,W. Tong, C. Gao, J. Shen, Polyelectrolyte microcapsules templated on poly(styrene sulfonate)-doped CaCO3 particles for loading and sustained release of daunorubicin and doxorubicin, Eur. Polym. J. 42 (2006) 3341–3351.

[183] A. Agarwal, Y. Lvov, R. Sawant, V. Torchilin, Stable nanocolloids of poorly soluble drugs with high drug content prepared using the combination of sonication and layer-by-layer technology, J. Control. Release 128 (2008) 255–260.

[184] A.K. Anal, W.F. Stevens, Chitosan-alginate multilayer beads for controlled release of ampicillin, Int. J. Pharm. 290 (2005) 45–54.

[185] A.J. Khopade, N. Arulsudar, S.A. Khopade, J. Hartmann, Ultrathin antibiotic walled microcapsules, Biomacromolecules 6 (2005) 229–234.

[186] K.N.A. Kumar, S.B. Ray, V. Nagaraja, A.M. Raichur, Encapsulation and release of rifampicin using poly(vinyl pyrrolidone)-poly(methacrylic acid) polyelectrolyte capsules, Mater. Sci. Eng. C 29 (2009) 2508–2513.

[187] S. Anandhakumar, M. Debapriya, V. Nagaraja, A.M. Raichur, Polyelectrolyte microcapsules for sustained delivery of water-soluble drugs, Mater. Sci. Eng. C 31 (2011) 342–349.

[188] Y. Chen, X. Lin, H. Park, R. Greever, Study of artemisinin nanocapsules and anticancer drug delivery systems, Nanomed. Nanotechnol. Biol. Med. 5 (2009) 316–322.

[189] D.J. Schmidt, J.S. Moskowitz, P.T. Hammond, Electrically triggered release of a small molecule drug from a polyelectrolyte multilayer coating, Chem. Mater. 22 (2010) 6416–6425.

[190] C.B. Woitiski, R.J. Neufeld, F. Veiga, R.A. Carvalho, I.V. Figueiredo, Pharmacological effect of orally delivered insulin facilitated by multilayered stable nanoparticles, Eur. J. Pharm. Sci. 41 (2010) 556–563.

[191] J. Zheng, X. Yue, Z. Dai, Y. Wang, S. Liu, X. Yan, Novel iron-polysaccharide multilayered microcapsules for controlled insulin release, Acta Biomater. 5 (2009) 1499–1507.

[192] J. Zhao, Y. Cui, A.Wang, J. Fei, Y. Yang, J. Li, Side effect of encapsulated hydrocortisone crystals by insulin/alginate shells, Langmuir 27 (2011) 1499–1504.

[193] S. Mehrotra, D. Lynman, R. Maloney, K.M. Pawelec, M.H. Tuszynski, I. Lee, C. Chan, J. Sakamoto, Time controlled protein release from layer-by-layer assembled multilayer functionalized agarose hydrogels,Adv. Funct.Mater. 20 (2010) 247–258.

[194] W. Qi, X. Yan, J. Fei, A. Wang, Y. Cue, J. Li, Triggered release of insulin from glucose-sensitive enzyme multilayer shells, Biomaterials 30 (2009) 2799–2806.

[195] E.M. Sauer, C.M. Jewell, J.M. Kuchenreuther, D.M. Lynn, Assembly of erodible, DNA-containing thin films on the surfaces of polymer microparticles: toward a layer-by-layer approach to the delivery of DNA to antigen-presenting cells, Acta Biomater. 5 (2009) 913–924.

[196] D.M. Lynn, R. Langer, Degradable poly(beta-amino esters): synthesis, characterization, and self-assembly with plasmid DNA, J. Am. Chem. Soc. 122 (2000) 10761–10768.

[197] X. Su, B.S. Kim, S.R. Kim, P.T. Hammond, D.J. Irvine, Layer-by-layer assembled multilayer films for trancutaneous drug and vaccine delivery, ACS Nano. 3 (2009) 3719–3729.

[198] C. Wang, C. He, Z. Tong, X. Liu, B. Ren, F. Zeng, Combination of adsorption by porous $CaCO_3$ microparticles and encapsulation by polyelectrolyte multilayer films for sustained drug delivery, Int. J. Pharm. 308 (2006) 160–167.

[199] N.G. Veerabadran, D. Mongayt, V. Torchilin, R.R. Price, Y.M. Lvov, Organized shells on clay nanotubes for controlled release of macromolecules, Macromol. Rapid Commun. 30 (2009) 99–103.

[200] Y. Zhu, J. Shi, A mesoporous core-shell structure of pH-controlled storage and release of water-soluble drug, Microporous Mesoporous Mater. 103 (2007) 243–249.

[201] E. Leguen, A. Chassepot, G. Decher, P. Schaaf, J.C. Voegel, N. Jessel, Bioactive coatings based on polyelectrolyte multilayer architectures functionalized by embedded proteins, peptides or drugs, Biomol. Eng. 24 (2007) 33–41.

[202] F. Daubiné, D. Cortial, G. Ladam, H. Atmani, Y. Haïkelm, J.C. Voegel, P. Clézardin, N. Benakirane-Jessel, Nanostructured polyelectrolyte drug delivery systems for bone metastasis prevention, Biomaterials 30 (2009) 6367–6373.

[203] P.M. Nguyen, N.S. Zacharia, E. Verploegen, P.T. Hammond, Extended release antibacterial layer-by-layer films incorporating linear-dendritic block copolymer micelles, Chem. Mater. 19 (2007) 5524–5530.

[204] B.S. Kim, S.W. Park, P.T. Hammond, Hydrogen-bonding layer-by-layer-assembled biodegradable polymeric micelles as drug delivery vehicles from surfaces, ACS Nano. 2 (2008) 386–392.

[205] E. Kharlampieva, V. Kozslovskaya, S.A. Sukhishvill, Layer-by-layer hydrogen bonded polymer films: from fundamentals to applications, Adv. Mater. 21 (2009) 3053–3065.

[206] B.S. Kim, R.C. Smith, Z. Poon, P.T. Hammond, MAD (multiagent delivery) nanolayer: delivering multiple therapeutics from hierarchically assembled surface coatings, Langmuir 25 (2009) 14086–14092.

[207] M. Malcher, D. Volodkin, B. Heurtault, P. André, Pierre Schaaf, H. Möhwald, J.C. Voegel, A. Sokolowski, V. Ball, F. Boulmedais, B. Frisch, Embedded silver ions containing liposomes in polyelectrolyte multilayers: cargos films for antibacterial agents, Langmuir 24 (2008) 10209–10215.

[208] D. Volodkin, H. Möhwald, J.C. Voegel, V. Ball, Coating of negatively charged liposomesby polylysine: drug release study, J. Control. Release 117 (2007) 111–120.

[209] S. Madrigal-Carballo, S. Lim, G. Rodriguez, A.O. Vila, C.G. Krueger, S. Gunasekaran, J.D. Reed, Biopolymer coating of soybean lecithin liposomes via layer-by-layer self-assembly as novel delivery system for ellagic acid, J. Funct. Foods 2 (2010) 99–106.

[210] J.I. Anzai, N. Nakamura, Preparation of active avidin films by a layer-by-layer deposition of poly(vinyl sulfate) and avidin on a solid surface, J. Chem. Soc., Perkin Trans. 2 (1999) 2413–2414.

[211] J.S. Maciel, P.M. Kosaka, R.C.M. de Paula, J.P.A. Feitosa, D.F.S. Petri, Formation of cashew gum thin films onto silicon wafers or amino-terminated surfaces and the immobilization of concanavalin A on them, Carbohydr. Polym. 69 (2007) 522–529.

[212] T. Hoshi, H. Saiki, J.I. Anzai, Layer-by-layer deposition of avidin and biotin-labeled antibody on a solid surface to prepare a multilayer array of antibody, J. Chem. Soc., Perkin Trans. 2 (1999) 1293–1294.

[213] J.I. Anzai, Y. Kobayashi, Construction of multilayer thin films of enzymes by means of sugar-lectin interactions, Langmuir 16 (2000) 2851–2856.

[214] R. Wilson, M. Mehrabi, I.A. Prior, A. Beckett, A. Hutchinson, A reliable method for attaching biological molecules to layer-by-layer self-assemblies, Chem. Commun. (2009) 2487–2489.

[215] M. Fischlechner, O. Zschörning, J. Hoffman, et al., Engineering virus functionalities on colloidal polyelectrolyte lipid composites, Angew. Chem. Int. Ed. 44 (2005) 2892–2895.

[216] C. Cortez, E. Tomaskovic-Crook, A.P.R. Johnston, A.M. Scott, E.C. Nice, J.K. Heath, F. Caruso, Binding of A33 antigen-targeted multilayered particles and capsules to colorectal cancer cells, ACS Nano. 1 (2007) 93–102.

[217] Y. Hu, K. Cai, Z. Luo, C. Chen, H. Dong, J. Hao, L. Yang, L. Deng, Fabrication of galactosylated polyethylenimine and plasmid DNA multilayers on poly(D, L-lactic acid) films for in situ targeted gene transfection, Adv. Eng. Mater. 11 (2009) B30–B34.

[218] F. Zhang, Q. Wu, L.J. Liu, Z.C. Chen, X.F. Lin, Thermal treatment of galactose branched microcapsules to improve drug delivery with reserved targetability, Int. J. Pharm. 357 (2008) 22–31.

CHAPTER 2

This chapter was submitted to the International Journal of Pharmaceutics.

STRYDOM, S.J., OTTO, D.P., LIEBENBERG, W., LVOV, Y.M. & DE VILLIERS, M.M. 2011. Preparation and characterization of directly compactible layer-by-layer nanocoated cellulose. International journal of pharmaceutics, 404: 57-65.*

IMPACT FACTOR: 3.991

INSTRUCTIONS TO AUTHORS (SUMMARY)

The *International Journal of Pharmaceutics* publishes innovative papers, reviews, mini-reviews, rapid communications and notes dealing with physical, chemical, biological, microbiological and engineering studies related to the conception, design, production, characterisation and evaluation of drug delivery systems *in vitro* and *in vivo*. "Drug" is defined as any therapeutic or diagnostic entity, including oligonucleotides, gene constructs and radiopharmaceuticals.

Areas of particular interest include: pharmaceutical nanotechnology; physical pharmacy; polymer chemistry and physical chemistry as applied to pharmaceutics; excipient function and characterisation; biopharmaceutics; absorption mechanisms; membrane function and transport; novel routes and modes of delivery; responsive delivery systems, feedback and control mechanisms including biosensors; applications of cell and molecular biology to drug delivery; prodrug design; bioadhesion (carrier-ligand interactions); and biotechnology (protein and peptide formulation and delivery).

Types of paper

(1) **Full Length Manuscripts** (2) **Rapid Communications** (a) These articles should not exceed 1500 words or equivalent space. (b) Figures should not be included otherwise delay in publication will be incurred. (c) Do not subdivide the text into sections. An Abstract should be included as well as a full reference list. (3) **Notes** Should be prepared as described for full length manuscripts, except for the following: (a) The maximum length should be 1500 words, including figures and tables. (b) Do not subdivide the text into sections. An Abstract and reference list should be included. (4) **Reviews and Mini-Reviews** Suggestions for review articles will be considered by the Review-Editor. "Mini-reviews" of a topic are especially welcome.

Authorship

All authors should have made substantial contributions to all of the following: (1) the conception and design of the study, or acquisition of data, or analysis and interpretation of data, (2) drafting the article or revising it critically for important intellectual content, (3) final approval of the version to be submitted.

Copyright

This journal offers authors a choice in publishing their research: Open Access and Subscription.

Submission

Submission to this journal proceeds totally online and you will be guided stepwise through the creation and uploading of your files. The system automatically converts source files to a single PDF file of the article, which is used in the peer-review process. Please note that even though manuscript source files are converted to PDF files at submission for the review process, these source files are needed for further processing after acceptance. All correspondence, including notification of the Editor's decision and requests for revision, takes place by e-mail removing the need for a paper trail. Authors must state in a covering letter when submitting papers for publication the novelty embodied in their work or in the approach taken in their research. Routine bioequivalence studies are unlikely to find favour. No paper will be published which does not disclose fully the nature of the formulation used or details of materials which are key to the performance of a product, drug or excipient. Work which is predictable in outcome, for example the inclusion of another drug in a cyclodextrin to yield enhanced dissolution, will not be published unless it provides new insight into fundamental principles.

Referees

Please submit, with the manuscript, the names, addresses and e-mail addresses of at least three potential reviewers. Reviewers who do not have an institutional e-mail address will only be considered if their affiliations are given and can be verified. Preferably international reviewers should be nominated, and their areas of expertise must be stated clearly. Note that the editor retains the sole right to decide whether or not the suggested reviewers are used.

Article structure ***Subdivision - numbered sections***

Divide your article into clearly defined and numbered sections. Subsections should be numbered 1.1 (then 1.1.1, 1.1.2, ...), 1.2, etc. (the abstract is not included in section numbering). Use this numbering also for internal cross-referencing: do not just refer to 'the text'. Any subsection may be given a brief heading. Each heading should appear on its own separate line.

Introduction

State the objectives of the work and provide an adequate background, avoiding a detailed literature survey or a summary of the results.

Material and methods

Provide sufficient detail to allow the work to be reproduced. Methods already published should be indicated by a reference: only relevant modifications should be described.

Results

Results should be clear and concise.

Discussion

This should explore the significance of the results of the work, not repeat them. A combined Results and Discussion section is often appropriate. Avoid extensive citations and discussion of published literature.

Conclusions

The main conclusions of the study may be presented in a short Conclusions section, which may stand alone or form a subsection of a Discussion or Results and Discussion section.

Title

Concise and informative. Titles are often used in information-retrieval systems. Avoid abbreviations and formulae where possible.

Author names and affiliations

Where the family name may be ambiguous (e.g., a double name), please indicate this clearly. Present the authors' affiliation addresses (where the actual work was done) below the names. Indicate all affiliations with a lower-case superscript letter immediately after the author's name and in front of the appropriate address. Provide the full postal address of each affiliation, including the country name and, if available, the e-mail address of each author.

Corresponding author

Clearly indicate who will handle correspondence at all stages of refereeing and publication, also post-publication. Ensure that phone numbers (with country and area code) are provided in addition to the e-mail address and the complete postal address. Contact details must be kept up to date by the corresponding author.

Present/permanent address

If an author has moved since the work described in the article was done, or was visiting at the time, a 'Present address' (or 'Permanent address') may be indicated as a footnote to that author's name. The address at which the author actually did the work must be retained as the main, affiliation address. Superscript Arabic numerals are used for such footnotes.

Abstract

A concise and factual abstract is required. The abstract should state briefly the purpose of the research, the principal results and major conclusions. An abstract is often presented separately from the article, so it must be able to stand alone. For this reason, References should be avoided, but if essential, then cite the author(s) and year(s). Also, non-standard or uncommon abbreviations should be avoided, but if essential they must be defined at their first mention in the abstract itself. The abstract must not exceed 200 words.

Graphical abstract

A Graphical abstract is mandatory for this journal. It should summarize the contents of the article in a concise, pictorial form designed to capture the attention of a wide readership online. Authors must provide images that clearly represent the work described in the article. Graphical abstracts should be submitted as a separate file in the online submission system. Image size: please provide an image with a minimum of 531 × 1328 pixels (h × w) or proportionally more, but should be readable on screen at a size of 200 × 500 pixels (at 96 dpi this corresponds to 5 × 13 cm). Bear in mind readability after reduction, especially if using one of the figures from the article itself. Preferred file types: TIFF, EPS, PDF or MS Office files. See http://www.elsevier.com/graphicalabstracts for examples.

Keywords

Immediately after the abstract, provide a maximum of 6 keywords, using American spelling and avoiding general and plural terms and multiple concepts (avoid, for example, 'and', 'of').

Be sparing with abbreviations: only abbreviations firmly established in the field may be eligible. These keywords will be used for indexing purposes.

Abbreviations

Define abbreviations that are not standard in this field in a footnote to be placed on the first page of the article. Such abbreviations that are unavoidable in the abstract must be defined at their first mention there, as well as in the footnote. Ensure consistency of abbreviations throughout the article.

Acknowledgements

Collate acknowledgements in a separate section at the end of the article before the references and do not, therefore, include them on the title page, as a footnote to the title or otherwise. List here those individuals who provided help during the research (e.g., providing language help, writing assistance or proof reading the article, etc.).

Figure captions

Ensure that each illustration has a caption. Supply captions separately, not attached to the figure. A caption should comprise a brief title (**not** on the figure itself) and a description of the illustration. Keep text in the illustrations themselves to a minimum but explain all symbols and abbreviations used.

Tables

Number tables consecutively in accordance with their appearance in the text. Place footnotes to tables below the table body and indicate them with superscript lowercase letters. Avoid vertical rules. Be sparing in the use of tables and ensure that the data presented in tables do not duplicate results described elsewhere in the article.

References

Citation in text Please ensure that every reference cited in the text is also present in the reference list (and vice versa). Any references cited in the abstract must be given in full. Unpublished results and personal communications are not recommended in the reference list, but may be mentioned in the text. If these references are included in the reference list they should follow the standard reference style of the journal and should include a substitution of the publication date with either 'Unpublished results' or 'Personal communication'. Citation of a reference as 'in press' implies that the item has been accepted for publication and a copy of the title page of the relevant article must be submitted.

Reference formatting There are no strict requirements on reference formatting at submission. References can be in any style or format as long as the style is consistent. Where applicable, author(s) name(s), journal title/book title, chapter title/article title, year of publication, volume number/book chapter and the pagination must be present. Use of DOI is highly encouraged. The reference style used by the journal will be applied to the accepted article by Elsevier at the proof stage. Note that missing data will be highlighted at proof stage for the author to correct. If you do wish to format the references yourself they should be arranged according to the following examples:

Reference style *Text:* All citations in the text should refer to: 1. *Single author:* the author's name (without initials, unless there is ambiguity) and the year of publication; 2. *Two authors:* both authors' names and the year of publication; 3. *Three or more authors:* first author's name followed by 'et al.' and the year of publication. Citations may be made directly (or parenthetically). Groups of references should be listed first alphabetically, then chronologically. Examples: 'as demonstrated (Allan, 2000a, 2000b, 1999; Allan and Jones, 1999). Kramer et al. (2010) have recently shown ....' *List:* References should be arranged first alphabetically and then further sorted chronologically if necessary. More than one reference from the same author(s) in the same year must be identified by the letters 'a', 'b', 'c', etc., placed after the year of publication. *Examples:* Reference to a journal publication: Van der Geer, J., Hanraads, J.A.J., Lupton, R.A., 2010. The art of writing a scientific article. J. Sci. Commun. 163, 51–59. Reference to a book: Strunk Jr., W., White, E.B., 2000. The Elements of Style, fourth ed. Longman, New York. Reference to a chapter in an edited book: Mettam, G.R., Adams, L.B., 2009. How to prepare an electronic version of your article, in: Jones, B.S., Smith , R.Z. (Eds.), Introduction to the Electronic Age. E-Publishing Inc., New York, pp. 281–304.

Journal abbreviations source Journal names should be abbreviated according to the List of Title Word Abbreviations:http://www.issn.org/services/online-services/access-to-the-ltwa/.

International Journal of Pharmaceutics

Preparation and characterization of directly compactible layer-by-layer nanocoated cellulose (2011)

Schalk J. Strydom[1], Daniel P. Otto[1], Wilna Liebenberg[2], Yuri M. Lvov[3] and Melgardt M. de Villiers[1]*

1. School of Pharmacy, University of Wisconsin-Madison, Madison, Wisconsin 53705, USA
2. Unit for Drug Research and Development, Faculty of Health Sciences, North-West University, Potchefstroom, 2520, South Africa
3. Institute for Micromanufacturing and Biomedical Engineering Program, Louisiana Tech University, Ruston, Louisiana 71272, USA

*To whom correspondence should be addressed.

Melgardt M. de Villiers, PhD. University of Wisconsin-Madison, School of Pharmacy, 777 Highland Avenue, Madison WI 53705-2222, USA. Phone: 608-890-0732. Fax: 608-262-5345. E-mail: mmdevilliers@pharmacy.wisc.edu.

Abstract

Microcrystalline cellulose is a commonly used direct compression tablet diluent and binder. It is derived from purified α-cellulose in an environmentally unfriendly process that involves mineral acid catalysed hydrolysis. In this study Kraft softwood fibers was nanocoated using a layer-by-layer self-assembling process. Powder flow and compactibility results showed that the application of nano thin polymer layers on the fibers turned non-flowing, non-compacting cellulose into powders that can be used in the direct compression of tablets. The powder flow properties and tableting indices of compacts compressed from these nanocoated microfibers were similar or better than that of directly compactible microcrystalline cellulose powders. Cellulose microfibers coated with four PSS/PVP bilayers had the best compaction properties while still producing tablets that were able to absorb water and disintegrate and did not retard the dissolution of a model drug acetaminophen. The advantages of nanocoating rather than traditional pharmaceutical coating are that it add less than 1 % to the weight of the fibers and allows control of the molecular properties of the surface and the thickness of the coat to within a few nanometers. This process is potentially friendlier to the environment because of the type and quantity of materials used. Also, it does not involve acid-catalyzed hydrolysis and neutralization of depolymerized cellulose.

Key words: layer-by-layer, selfassembling, nanocoating, cellulose, direct compression

Running title: Directly compactible nanocoated cellulose

Introduction

Tablets, and in particular directly compressed tablets, are considered to be the most desirable dosage form for drug delivery since it is affordable and convenient for patients, and it has a straightforward, easily controllable and low cost manufacturing process which is attractive for pharmaceutical manufacturers and friendlier to the environment (De la Luz Reus Medina and Kumar, 2007; McCormick, 2005). Also, the process of direct compression consists of only two manufacturing steps including mixing of the constituent powders and compression to produce the final tablet dosage form, and this is beneficial in the pharmaceutical industry since it reduces the risk that an error may be introduced during the manufacturing process which could compromise the safety and stability of the final product (McCormick, 2005).

Most dosage forms require the addition of excipients in order to assist in the manufacture and delivery of the dosage form, and for directly compressed tablets these include diluents, binders, lubricants, disintegrants and glidants (Aulton, 2000; De la Luz Reus Medina and Kumar, 2006; Peck et al., 1989). Cellulose fibers, manufactured from the purification and size reduction of α-cellulose fibers from the pulp of fibrous plant materials, serves as the basis for the manufacture of a variety of these excipients but it is not used in its unmodified form due to its poor flow properties (Aulton, 2000; De la Luz Reus Medina and Kumar, 2007). A modified cellulose, microcrystalline cellulose (MCC) is the most commonly used diluent or binder in directly compressed tablets. MCC is derived from purified wood α-cellulose by the treatment of the cellulose fibers with mineral acids (De la Luz Reus Medina and Kumar, 2006; Doelker, 1993). This acid treatment results in the hydrolysis of the amorphous cellulose fibers which also reduces the degree of polymerization in the cellulose chains, and this leads to the formation of aggregates of microcrystals with an average particle size in the micrometer range (Chuayjuljit et al., 2008, Doelker, 1993). The reason for this modification is that the unmodified cellulose fibers have poor flow and compression properties compared to MCC, and these two properties play an essential role in the manufacturing of tablets through direct compression since it influences the weight uniformity, compressibility and tensile strength of the tablets (Lindner and Kleinebudde, 1994). However the process through which MCC is manufactured is environmentally unfriendly since it consumes large quantities of fresh water which is difficult to recycle as a result of the treatment with strong mineral acids. More environmentally friendly methods for preparing MCC have been suggested. (Chuayjuljit et al., 2008; Stupińska et al., 2007). There are two possible

options available in order to be more environmentally conscious during the manufacturing of directly compressed tablets, and these are to either develop another environmentally friendly method for the production of MCC, or to develop method of altering the flow and compression properties of the unmodified cellulose fibers in order for it to be suitable for the manufacture of directly compressed tablets. The latter was explored during this study through the nanocoating of aqueous suspensions of Kraft softwood fibers with various polymers, using a layer-by-layer (LbL) self-assembly process.

The layer-by-layer (LbL) coating process is the sequential application of alternate polyelectrolytes or charged nanoparticles onto the surface of a charged substrate (Lvov et al., 1993). These ultrathin coatings can be functionalized for controlled drug delivery purposes (Ai et al. 2003, De Geest et al., 2006) or to adjust the properties of the coated substrate (Lu et al., 2007), and the properties of this coating depends on the nature of the molecules that make up the coating. It has been shown that colloidal SiO_2 is suitable for coating lignocellulose wood microfibers in order to improve the tensile strength of paper sheets made from these cellulose fibers, and cellulose fibers have also been coated with polymers in order to alter the surface properties of these fibers (Huang et al., 2005; Lu et al., 2007). This thus indicates that the LbL coating method might be a well suited technique to alter the properties of unmodified cellulose for making it suitable for use during direct compression. The aim of this study is to determine the feasibility of the LbL technique in coating cellulose fibers with polyelectrolytes commonly used in LbL coating and other biocompatible polymers in order to improve the flow, compression and tableting properties of cellulose fibers.

Materials and Methods

Materials

Beaten, bleached (TCF) Kraft softwood fibers from Southern Pine (dried after beating) were supplied by International Paper Company, Bastrop, LA. Short damaged fibers were prepared by Wiley milling the dry pulp strips and passing it through a 60 mesh screen (resulted fiber length was 0.2 ± 0.1 mm). Fluorescein-5-isothiocyanate (FITC), cationic poly(dimethyldiallyl ammonium chloride) (PDDA; MW 200,000), anionic sodium poly(styrenesulfonate) (PSS; MW 70,000), polyvinylpyrrolidone (PVP, K30, MW ~ 40,000) and the charged polypeptides, gelatin type B (alkali processed or bovine gelatin; Bloom strength 225, MW 50,000~100,000) and

chitosan (medium molecular weight), was purchased from Sigma-Aldrich (St. Louis, MO, USA). Microcrystalline cellulose USP/NF, Avicel® PH101 and PH102 were purchased from FMC Corporation (Newark, DE, USA). Milli-Q water with a resistivity of 18.2 MΩ/cm was used throughout this study in the preparation of the dissolution media, and all other reagents were analytical grade unless otherwise stated.

LbL nanocoating of cellulose fibers

Based on the negative charge on the suspended cellulose fibers, 1 g of the fibers were suspended in 100 ml of a PDDA solution (2 mg/ml in PBS buffer pH 5.8). The isoelectric point of PDDA is 12 and therefore has a net positive charge at pH 5.8. The suspension was then sonicated for 15 min, transferred to centrifuge tubes and centrifuged at 10 000 RPM for 5 min. The separated coated fibers were washed three times with PBS buffer. Zeta potential measurements indicated reversal to positive charge due to PPDA masking the negative drug particle surface charge. The particles were then resuspended in 100 ml of PSS solution (2 mg/ml at pH 5.8), stirred for 20 min to ensure coating, centrifuged, and then washed three times. At this pH, PSS carries a net negative charge because the isoelectric point of PSS is below 1.0. This completes the assembly of the first bilayer. When gelatin B was used in the assembling process, it was dissolved in the PBS pH 5.8 at a concentration of 2 mg/ml. It was layered with PDDA because it has a negative charge at pH 5.8 (isoelectric point, ~4-5). Due to the low solubility of chitosan at pH 5.8 it was dissolved in 0.1 M HCl. At this pH chitosan has a net positive charge. When PVP (2 mg/ml in 0.1 M HCl) was used in the coating it was layered with PSS. In each case at least four bilayers were applied to the cellulose particles.

Characterization of LbL nanocoating

Prior to polyion multilayer formation on the cellulose fibers, the coating procedure was elaborated on gold electrode resonators of 9-MHz quartz crystal microbalance (QCM; USI-Systems Inc., Kyoto, Japan). The resonators were immersed in the polyion solutions for 25 min, removed, and dried. The added mass and the coating thickness (ΔL) can be calculated from the frequency shift (ΔF), according to the Sauerbrey equation and using a special scaling. For the instrument used in this study, the calibration was $\Delta L\ (nm) = 0.017\Delta F(Hz)$. These optimized assembly conditions were applied to the LbL nanocoating on the cellulose particles. To ensure the reversal of charge after each polyion coating, the zeta-potential of the suspended particles

were measured with a Zeta-plus photon correlation spectroscopy and microelectrophoresis instrument (Brookhaven Instruments, Holtsville, NY, USA). Since the coating with PVP depended more on hydrogen bonding than charge the layering of PVP with PSS was also followed by depositing the film on quartz slides (Yang et al., 2007). Before film preparation, the quartz slides were thoroughly cleaned by immersion in boiling H_2SO_4/H_2O_2 (70:30 v/v) for 30 min, followed by rinsing with deionized water and drying with a stream of pure N_2. The quartz slides were also modified before LbL deposition of PVP by coating with two PDDA/PSS layers. The UV-Vis absorbance measurements were obtained with an Agilent 8453 UV-Vis spectrophotometer (Santa Clara, CA, USA).

Microscopic analysis

Scanning electron microscopy (SEM) studies were performed on samples that were affixed on carbon-taped stubs and thinly coated with Au/Pd. Both a Hitachi S570 and a Hitachi S-900 FESEM was used to photograph the samples (Hitachi High Technologies, Pleasanton, CA, USA). All micrographs were recorded with a crystal emission of 10 keV. Additional SEM micrograph analysis was conducted with automated image analysis routines available in ImageJ 1.42 imaging analysis software. Confocal laser scanning microscopy (model DMI RE2; Leica, Allendale, NJ, USA) and fluorescent spectrometry (Photon Technology International, Lawrenceville, NJ, USA) were used to visualize the LbL coating. For fluorescence, the cellulose particles were coated with FITC labeled PDDA (Ai et al., 2003).

Powder flow properties

Prior to making measurements all powder were dried under vacuum for at least 24 hours. Angle of repose measurements were made by allowing powder samples to fall freely from a height of 45 mm onto a constant base with a diameter of 40 mm, through a glass funnel. The angle of repose was determined by taking photographs of the powder mound and measuring the angle formed between the horizontal surface of the base and the incline using ImageJ picture editing software. The Hausner ratio and Carr's index for each sample was determined by pouring a known weighed quantity of powder, equal to approximately 2 g powder, into a graduated 50 ml cylinder. The initial powder volume (bulk volume) was measured after which the cylinder was tapped on a hard surface for 2 minutes (approximately 200 taps), or until the powder volume remained constant, and a second volume measurement (tapped volume) was made. The Hausner ratio was calculated

as the ratio between the tapped and bulk densities of each sample, whereas the Carr's index was calculated using equation 1 (Carr, 1965):

$$C_{\%} = \frac{\rho_t - \rho_b}{\rho_t} \times 100\% \qquad (1)$$

where ρ_t and ρ_b are the tapped and bulk densities respectively. All measurements were repeated five times for each sample.

Compaction properties

The powder samples were compacted into tablets with a Carver auto bench top press (Wabash, IN). The tablets had a diameter of 12 mm and weighed approximately 250 mg. Each powder was kept under pressure for 30 s before the pressure was removed. Six different compaction forces: 60, 120, 180, 240, 300 and 360 MPa were used. Before compaction, the powders were dried under vacuum for at least 24 hours and afterwards the tablets were rested for 12 hours before the tablet weight and dimensions were measured. Diametrical tablet hardness was measured with a Varian VK 200 tablet hardness test unit (Varian, Palo Alto, CA), and this enabled the calculation of the tensile strength (σ) (Fell & Newton, 1970):

$$\sigma = \frac{2P}{\pi D t} \qquad (2)$$

where P is the crushing strength, D the diameter and t the thickness of the tablets. The brittle fracture index (BFI) of the tablets was calculated using the following equation

$$BFI = 0.5\left[\left(\frac{\sigma}{\sigma_0}\right) - 1\right] \qquad (3)$$

Where σ is the tensile strength of the tablet without a hole and σ_0 the tensile strength of a tablet with a hole. A modified punch and die set with upper and lower sides having a hole and a pin at their centers permitted the formation of compacts with a centrally located hole (~1.0 mm diameter) that acted as a stress concentration defect during tensile testing. BFI values were calculated for tablets compacted to comparable tensile strength and porosity.

The porosity of tablets, ε, was calculated using Eq. (4).

$$\varepsilon = 1 - \frac{\rho_{tablet}}{\rho_{true}} \qquad (4)$$

where ρ_{tablet} is the density calculated using the volume and weight of each tablet and ρ_{true} is the true density of the material measured using a Quantachrome Model MPY-2 helium displacement pycnometer (Quantachrome Corporation, Syosset, NY).

Compactibility plots of tensile strength versus porosity was analysed with the Ryshkewitch equation (Ryshkewitch, 1953)

$$\sigma = \sigma_0 e^{-b\varepsilon} \qquad (5)$$

where ε is the tablet porosity and σ is the tablet tensile strength. The constant σ_0 is the maximum tensile strength at zero tablet porosity and b is an empirical constant that has been related to the pore distribution within a tablet (Roberts et al., 1995).

Heckel plots were constructed by plotting the natural log of the inverse of the compact porosity against the respective compaction pressures in accordance to the Heckel equation

$$\ln\left(\frac{1}{\varepsilon}\right) = KP + A \qquad (6)$$

where K and A are slope and intercept, respectively, and P is the compaction pressure applied.. Regression analysis was performed on the linear portion of each curve, and the slope value (K) obtained was converted to mean deformation, yield, pressure (Py) using the relationship

$$P_y = \frac{1}{K} \qquad (7)$$

The areas under the Heckel curves (AUC_H) were calculated using TableCurve 2D and it was used as a measure of the extent of volume reduction that the material experienced over the entire compaction pressure range (60-360 MPa).

Disintegration time and dissolution testing

Tablets for the disintegration study were prepared to have similar solid fractions (1-ε) and tensile strengths. The disintegration test was performed according to the US Pharmacopoeia/National Formulary disintegration method using water at 37ºC and an Erweka GmbH apparatus (type 712, Erweka, Offenbach, Germany). The disintegration times reported are averages of five

determinations.

Dissolution testing was performed on six tablets made from cellulose, nanocoated cellulose or MCC, and acetaminophen (APAP) powder mixtures. Tablets made from the powder mixtures that contained 30 and 60% (w/w) acetaminophen were used for the dissolution testing. Tablets prepared with acetaminophen concentrations of greater than 60% (w/w) were too brittle to handle, and were deemed not practically acceptable. The dissolution method for acetaminophen tablets from the United States Pharmacopoeia 2007 was followed (USP 2007), and dissolution apparatus 2 (the rotating paddle method) was used during the dissolution testing of these samples. A Varian VK 7000 dissolution apparatus (Palo Alto, CA) was used with 900 ml phosphate buffer USP (pH 5.8) as the dissolution media, made with potassium phosphate monobasic (KH_2PO_4) and sodium hydroxide (NaOH). The paddles were rotated at 50 rpm and 2.5 ml of dissolution media were withdrawn at predetermined time intervals, up to 2 hours, and it was immediately replaced with an equal amount of fresh dissolution media. The amount of AAP in solution was calculated by determining the ultraviolet (UV) absorbance of the withdrawn solutions at a wavelength of 243 nm (USP 2007), and this value was converted to a concentration value using a calibration curve.

Results and discussion

Particle morphology

This paper reports the use of the LbL coating on small soft wood cellulose fibers and demonstrates the use of these nanocoated particles as a direct compaction tablet diluent. Direct compression is a process by which tablets are compressed directly from powder blends of the active ingredient and suitable excipients without pre-treatment by wet or dry granulation. Cellulose and especially MCC, purified partially depolymerized cellulose prepared by treating α-cellulose with mineral acids, is a diluent often used in direct compression. Examination of commercially available MCC powders reveals that many have similar particle morphology but they differ significantly in particle size. The SEM images in Figure 1 show MCC particles that appear very rough, with many wrinkles and folds, irregular in shape, and with aspect ratios from 1.5 to 3 (Shangraw et al., 1987). Closer inspection of the surface reveals a crystalline powder composed of agglomerated porous microfibers (Figure 1b).

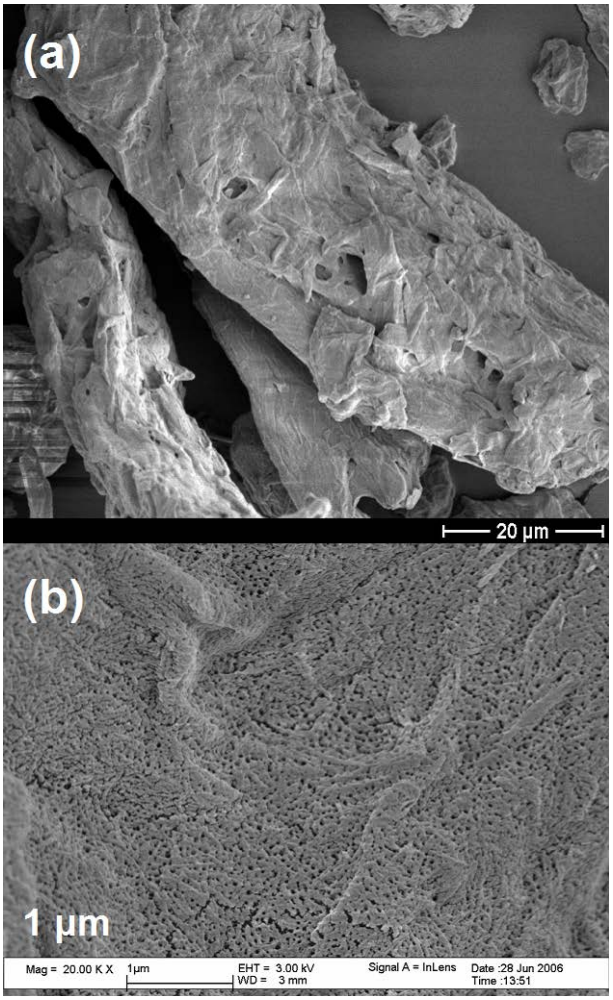

Figure 1. SEM photomicrographs of (a) MCC (Avicel PH102) particle and (b) the surface of the MCC particle.

SEM and laser confocal fluorescent photomicrographs of the milled softwood cellulose fibers are shown in Figure 2. Milling damaged the ends of the fibers but caused little wall separation of the porous microfibers (Lvov et al., 2006). The majority of the fibers were very short (0.2 ± 0.1 mm) with aspect ratios similar to that of the MCC particles. Microscopically, Figure 2a, the morphology and size of the uncoated cellulose and MCC particles appeared similar.

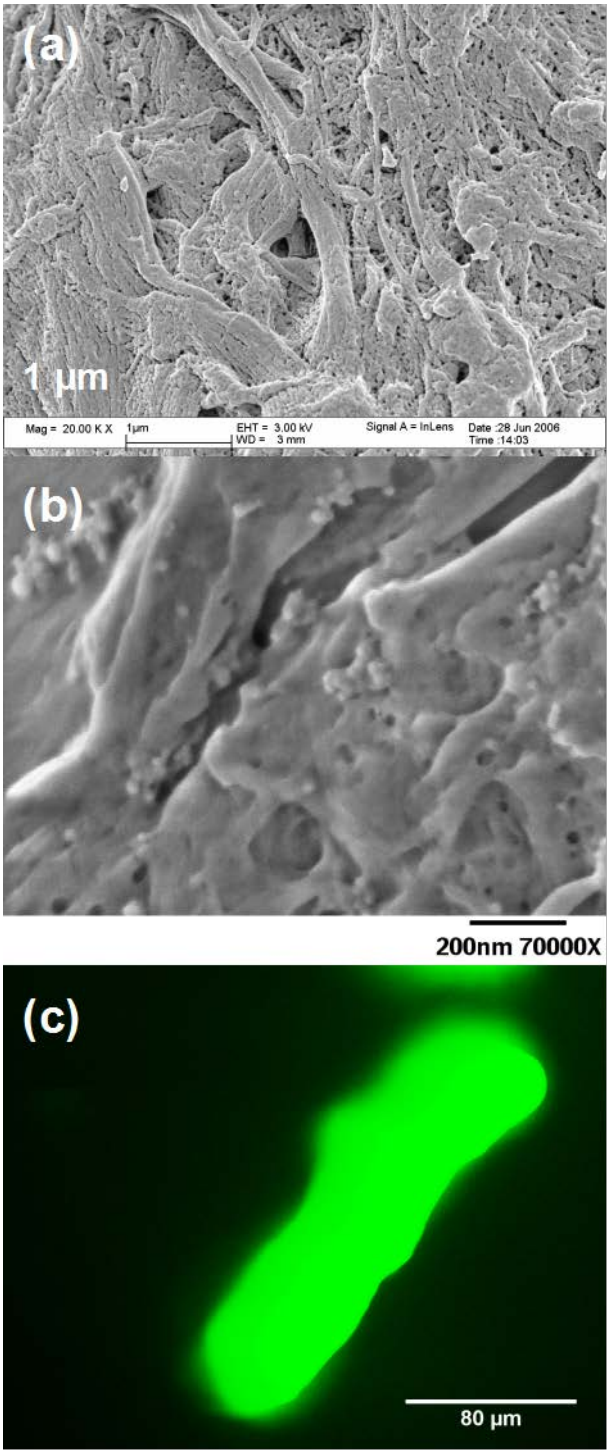

Figure 2. SEM photomicrographs of the surface of (a) cellulose particle and (b) a cellulose particle coated with $(PDDA/(PSS/PVP)_3)$. (c) Laser confocal fluorescent image of a cellulose particle coated with labeled $(PDDA\text{-}FITC/PSS)_8$.

Characterization of the LbL nanocoating

The cellulose fibers were coated with polyelectrolytes commonly used in the LbL process (PDDA and PSS) and also GRAS and biocompatible polymers (gelatin, chitosan and PVP). The surface charge (ζ-potential) and change in surface charge is important for the LbL nanocoating process. The cellulose fibers had a negative potential of -30±2.1 mV. The first precursor polyelectrolyte layers provided even coating and showed a change in surface potential with values of +35±3.0 mV for cationic PDDA and -27±1.9 mV for anionic PSS. Overall, alternate ζ-potential values were observed for all multilayer films (Figure 3). The results shown in Figure 3 confirmed the LbL nanocoating of PDDA/PSS, PDDA/gelatin, PSS/chitosan or chitosan/gelatin in organized alternating layers. For each layer deposited, the underneath layer could have a different molecular distribution and conformation, which may explain the slight variations of the measured ζ-potential values for a specific polyelectrolyte when combined with different oppositely charged polyelectrolytes. SEM photomicrographs, Figure 2b, also showed the coating because compared to uncoated particles smoother particle edges, and filled cracks and pores were observed after coating. Confocal images, Figure 2c, of the bright green fluorescence of microfibers coated with eight layers of labeled FITC–PDDA alternated with PSS also confirmed the uniform polymer nanocoating on the surface of the fibers. Confocal microscopy was used as a measurement to confirm the LbL coating.

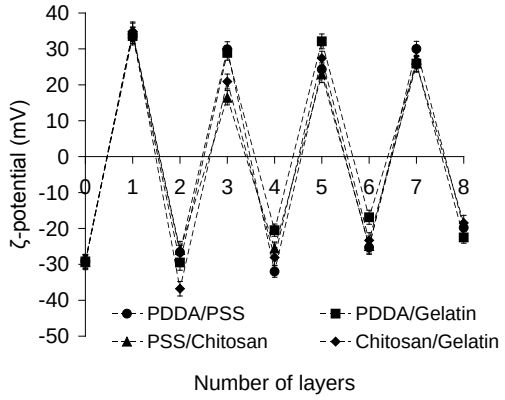

Figure 3. Change in the cellulose particles ζ-potential during the LbL nanocoating.

The coating thickness was estimated from QCM measurements. A resonance frequency shift, Figure 4, of the LbL nanocoated QCM-resonator enabled the calculation of the thickness of deposited polyelectrolyte multilayers. On the resonator each step of the PDDA/PSS

polycation/polyanion deposition added approximately 2–5 nm thickness to the nanocoating thickness (Figure 4). From this it was estimated that the total thickness of the PDDA/PSS nanocoat was ~15 nm. This added about 0.15 % to the total weight of each fiber. Similarly the thickness of the PDDA/gelatin nanocoat was ~29 nm, the PSS/chitosan nanocoat ~25 nm and the chitosan/gelatin nanocoat ~64 nm. The 0.6 % increase in weight for the chitosan/gelatin nanocoat was double that for the PDDA/gelatin and PSS/chitosan (0.3 %), and four times that of the PDDA/PSS nanocoat. Together the QCM results showed that these ultrathin coatings added less than 1 % to the weight of the cellulose fibers. This is significant because addition of these coatings by processes such as blending, granulation or spray coating would require significantly larger quantities of the polymers.

Since the adsorption of PVP depends on hydrogen bonding more than change interactions, the absorption of PSS/PVP bilayers were followed by UV spectroscopy at λ = 225 nm. This wavelength corresponds to absorbency of benzyl rings of PSS (Lvov et al., 1994).

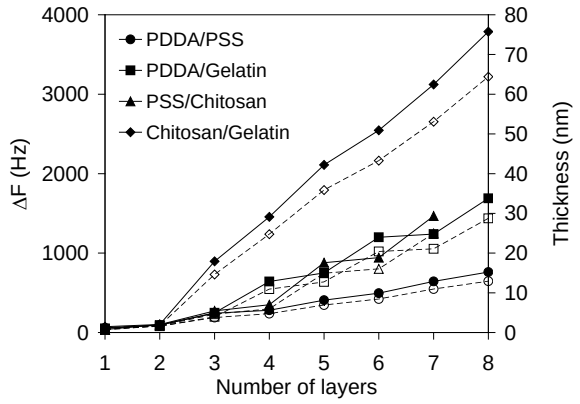

Figure 4. QCM monitoring of resonance shifts by the subsequent nanoassembly of multiple layers on quartz resonators (solid lines and closed symbols) and thickness of layers relative derived from QCM data (broken lines and open symbols). Adsorption time is 25 min for every step.

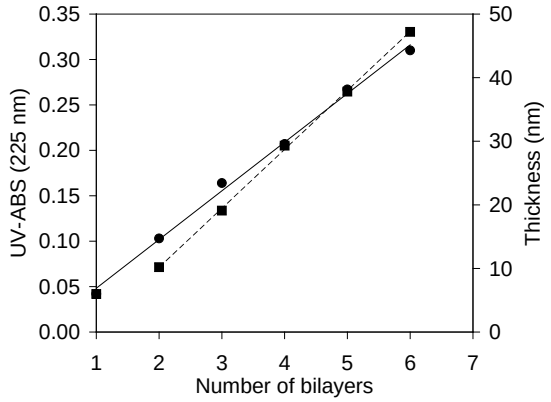

Figure 5. (a) Monitoring of the LbL PSS/PVP assembly process by UV/Vis spectroscopy (λ = 226 nm) (solid line). (b) Thickness of PSS/PVP bilayers derived from QCM monitoring of resonance shifts on quartz resonators (broken line).

Since the deposition was done on both sides of the glass slide the increase in absorbance, Figure 5, correspond to the absorbance value of double the number of bilayers deposited. There was a linear increase in absorbency with number of bilayers; therefore, the mass of the film was increasing linearly too. The thickness of the PSS/PVP layers deposited by the LbL technique was calculated from QCM data and Figure 5 shows the film thickness versus number of bilayers. The average thickness of each PSS/PVP bilayer was estimated to be 9±0.7 nm. Since the results in Figure 4 showed that a single PSS layers is about 2-3 nm thick, each bilayer is composed mostly of PVP. The total thickness of the nanocoat containing PVP in three of the bilayers and on the outer surface was 30 nm which included the 2-3 nm thick PDDA precursor layer. This increased the weight of each particle by approximately 0.3 %. These results demonstrate the successful selfassembling of a PSS/PVP nanocoat on the cellulose fibers.

Powder flow properties of nanocoated cellulose

The flow properties of powders are of critical importance in the production of tablets by the direct compression method. The powder flow properties of the nanocoated cellulose fibers are listed in Table 1. For powders that flow the angle of repose is often used to indicate differences in flow properties. Angles ≤ 25º corresponds to excellent flow while angles > 50º indicates very poor flow. The uncoated cellulose fibers had an angle of repose of 64º indicating unsatisfactory flow. Although the angle of repose values, Table 1, indicated that the flow properties of the nanocoated powders were only passable (between 30-40º) it was similar to that of commercially available MCC powders (Geldart et al., 1990). According to Geldart's classification of powders

a Hausner ratio of 1.96 of the uncoated cellulose powder means it is poorly flowable and difficult to fluidize (Geldart, 1970). The Hausner ratios of all the nanocoated powders were < 1.25 indicating that they were non-cohesive with good flow, similar to that of Avicel PH102. Angle of repose and Hausner ratios was confirmed by the Carr's compressibility values listed in Table 1 (Hiestand, 2002). These powder flow property values indicated that LbL nanocoating changed the flow properties of the cellulose fibers from exceedingly poor to good. It also converted the cellulose fibers into powders that flowed as well or better than MCC powders. Powder flow was again tested on samples stored for 36 months at room temperature and the values obtained was within 5 % of the original test results. This shows the stability or the coatings.

Table 1. Compressibility and powder flow properties of the nanocoated cellulose particles. Type of flow was characterized according to Carr's compressibility values (Hiestand, 2002).

Nanocoating	Angle of Repose (°)	Hausner ratio	$C_{\%}$	Type of flow
Uncoated cellulose	64	1.96	49	Exceedingly poor
PDDA/PSS	38	1.23	15	Good
PDDA/Gelatin	38	1.16	17	Fair
PSS/Chitosan	41	1.22	28	Poor
Chitosan/Gelatin	38	1.18	20	Fair
PDDA + PSS (1:1)	37	1.17	15	Good
PSS/PVP	37	1.16	14	Good
Avicel PH101	41	1.32	24	Passable
Avicel PH102	36	1.17	14	Good

Compaction properties of nanocoated cellulose

Compaction studies, because they mimic the tableting process, were used to assess the mechanical properties of the nanocoated cellulose fibers. In Figure 6 the change in tensile strength versus compaction pressure for the nanocoated cellulose fibers is shown. In this study this relationship was used to measure the tabletability of vacuum dried powders using zero-pressure measurements (Sun, 2008). Since at both low and very high pressures considerable deviations of the experimental data occur due to particle rearrangements and strain hardening a pressure range of 60-360 MPa was used (Sun, 2008). Within this pressure range both cellulose and MCC undergo plastic deformation of the primary particles that contributed predominantly to the formation of compacts (Doelker, 1993). In this study the MCC powders used as controls formed intact tablets within this compaction pressure range. The results in Figure 6a show that cellulose fibers coated with a PSS/PVP nanocoat and tablets made from a 1:1 mixture of fibers with PDDA or PSS on the outer surface had the highest tensile strength over the entire compression range. The significantly higher tensile strength of the tablets containing PVP could be due to the excellent tablet binding properties of PVP (Horn and Ditter, 1982). In addition, a previous study has shown that when mixing oppositely charged LbL-treated pulps, then in addition to inter fiber hydrogen bonding, the electrostatic interactions between positive and negative fibers provide stronger bonding in the paper (Zheng et al., 2006). The PSS/chitosan coated cellulose compacts had the lowest tensile strength at each compaction pressure. There was no significant difference between the compaction properties of the other nanocoated fibers and the MCC powders. Tensile strength was measured for samples stored for 36 months at room temperature and the values obtained was within 5 % of the original test results for all the coated samples. This shows the stability of the coated cellulose fibers.

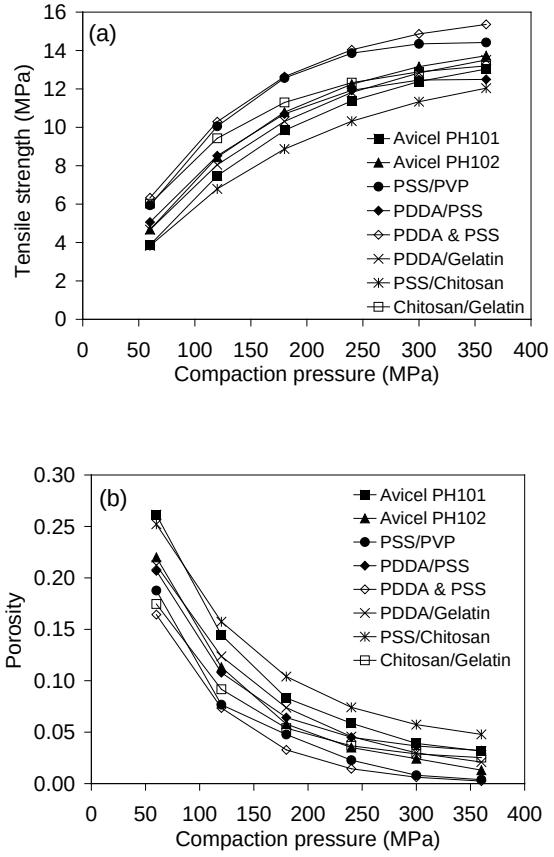

Figure 6. Influence of LbL nanocoating on the (a) tensile strength and (b) porosity of cellulose compacts as a function of compaction pressure. Each nanocoat was composed of four bilayers of the polyelectrolytes which included a precursor PDDA layer or PDDA/PSS bilayer. For comparison the compaction properties of Avicel PH101 and PH102 are also shown.

In powder compaction the observations of Heckel is often used to evaluate the stress of a material during compression (Heckel, 1961). In Figure 6b the effect of compression on the porosity of the powder compacts is shown. With increasing pressure, the density of all the powder increased leading to decreasing porosity. Within the pressure range studied a near straight-line relationship (mean R^2 = 0.994±0.003) existed between ln[1/1(1-D) and P (equation 6) for Avicel PH102, the PDDA/gelatin and PSS/PVP coated, and a 1:1 mixture of fibers with PDDA or PSS on the outer surface (Figure 7). For these powders tablet density approached zero porosity faster. This meant that they undergo more permanent plastic deformation to more effectively eliminate pores.

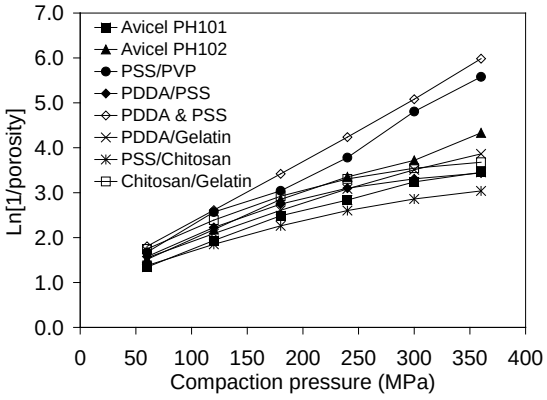

Figure 7. Heckel plots for LbL nanocoated cellulose particles and Avicel PH101 and PH102.

For these powders lower tablet porosity also resulted in larger areas of interparticulate bonding thus stronger tablets. Although linearity was not observed over the whole compression pressure range for the other nanocoated powders, linearity was seen for at least 60-240 MPa (mean R^2 = 0.99±0.004, Table 2). The mean yield pressure values calculated from the slope of the Heckel curve (equation 7) (Table 2) show that, compared to Avicel PH102, the PSS/PVP coated fibers and a 1:1 mixture of fibers with PDDA or PSS on the outer surface undergo plastic deformation at a lower compaction pressure. The greater compactibility of these powders was also evident from the AUC_H values because the AUC_H for the PSS/PVP powder was 1.3 and the mixture of positive and negative particles 1.2 large than that of Avicel PH102. The mean yield pressure and AUC_H indicate that these two nanocoated powders were the most ductile materials. Except for the PSS/chitosan coated fibers that was the least ductile the yield pressures and AUC_H values of the other nanocoated cellulose fibers were comparable to that of the MCC powders.

Even though cellulose powders are generally compactible the stability of these compacts depends on the ability of the materials to relieve stresses without undergoing brittle fracture. For example the uncoated cellulose powders formed compacts but were not able to relieve stress rapidly enough and the tablets always capped or laminated. In this study BFI values (equation 3) was used to measure the ability of compacts to withstand fracture (Hiestand, 1996). The BFI values (Table 2) for all the powders were < 0.2 and except for the Avicel PH102 that had the smallest BFI value, the BFI values of all the other powders were not significantly different ($p < 0.05$).

Table 2. BFI values and the mechanical properties of coated cellulose particles derived from Heckel analysis. The AUC_H was calculated over the entire compaction pressure range of 60-360 MPa. Results for the uncoated cellulose particles is not shown because compacts laminated upon compression over the entire compaction pressure range.

Nanocoating	Compaction pressure range (MPa)	BFI[a]	Py (MPa)	Heckel R^2	AUC_H
PDDA/PSS	60-240	0.11±0.03	118	0.989	892
PDDA/Gelatin	60-360	0.12±0.02	129	0.995	835
PSS/Chitosan	60-240	0.18±0.02	147	0.987	699
Chitosan/Gelatin	60-240	0.15±0.03	115	0.990	879
PDDA + PSS (1:1)	60-360	0.11±0.02	72	0.998	1157
PSS/PVP	60-360	0.09±0.02	78	0.992	1073
Avicel PH101	60-300	0.08±0.01	128	0.989	765
Avicel PH102	60-360	0.05±0.01	108	0.991	897

a BFI were calculated for tablets compacted to comparable tensile strength and porosity (see Table 3).

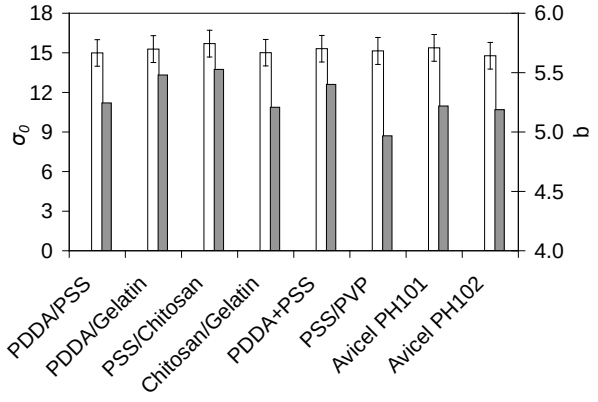

Figure 8. Change in the compactibility parameters σ_0 (non filled bars) and b (filled bars) for nanocoated cellulose fibers derived from the Ryshkewitch equation.

BFI values < 0.2 indicated that all the compacts were able to relieve stresses sufficiently such that brittle fracture was not significant (Hiestand, 1996). This meant that tablets made with the nanocoated cellulose fibers were not likely to cap or laminate when compacted under the compaction pressures used in this study. In addition, according to Hiestand (1996) experience has also taught that when BFI values are < 0.2, there will be no problem with fracture during tableting on a rotary press unless the bonding is very weak.

Compactibility can also be represented by a plot of tablet tensile strength versus porosity. In this study tensile strength versus porosity for the powders was plotted and the data were extrapolated using the exponential relationship shown in Equation 5 (Ryshkewitch, 1953; Roberts et al., 1995). For all the materials, except the uncoated cellulose fibers that did not form intact compacts, the correlation coefficient of the non-linear regression, R^2, was > 0.995. From these fits the maximum tensile strength at zero tablet porosity (σ_0) were extrapolated and the values are given in Figure 8. The mean σ_0 for all the powders was 15±0.3 MPa indicating no statistically significant difference ($p < 0.05$). This means that tablet tensile strength at a common porosity was approximately constant for all the nanocoated and MCC powders. The constant b in Equation 5 has been related to the pore distribution within a tablet (Roberts et al., 1995; Sun, 2008; Sun and Grant, 2001). Lower values of b are characteristic of homogeneous pore distribution, whereas higher values of b are indicative of inhomogeneous porosity. The results in Figure 8 show the b values for the materials used in this study. The average b = 5.3±0.2 (maximum 5.5 and minimum 5.0) is similar to that reported by others for MCC and indicate that in terms of tablet porosity, within the studied pressure range evaluated, the nanocoated cellulose produced compacts that were similar or better than MCC tablets. Although statistically not significant the b value for the PSS/PVP coated cellulose was the lowest and contributed most to the variance. Since b is the slope of the $\ln(\sigma)$ versus ε line, the lower b value corresponds to a slower increase in tensile strength as porosity is reduced.

Disintegration of compacts

The disintegration times of tablets compressed to similar solid fractions (0.94-0.96) and tensile strengths (11-13 MPa) are listed in Table 3. The uncoated cellulose compacts disintegrated the fastest because it formed very poor compacts that capped and laminated. Compacts of both Avicel PH101 and Avicel PH102 did not disintegrate within 100 minutes because although MCC

is a strong binder and good wicking agent it does not swell and when compacted on its own, does not disintegrate (Kumar et al., 2002). Tablets made with the PDDA/PSS nanocoated fibers and a 1:1 mixture of fibers with PDDA or PSS on the outer surface also did not disintegrate within 100 minutes. Compared to these and the MCC compacts tablets prepared with the LbL nanocoated cellulose fibers coated with gelatin, chitosan and PVP disintegrated within 50 minutes. Although the disintegration times was faster for compacts made with these powders tensile strength and porosity values still indicate that these powders are strong binders. Since, the tensile strength and solid fraction values obtained for tablets were comparable it appears that the difference seen in the disintegration times must be due to the wettability of the nanocoating (Wu et al., 2007). Contact angle measurements of the coated quartz resonators used for QCM analysis indicated that PDDA or PSS coating had contact angles between 30-40º while water spread completely on those coatings having chitosan, gelatin or PVP on the surface. This would make it easier for water to access and enter the compacts which in turn would promote disintegration.

Table 3. Disintegration times of tablets compacted to comparable tensile strength and porosity.

Nanocoating	Compaction pressure (MPa)	Tensile strength (MPa)	Solid fraction (%)	Disintegration time (min)
Cellulose	360	-	95.1	4±1
PDDA/PSS	240	11.4	95.5	> 100
PDDA/Gelatin	240	11.9	95.4	35±7
PSS/Chitosan	360	11.8	95.2	> 100
Chitosan/Gelatin	180	12.0	94.6	42±6
PDDA + PSS (1:1)	180	11.3	96.0	> 100
PSS/PVP	180	12.6	95.2	26±5
Avicel PH101	240	11.4	94.1	> 100
Avicel PH102	180	10.8	94.2	> 100

In order to determine if the nanocoatings have an influence on the release rate of a drug from tablets, dissolution tests were performed on tablets prepared from powder mixtures between coated cellulose fibers or MCC and APAP. The dissolution of tablets containing 30% and 60 % APAP were tested. APAP is poorly released from the tablets prepared from unmodified cellulose.

This is due to the fact that these tablets did not completely disintegrate during the dissolution analysis which slowed down the release of the drug from these tablets. However, it was seen that the dissolution profiles of the acetaminophen tablets made from coated fibers, and containing both 30% and 60% (w/w) APAP, were similar to the dissolution profiles of the tablets made with the MCC powder. Similarity was confirmed by f_2 calculations (SUPAC-IR, 1995). SUPAC-IR suggest that similarity between two dissolution profiles be concluded if f_2 is between 50 and 100, where 50 represents an average 10% difference at all sampling time points and 100 is the upper bound of f_2 when the distance at all sampling time points is 0. The results from the dissolution tests for cellulose fibers coated with PSS/PVP compared to uncoated fibers and MCC are shown in Figure 9.

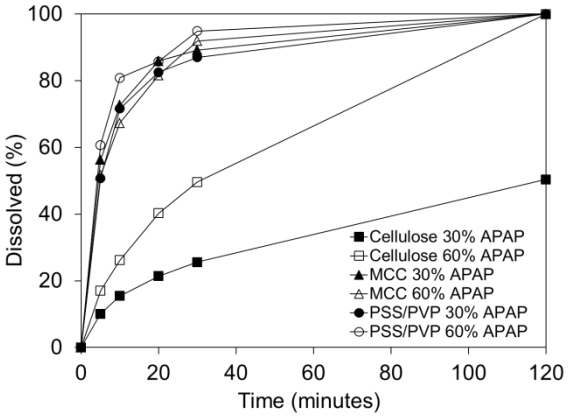

Figure 9. Dissolution profiles for APAP tablets prepared from blends of the drug and uncoated lignocellulose, lignocellulose LbL coated with PSS/PVP and uncoated MCC.

Conclusion

The results for the compactibility of nanocoated soft wood microfibers obtained in this study showed that LbL selfassembling of nano thin polymer layers on cellulose fibers can be used to produce cellulose based directly compactible tablet diluents. The powder flow properties and tableting indices of compacts compressed from these nanocoated microfibers were similar or

better than that of directly compactible MCC powders. Cellulose microfibers coated with four PSS/PVP bilayers had the best compaction properties while still producing tablets that were able to absorb water and disintegrate and for a model drug, APAP, produced tablets with similar dissolution profiles. Although the mechanism for improve compactibility of the coated cellulose fibers is not completely understood it is thought that a combination of better flow, better compression, and the addition of a nanocoat of the polymers that act as a binder all contributes to the improved performance of the nanocoated fibers when compared to MCC.

The advantages of using LbL nanocoating rather than traditional pharmaceutical coating processes are that it allows control of the molecular properties of the surface and the thickness of the coat to within a few nanometers, and that it add less than 1 % to the weight of the fibers. Although the LbL coating process involved milling, suspension, centrifuging (or filtering) and drying of coated fibers, this process is potentially friendlier to the environment because it uses biocompatible and degradable materials and does not involve acid-catalyzed hydrolysis and neutralization of depolymerized cellulose.

Acknowledgements

We are grateful to the University of Wisconsin, the North-West University, Louisiana Tech University and the National Research Foundation of South Africa (NRF) for research support. We want to thank Louwrens R. Tiedt from the Laboratory for Electron Microscopy, Faculty of Natural Sciences, North-West University, Potchefstroom, South Africa and Joseph Heintz from the Biological and Biomaterials, Preparation, Imaging and Characterization (BBPIC) laboratory at UW – Madison, Animal Sciences, for their assistance with the SEM and confocal microscopy.

References

Ai, H., Jones, S.A., De Villiers, M.M., Lvov, Y.M., 2003. Nano-encapsulation of furosemide microcrystals for controlled drug release. J. Controlled Release. 86(1), 59-68.

Aulton, M.E., 2000. Cellulose, powdered, in: Kibbe, A.H. (Ed.), Handbook of pharmaceutical excipients. Pharmaceutical Press, London, pp. 107-109.

Carr, R.L., Jr., 1965. Classifying flow properties of solids. Chem. Eng. 72(3), 69-72.

Chuayjuljit, S., Su-Uthai, S., Tunwattanaseree, C., Charuchinda, S., 2008. Preparation of microcrystalline cellulose from waste-cotton fabric for biodegradability enhancement of natural rubber sheets. J. Reinf. Plast. Compos. 28, 1245-1254.

De la Luz Reus Medina, M., Kumar, V., 2006. Evaluation of cellulose II powders as a potential multifunctional excipient in tablet formulations. Int. J. Pharm. 322, 31-35.

De la Luz Reus Medina, M., Kumar, V., 2007. Modified cellulose II powder: preparation, characterization, and tableting properties. J. Pharm. Sci. 96, 408-420.

De Geest, B.G., Déjugnat, C., Verhoeven, E., Sukhorukov, G.B., Jonas, A.M., Plain, L., Demeester, J., De Smedt, S.C., 2006. Layer-by-layer coating of degradable microgels for pulsed drug delivery, J. Controlled Release. 116, 159-169.

Doelker, E., 1993. Comparative compaction properties of various microcrystalline cellulose types and generic products. Drug Dev. Ind. Pharm. 19(17-18), 2399-2471.

Fell, J. T., Newton, J.M., 1970. Determination of tablet strength by the diametral-compression test. J. Pharm. Sci. 59(5), 688-691.

Geldart, D., 1973. Types of gas fluidization. Powder Technol. 7, 285-292.

Geldart, D., Mallet, M.F., Rolfe, N., 1990. Assessing the flowability of powders using angle of repose. Powder Handling & Processing. 2(4), 341−346.

Guidance for Industry: Immediate Release Solid Oral Dosage Forms; Scale-up and Postapproval Changes: Chemistry, Manufacturing, and Controls; In Vitro Dissolution Testing; In Vivo Bioequivalence Documentation. Center for Drug Evaluation and Research, Food and Drug Administration, November 1995.

Heckel, R.W., 1961. Density-pressure relations in powder compaction. Trans. Am. Inst. Min. Metall. Pet. Eng. 221, 671-675.

Hiestand, E.N., 1996. Rationale for and the measurements of tableting indices, in: Alderborn, G., Nystrom, C. (Eds), Pharmaceutical Powder Compaction Technology, Marcel Dekker, New York, pp. 219-244.

Hiestand, E.N., 2002. Mechanical and physical principles for powders and compacts. 2nd ed. SSCI, West Lafayette.

Horn, D., Ditter, W., 1982. Chromatographic study of interactions between poly(vinylpyrrolidone) and drugs. J. Pharm. Sci. 71(9), 1021-1026.

Huang, J., Ichinose, I., Kunitake, T., 2005. Nanocoating of natural cellulose fibers with conjugated polymer: hierarchical polypyrrole composite materials. Chem. Comm. 13, 1717-1719.

Kothari, S.H., Kumar, V., Banker, G.S., 2002. Comparative evaluations of powder and mechanical properties of low crystallinity celluloses, microcrystalline celluloses, and powdered celluloses. Int. J. Pharm. 232(1-2), 69-80.

Kumar, V., De la Luz Reus-Medina, M., Yang, D., 2002. Preparation, characterization, and tabletting properties of a new cellulose-based pharmaceutical aid. Int. J. Pharm. 235, 129-140.

Lieberman, H.A., Lachman, L., Schwartz, J.B. (Eds.), Pharmaceutical dosage forms: tablets. Marcel Dekker Inc., New York, pp. 362-387.

Lindner, H., Kleinebudde, P., 1994. Use of powdered cellulose for the production of pellets by extrusion spheronization. J. Pharm. Pharmacol. 46, 2-7.

Lvov, Y., Ariga, K., Ichinose, I., Kunitake, T., 1995. Assembly of multicomponent protein films by means of electrostatic layer-by-layer adsorption. J. Am. Chem. Soc. 117(22), 6117-6123.

Lvov, Y., Ariga, K., Kunitake, T., 1994. Layer-by-layer assembly of alternate protein/polyion ultrathin films. Chem. Lett. 12, 2323-2326.

Lvov, Y., Ariga, K., Onda, M., Ichinose, I., Kunitake, T., 1999. A careful examination of the adsorption step in the alternate layer-by-layer assembly of linear polyanion and polycation. Colloids Surf., A. 146(1-3), 337-346.

Lvov, Y., Decher, G., Möhwald, H., 1993. Assembly, structural characterization, and thermal behavior of layer-by-layer deposited ultrathin films of poly(vinyl sulfate) and poly(allylamine). Langmuir. 9, 481-486.

Lvov, Y.M., Grozdits, G.A., Eadula, S., Zheng, Z., Lu, Z., 2006. Layer-by-layer nanocoating of mill broken fibers for improved paper. Nord. Pulp. Paper Res. J. 21(5), 552-557.

Lu, Z., Eadula, S., Zheng, Z., Xu, K., Grozdits, G., Lvov, Y., 2007. Layer-by-layer nanoparticle coating on lignocellulose wood microfibers. Colloids Surf., A. 292, 56-62.

McCormick, D., 2005. Evolution in direct compression. Pharm. Technol. 4, 52-62.

Peck, G.E., Baley, G.J., McCurdy, V.E., Banker, G.S., 1989. Tablet formulation and design, in: Lieberman, H.A., Lachman, L., Schwartz, J.B. (Eds.), Pharmaceutical Dosage Forms: Tablets. Marcel Dekker Inc., New York, pp. 108-110.

Roberts, R.J., Rowe, R.C., York, P., 1995. The relationship between the fracture properties, tensile strength and critical stress intensity factor of organic solids and their molecular structure. Int. J. Pharm. 125, 157–162.

Ryshkewitch, E., 1953. Compression strength of porous sintered alumina and zirconia: 9th communication to ceramography. J. Am. Ceram. Soc. 36, 65-68.

Shangraw, R.F., Wallace, J.W., Bowers, F.M., Morphology and functionality in tablet excipients for direct compression. Pharm. Technol., 11, 136-143.

Stupińska, H., Iller, E., Zimek, Z., Wawro, D., Ciechańska, D., Kopania, E., Palenik, J., Milczarek, S., Steplewski, W., Krzyzanowska, G., 2007. An environment-friendly method to prepare microcrystalline cellulose. Fibres Text. East. Eur. 15, 167-172.

Sun, C.C., 2008. Mechanism of moisture induced variations in true density and compaction properties of microcrystalline cellulose. Int. J. Pharm. 346, 93-101.

Sun, C.C., Grant, D.J.W., 2001. Effects of initial particle size on the tableting properties of L-lysine monohydrochloride dihydrate powder. Int. J. Pharm. 215, 221–228.

Wu, T., Sun, Y., Li, N., De Villiers, M.M., Yu, L., 2007. Inhibiting surface crystallization of amorphous indomethacin by nanocoating. Langmuir. 23(9), 5148-5153.

Yang, S., Zhang, Y., Zhang, X., Guan, Y., Xu, J., Zhang, X., 2007. From cloudy to transparent: chain rearrangement in hydrogen-bonded layer-by-layer assembled films. ChemPhysChem. 8(3), 418-424.

Zheng, Z., McDonald, J., Khillan, R., Su, Y., Shutava, T., Grozdits, G., Lvov, Y.M., 2006. Layer-by-layer nanocoating of lignocellulose fibers for enhanced paper properties. J. Nanosci. Nanotech. 6(3), 624-632.

CHAPTER 3

This chapter was submitted to Nanomedicine: Nanotechnology, Biology and Medicine Journal.

STRYDOM, S.J., ROSE, W.E., OTTO, D.P., LIEBENBERG, W. & DE VILLIERS, M.M. 2013. Poly(amidoamine) Dendrimer-Mediated Synthesis and Stabilization of Silver Sulfonamide Nanoparticles with Increased Antibacterial Activity. Nanomedicine: Nanotechnology, biology and medicine, 9:85-93.

IMPACT FACTOR: 7.647

INSTRUCTION TO AUTHORS (SUMMARY)

Aims and Scope of the Journal

The mission of *Nanomedicine: Nanotechnology, Biology, and Medicine (Nanomedicine: NBM)* is to promote the emerging interdisciplinary field of nanomedicine. The scope of the journal is publishing medical research related to nanoscience and nanotechnology in the life sciences, with a special emphasis on theoretical, basic, preclinical, and clinical studies addressing diagnosis, treatment, monitoring, prediction, and prevention of diseases. Preferred topics include mechanistic insight into how nanoparticles influence cellular and sub-cellular mechanisms; improve imaging, diagnostics, and therapeutics; bioavailability, and toxicological assessment of nanomedicines; interactions of nanomaterials and nanodevices with cells, tissues, and living organisms; targeted delivery, pharmacokinetics and pharmacodynamics of nanomedicines; regenerative medicine; translational models for nanomedicine research, case studies, and clinical trials. The journal website also presents important nanomedicine-related information, such as future meetings, meeting summaries, Virtual Issues, news, funding opportunities, societal subjects, public health, point of care monitoring, nutrition, and ethical issues of nanomedicine. Manuscripts must fit the scope of the journal, i.e., it must be directly or closely related to medicine (diagnosis, treatment, monitoring, prognosis and prevention of diseases) and supporting biology, especially understanding biologic mechanisms related to nanoscience, nano-engineering and nano-technology research, i.e., research of man-made nanoscale objects, materials, and devices that improve medical procedures. Application of a nanoscale characterization techniques, such as STM, AFM, TEM, etc. is itself insufficient to qualify a work as nanomedicine. In vitro testing of materials and procedures is required, but in vivo is preferred with statistical

evaluation. Case studies are welcome. To ensure that a submitted manuscript fits the scope of the journal, authors may solicit a preliminary scope assessment from the Editor-in-Chief by emailing a brief synopsis (title, topic, authors, and abstract) to nnbm.editor@yahoo.com or nnbm.editor@gmail.com and cc their message to nnbm.journaloffice@gmail.com. The purpose of this is to eliminate those abstracts, which are undoubtedly out of scope. This evaluation is merely an advice and not an invitation. A positive scope assessment does not guarantee acceptance in any way, as adherence to scope is only one of the fundamental requirements.

Nanomedicine: NBM requires a $100 nonrefundable administrative fee for communications, original articles, scientific reviews, and case studies. Payment must be made through Submission Start. Exempt from this submission fee are Editorials, Perspectives, Letters, and manuscripts in which the corresponding author is an editorial board member or one of the Journal's top reviewers (those who have completed 5 or more reviews in the previous calendar year, or more than fifteen reviews over several years). In recent years, the number of manuscripts submitted each year has more than doubled, leading to a significant increase in the expenses related to the peer review process; the submission fee will help to offset a small portion of these expenses. Although this is the only fee required by the journal, this fee is non-refundable.

General Policies and Instructions for Authors

GENERAL REQUIREMENTS

1) The manuscript must be of INTERDISCIPLINARY nature, representing the overlapping fields of biology, and medicine with nanotechnology. 2) NOVELTY and ORIGINALITY are of primary importance. The results presented must significantly advance the field and improve scientific knowledge. Manuscripts with similar approaches that have already been undertaken by other groups should be submitted to appropriate journals. Originality of submissions is routinely checked by the editors using professional software. 3) SIGNIFICANCE: Accounts of research must appeal to a broad readership. In the cover letter, authors should provide a paragraph explaining how the work differs from the knowledge available in the literature and describe how it improves or has the potential to improve medicine. Experimental studies must include at least in vitro results, although in vivo is preferred. Accordingly, synthesis and characterization of nanotechnology-based medicines (i.e., substances that promote healing) must accompany bioavailability and toxicity data and

their comprehensive evaluation. Manuscripts that do not satisfy these general requirements will not be sent out for peer review and will be returned to the authors.

Article Types

Selection of the appropriate article type is very important because requirements do differ.

COMMUNICATIONS

Communications are to disseminate new observations quickly to the scientific community. Length of communications should not exceed 1,200 words (including body text, and figure legends), and the article should have no more than 4 figures. No more than 20 references should be cited. Include an Abstract of 150 words or less without internal subheadings.Upon acceptance, Communications enjoy priority in publishing and are entered into the next available issue.

ORIGINAL ARTICLES

Full-length articles describe a full account about hypothesis-based research or theory in nanomedicine. Length should not exceed 5,000 words (including body text, and figure legends), and the article should have no more than 6 figures in the main article. No more than 50 references should be cited. Include an Abstract of 150 words or less without internal subheadings. The body text should include the four separate headings: Background, Methods, Results, and Discussion. Use of supplementary materials is recommended for detailed descriptions (see below).

REVIEWS

Critical reviews of selected important topics in nanomedicine research are solicited from opinion leaders. Authors wishing to submit an unsolicited review should send the topic and title of the planned review along with names of authors and a brief, 250-word synopsis to nanomedicine@cox.net for pre-submission approval by the Editor-in-Chief. Length should not exceed 10,000 words (including body text, and figure legends), and the article should have no more than 15 figures. No more than 150 references should be cited in the review; additional references should be moved to the supplementary file(s). Include an Abstract of 150 words or less without internal subheadings.

PERSPECTIVES IN NANOMEDICINE

Invited articles or brief editorial comments that represent opinions of recognized leaders in nanomedicine research and are written for the general scientific readership. Length should not exceed 3,000 words (including body text, and figure legends).

LETTERS TO THE EDITOR

Letters to the Editor serves the purpose to comment on research published in *Nanomedicine: NBM*, including critical issues. Letters may not exceed 500 words with maximum 10 references, one illustration, and one table.

TECHNICAL AND COMMERCIALIZATION NOTES

Information regarding new technologies, business issues, commercialization of new products in the field, including intellectual property and patenting, nanotechnology law, etc. Length of technical notes should not exceed 1,500 words (including body text, and figure legends), 4 figures, and 10 references. Include an Abstract of 150 words or less without internal subheadings.

CASE STUDIES

These articles are descriptive or explanatory reports on actual clinical events based on an in-depth investigation of a single patient or small group of individuals, related to nanoparticles, nanostructures, or use of nanomedicines in real-life context. Length of case studies should not exceed 3,500 words (including body text, and figure legends) with a maximum of 6 figures and 20 references. Include an Abstract of 150 words or less without internal subheadings. Accepted case studies enjoy priority in publishing. Authors should provide in the manuscript only information essential for the discussion of results, and utilize the Supporting Materials file to provide all experimental details and other non-essential supporting information. There are no limitations for length, figures, and references in Supplementary Material. Communications and Original Articles complete with Supporting Materials must contain sufficient information to reproduce the experiments and data by someone experienced in the art.

Nanomedicine: Nanotechnology, Biology and Medicine

Poly(amidoamine) Dendrimer-Mediated Synthesis and Stabilization of Silver Sulfonamide Nanoparticles with Increased Antibacterial Activity (2013)

Schalk J. Strydom, MSc[a,b], Warren E. Rose, PharmD[a], Daniel P. Otto, PhD[c], Wilna Liebenberg, DSc[b], and Melgardt M. de Villiers, PhD[a,]*

[a]School of Pharmacy, University of Wisconsin-Madison, Madison, Wisconsin 53705-2222

[b]Unit for Drug Research and Development, Faculty of Health Sciences, North-West University, Potchefstroom, 2520, South Africa

[c]Catalysis and Synthesis Research Group, Chemical Resource Beneficiation Focus Area, Faculty of Natural Sciences, North-West University, Potchefstroom, 2520, South Africa

Short title: Dendrimer-coated silver antibiotic nanoparticles

This study was work was supported by NSF grant no. 0210298 "Nanoengineered Shells" and by a grant from AstraZeneca.

*Corresponding author. University of Wisconsin-Madison, School of Pharmacy, 777 Highland Avenue, Madison WI 53705-2222, USA. Phone: 608-890-0732. Fax: 608-262-5345. E-mail: mmdevilliers@pharmacy.wisc.edu.

Abstract

Silver sulfadiazine (AgSD) is a topical antibiotic with limited aqueous solubility. In this study, it was shown that poly(amido amine) (PAMAM) dendrimer complexes with sulfadiazine (SDZ) and silver could be used for a bottom-up approach to synthesize highly-soluble AgSD nanoparticles. These nanoparticles were stabilized against crystal growth by electrostatic layer-by-layer (LbL) coating with various PAMAM dendrimers. Additionally, silver nanoparticles can be incorporated in the dendrimer shells which augmented AgSD release. Nanoparticle formulation in a cream base provided a topical drug delivery platform with enhanced antibacterial properties against burn wound infections, comprising of three nanostructures i.e., AgSD and silver nanoparticles as well as PAMAM dendrimers, in one efficient, elegant nanosystem.

Keywords

silver antibiotic nanoparticles, PAMAM dendrimer, solubility, release, antibacterial

Background

The skin is essential for human survival since it provides a protective barrier between the internal tissues and the environment.[1] Burn wounds compromise this protective immune system barrier, subsequently easing the manifestation of bacterial infections in these wounds.[2] Burn wounds are protein-rich and consist of avascular necrotic tissues which limits the effective permeation of systemically-administered antibiotics in the treatment of these wounds.[3] Subsequently, topical antibacterial preparations are the basis for burn wound treatment and topical silver sulfadiazine (AgSD) is seen as the gold standard.[1,4] AgSD, a sulfonamide antibiotic, effects a dual inhibitory action on bacterial growth by its sulfa moiety (sulfadiazine – SDZ) that prevents bacterial folate absorption and subsequent DNA synthesis, whereas the silver that is released from AgSD binds and disrupts the DNA structure, precluding bacterial DNA replication.[5]

Poly(amidoamine) (PAMAM) dendrimers are dendritic polymers characterized by regular branching and radial symmetry.[6,7] PAMAM dendrimers have illustrated useful drug delivery and antimicrobial applications with amino-terminated dendrimers showing high antibacterial efficacy.[8,9,10,11] This is attributed to the electrostatic interaction between the cationic dendrimer and the anionic bacterial cell surface with resultant disruption of the lipid bilayer and consequent cell lysis.[8,12] Thus, by combination of an antibiotic such as sulfamethoxazole and PAMAM dendrimers, a synergetic antibacterial effect was demonstrated on bacterial cultures.[13]

The advent of nanotechnology and nanomedicine enabled scientists to synthesize and manipulate particles of highly insoluble drugs on the nanoscale, which subsequently increases the solubility of these drugs.[14] Since the antibacterial effect of AgSD is limited by its poor aqueous solubility, co-formulation with PAMAM dendrimers and/or the preparation of nanoparticles, represent alternative methods of improving its solubility and/or antibacterial effect, and this was subsequently studied.[14,15] Additionally, the thermodynamically favorable bottom-up synthesis approach employed here, illustrated a unique application of dendrimers in producing antibiotic nanoparticles that were also stabilized on a colloidal level by employment of the dendrimers for layer-by-layer (LbL) coating. This study reports one of the first accounts of the improved efficacy of the nanoparticles that were formulated in topical cream preparations as compared to commercial antibiotic equivalents.

Methods

Detailed descriptions of the materials methods can be found in the supplementary material.

Nanoparticle preparation by microfluidization

Ethylenediamine core PAMAM dendrimers were used in all instances to fabricate silver[16] and SDZ nanoparticle[17] complexes, utilizing microfluidization (microfluidizer model 110-Y, Microfluidics, Newton, MA, USA) (Figure 1 and supplemental material). Dendrimers are denoted in abbreviated form as generation(G)-PAMAM-terminal group. The optimized reactant mixture for production of the AgSD nanoparticles was G4.0-PAMAM-NH_2/Ag^+ (molar ratio of 1:1) and G4.5-PAMAM-COOH/SDZ (molar ratio of 1:1). The layer-by-layer coating process of the nanoparticles is described in the supplemental material.

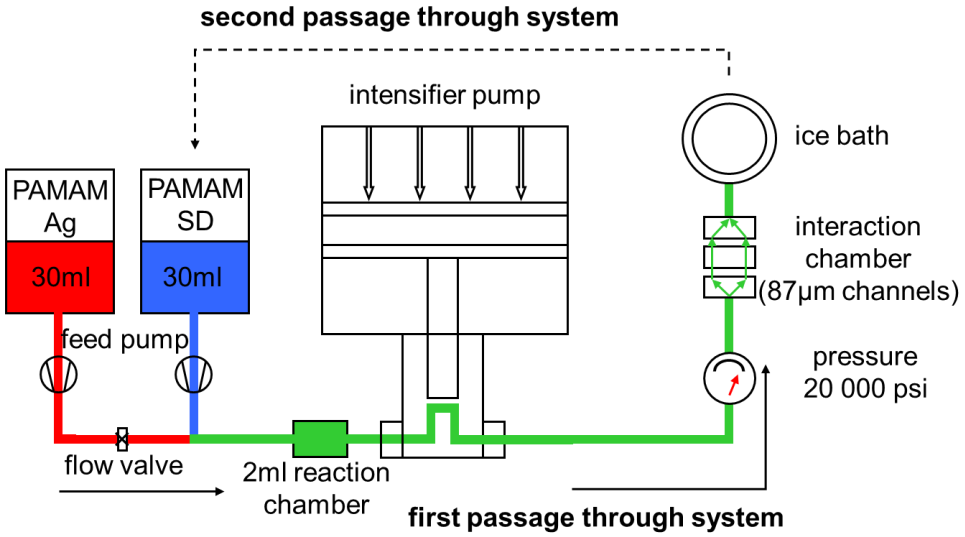

Figure 1: A schematic illustration of the microfluidizer used for preparing the AgSD nanoparticles.

Titration

Titration with ionic silver was employed to establish the degree of complexation between the dendrimers and SDZ.

Particle sizing

The size distribution and stability of these complexes were evaluated by dynamic light scattering (NICOMP 380 submicron particle sizer, Particle Sizing Systems, Santa Barbara, CA) for submicron sizing and light diffraction (Malvern Mastersizer X, Malvern, Worcestershire, UK) for particle sizing over 1 µm.

Particle morphology

Particle morphology was investigated by transmission electron microscopy (TEM) (JEOL USA, Inc., Peabody, MA, USA) and high resolution TEM with a Tecnai G2 S-Twin electron microscope (FEI, Hillsboro, Oregon, USA).

Structural analysis

X-ray powder diffraction (XRPD) (Bruker D8 Advanced diffractometer, Bruker, Germany) and Raman microscopy (Thermo Scientific DXR Raman microscope, Waltham, MA) revealed the structure and composition of the nanoparticles.

Quartz crystal microbalance with frequency dissipation

Quartz crystal microbalance frequency dissipation (QCM-D) (USI-Systems Inc., Fukuoka, Japan) was used to determine the layer thickness of coated nanoparticles.

Zeta potential measurements

Zeta potential measurements (Zeta-plus photon correlation spectroscopy and microelectrophoresis instrument, Brookhaven Instruments, Holtsville, NY) confirmed charge reversal during LbL coating.

Drug release

Enhancer cell accessories equipped to a dissolution tester (Vanderkamp 600, Van Kel Industries, NJ) was used to establish antibiotic release profiles from the formulated and dialysis for native nanoparticles (Slide-A-Lyzer dialysis cassettes) with the antibiotic assayed by high performance liquid chromatography (HPLC) (Thermo Separation Products, Waltham, MA) and silver by atomic absorption spectroscopy (Perkin Elmer model 5100 PC Zeeman atomic absorption spectrophotometer).

Antimicrobial efficacy

Antimicrobial efficacy was established through incubation of the nanoparticles and cream-based formulations thereof with burn-wound bacterial cultures.

Results

Characterization of complexes

The amount of Ag^+ that formed a complex with a single dendrimer molecule was calculated by titration of Ag^+ with standard solutions of amino- and/or carboxyl-terminated dendrimers (supplementary material Figure 3). G4.0 and G5.0-PAMAM-NH_2 dendrimers were complexed with 34 and 67 Ag^+ ions respectively. The G3.5 and G4.5-PAMAM-COOH dendrimers showed complexation values of 86 and 115 respectively. The PAMAM-NH_2 dendrimers had a lower Ag^+/dendrimer complex ratio compared to PAMAM-COOH dendrimers since a coordination complex between Ag^+ and the amine groups form, whereby two primary amines bind one silver ion.[16] Experimentally, this was correlated since the Ag^+/dendrimer ratios for G4.0 and G5.0-PAMAM-NH_2 were equal to approximately half the number of amino groups, 64 and 128, respectively.

For the G3.5- and G4.5-PAMAM-COOH dendrimers electrostatic complexes formed.[16] The Ag^+/dendrimer ratios for G3.5- and G4.5-PAMAM-COOH of 86 and 115 respectively, corresponded closer to the number of carboxylate functional groups of 64 for G3.5 and 128 for G4.5.[16] The weaker carboxylate-interaction complexes were selected to ensure the release of silver from the AgSD particles.

Similarly, the complexation efficiency between sulfadiazine (SDZ) and the dendrimers was studied in methanol. The number of SDZ associated with each dendrimer was calculated (supplementary material) as 24, 38, 38 and 68 molecules for G3.5-PAMAM-COOH, G4.0-PAMAM-NH_2, G4.5-PAMAM-COOH and G5.0-PAMAM-NH_2 respectively. Approximately a third of the carboxylate groups were complexed with SDZ for G3.5- and G4.5-PAMAM-COOH, whereas the number of SDZ molecules bound to the amino dendrimers approached half the number of amino groups in the G4.0- and G5.0-PAMAM-NH_2. The SDZ-amino dendrimer interaction was strongly electrostatic, whereas weak hydrogen bonding prevailed with carboxyl groups[17], therefore more SDZ molecules could complex with G4.0- and G5.0-PAMAM-NH_2 compared with G3.5- and G4.5-PAMAM-COOH dendrimers even though they have an equal number of terminal functional groups. Moreover, the SDZ has a large molecular volume compared to Ag^+ and experience steric hindrance to bonding at the surface. Despite the larger SDZ loading capacity on PAMAM-NH_2, weakly-complexed PAMAM-COOH was preferred to optimize the nanoparticle synthesis.

The motivation for using complexes comprising silver, dendrimers, and SDZ was dual purpose i.e., to increase the solubility of silver and SDZ, enhancing the reaction and yield of AgSD nanoprecipitates and to serve as templates the formation of nanoparticles from the molecules that they are complexed with.[18] The AgSD nanoparticle synthesis could only be effective if the silver and SDZ were free in solution[15], therefore the weak complexes, regardless of lower reagent loading, were selected for synthesis since it was still more effective than using raw materials. Ag^+ forms a weak complex with G4.0-PAMAM-NH_2 (34 Ag^+ complexed) and Ag^+ and SDZ reacts in a 1:1 stoichiometric ratio to form AgSD. Therefore, the weak G4.5-PAMAM-COOH/SDZ complex that contained 38 molecules of SDZ was utilized as counter reagent.

Dendrimers also aggregate with each other or other dendrimer molecules[19], due to hydrogen bonding, electrostatic interactions and/or physical entanglement of the dendrimer branches.[19,20] The Ag^+-loaded G4.0-PAMAM-NH_2 and SDZ-loaded G4.5-PAMAM-COOH dendrimers thus aggregated during AgSD nanoparticle synthesis due to electrostatic interaction optimized for pH[20] and AgSD nanoparticles precipitated by exceeding its poor aqueous solubility of 3.4 μg/mL.[15] Microfluidization was utilized to process the particles formed by the Ag-loaded G4.0-PAMAM-NH_2 and SDZ-loaded G4.5-PAMAM-COOH reactant mixture (Figure 1).

Particle size distribution and morphology

Dendrimer nanoaggregates

The G4.0-PAMAM-NH_2 and G4.5-PAMAM-COOH dendrimers showed bimodal size distributions as was anticipated if individual and self-aggregated dendrimer molecules present.[21] The mean particle size for 0.1 mM solutions of G4.0-PAMAM-NH_2 and G4.5-PAMAM-COOH were 23 nm and 18 nm respectively. However, a solution containing G4.0-PAMAM-NH_2 and G4.5-PAMAM-COOH dendrimers showed a unimodal size distribution with aggregates being 10-fold larger at 158 nm and 203 nm for 0.1 and 1 mM solutions respectively (supplemental material). The dendrimer mixtures illustrated a narrower size distribution, explained by the differences in the dominant intermolecular forces in the different aggregates of the system.[20] Aggregates comprising only a single type of dendrimer likely resulted from weak hydrogen bonding and physical entanglement, that could be abolished and reformed to produce size fluctuation. The stronger electrostatic interaction between G4.0-PAMAM-NH_2 and G4.5-PAMAM-COOH dendrimers produced more stable particle size distributions.[19,22]

AgSD nanoparticles and effect of dendrimer coating on AgSD nanoparticle size

AgSD nanoparticles processed with microfluidization were more uniform in size distribution as the number of process cycles was increased. After 3 processing cycles a unimodal size distribution was observed. The mean particle size increased with each of three successive cycles processing step, from 218 nm to 238 nm to 243 nm (Figure 2a).

The AgSD nanoparticles, suspended after three processing cycles, increased in particle size over the course of 240 minutes from 243 to 1400 nm (Figure 2b). The large surface free energy of the AgSD nanoparticles resulted in thermodynamic instability with resultant particle surface crystallization (Figure 2c) to minimize the free energy.[23]

Surface crystallization can be impeded by the application of a monomolecular polymer coating on a crystallizing surface.[24] Here, the electrostatic LbL method[25,26] was used to coat the silver sulfadiazine nanoparticles with polyions (supplementary material). Fig 2a and b show that the particle size growth was impeded by LbL coating, however not for anionic poly(styrene sulfonate) (PSS). AgSD nanoparticles showed a zeta potential of -23.9 to -25.9 mV in an aqueous medium (supplemental material). PSS has a negative surface charge resulting in weak repulsion[24] and phase separation of AgSD and PSS with resultant clustering and crystallization of the AgSD particles.

In contradiction, cationic poly(dimethyldiallyl ammonium chloride) (PDDA) completely suppressed surface crystallization due to inefficient complexation of silver ions which prevented their clustering

and crystallization. Additionally, PDDA layers have a greater magnitude in zeta potential than PSS[25] due to its quaternary ammonium substituent and this exceeded the limit for colloidal stability.

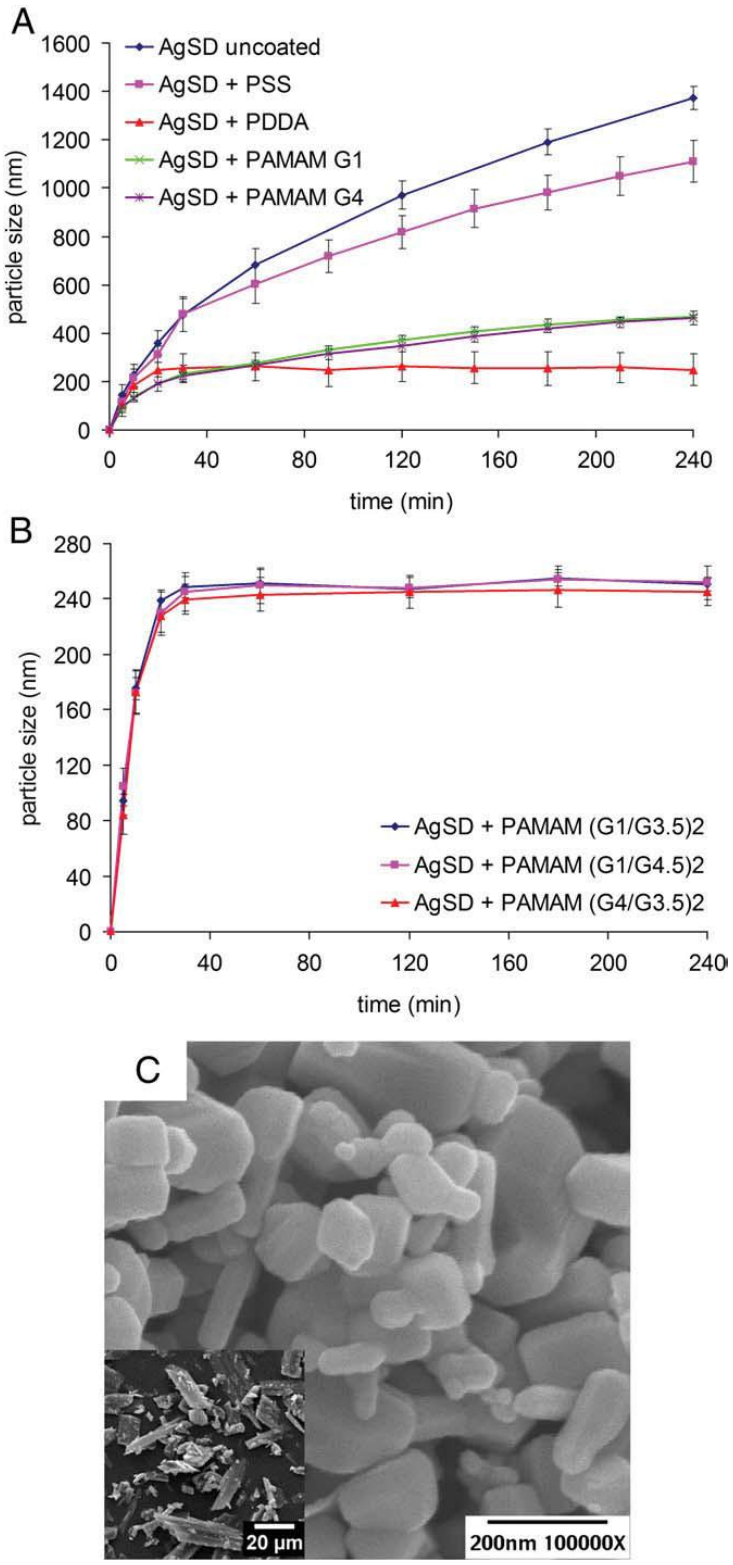

Figure 2. Time-correlated particle size analyses of the AgSD nanoparticles (a) uncoated, coated with polyions or dendrimers, (b) coated with different generation dendrimers and (c) SEM images of uncoated, crystallized AgSD nanoparticles suspended in water for 240 minutes and commercially available micronized AgSD with a mean particle size of 5.8 µm (insert).

The AgSD nanoparticles were also LbL coated with dendrimers[26,28,29] to determine if this would stabilize the nanoparticles. G1.0- and G4.0-PAMAM-NH_2 are cationic, G3.5- and G4.5-PAMAM-COOH are anionic. Since AgSD nanoparticles were anionic, the first nanocoat was either G1.0- or G4.0-PAMAM-NH_2 dendrimers, followed by either G3.5- or G4.5-PAMAM-COOH. The dendrimer double layers produced similar efficiency compared to PDDA without significant differences between the dendrimer generations (Figure 2a).

Dendrimer coatings averaged 0.73 nm thickness for G1.0-PAMAM-NH_2 dendrimer layers and 2.24 nm for G3.5- and G4.5-PAMAM-COOH layers. The application of two double layers of the dendrimers (Figure 2b) resulted in a 5.94 nm increase in the particle diameter which is equated to negligible 2.44% relative to the original 243 nm.

Furthermore, the thickness of each of the dendrimer coatings was less than the diameter of the individual dendrimer molecules i.e., 2.2 nm (G1.0-PAMAM-NH_2), 4.5 nm (G3.5-PAMAM-COOH) and 5.4 nm (G4.5-PAMAM-COOH)[6], suggesting that the dendrimer structure was highly compressed due to its multivalent grip on the substrate.[28]

Powder diffraction and Raman microscopy

The presence of silver and AgSD nanoparticles in the PAMAM-coated nanoparticles was observed from XRPD (supplementary material Figure 7). The diffraction peaks at 38.2°, 44.4°, 64.6°, 77.5°, and 81.6° 2θ correspond to silver and the high intensity peak at 10.3° 2θ is characteristic of AgSD.[15,33] The Raman spectra of the PAMAM-coated AgSD with additional added silver (supplemental material), agreed with that of the silver nanopowder, indicating the presence of silver nanoparticles. Both the XRPD and Raman microscopy results thus indicated that silver nanoparticles do form as a result of the interaction between ionic silver and the dendrimer molecules as reported.[33]

Drug release kinetics

Uncoated and PAMAM-coated AgSD micro- and nanoparticles

For AgSD nanoparticles to be effective in treating burn wounds the drug must be released from the nanostructure and comparative release studies of coated and uncoated systems were undertaken.

Comparative release profiles of SDZ from uncoated micronized and nanosized AgSD as well as dendrimer-coated nanoparticles with or without added silver followed the same trend (Figure 3).

AgSD nanoparticles illustrated a significantly faster initial zero-order release rate of 1.34 mg/h compared to the micronized AgSD (0.36 mg/h). This rate gradually decreases over time down to 0.35 mg/h to that of the micronized particles. During the initial phase of the release profile, the drug particles

still present a nanoscale size distribution and therefore expose a high surface area with a high rate of dissolution. However, the dissolution rate decelerated in the second phase since the nanoparticles have grown to microscale particles which present a comparatively lower dissolution surface area. This second phase dissolution rate approached that of the pristine microparticulate powders.

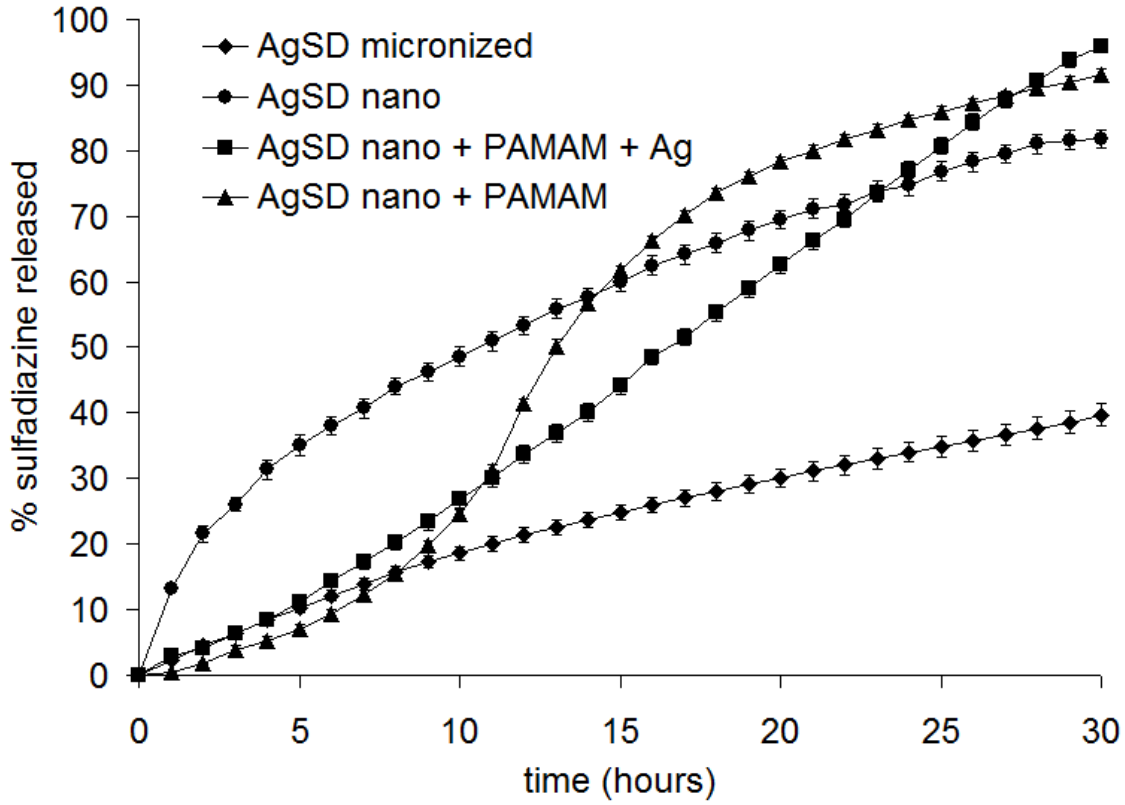

Figure 3. Release of sulfadiazine from uncoated microparticles, nanoparticles and PAMAM-coated nanoparticles with and without silver nanoparticles in the shell.

Moreover, the 81.8% of SDZ released from the nanoparticles after 30 hours was greater than the 39.7% from the micronized AgSD. This difference is attributed to the greater initial rate of release, resulting in a greater final amount of SDZ being released compared to that from micronized AgSD.

The initial release rate for dendrimer-coated nanoparticles of 0.30 mg/h (0 to 5 hours) was comparable to micronized AgSD. From 10 to 17 hours, the rate accelerated to 1.34 mg/h, similar to the initial dissolution rate of the uncoated AgSD nanoparticles. Thereafter, the rate tapered off to 0.26 mg/h (Figure 3). It was expected that the initial release rate from the PAMAM-coated particles would be similar to that of the uncoated nanoparticles due to their comparable size; however, this expectation was experimentally contradicted. Only after 10 hours could the release rate approach that of to the initial uncoated particles. This is explained by considering that the particles are surrounded by strongly interacting, compact PAMAM monolayers.[28] This nanocoating increased the path length of diffusion

slightly, however the coat was very compact suggesting interaction with the silver ions as cause of the significantly lower release rate of SDZ due to a decrease in the diffusion coefficient.[30]

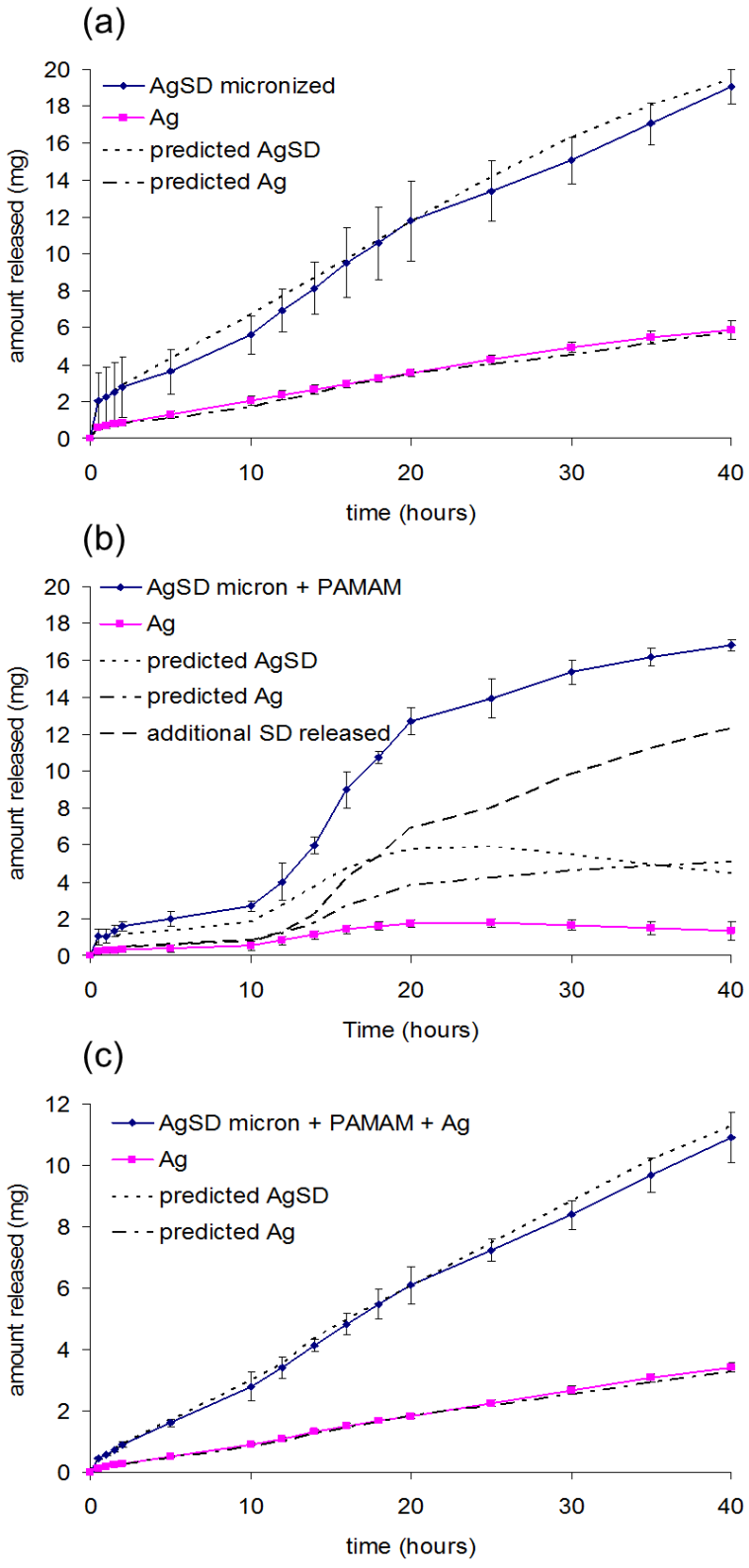

Figure 4. The experimental and predicted amounts of sulfadiazine and silver released from (a) uncoated micronized AgSD, (b) PAMAM-coated AgSD and (c) AgSD coated with PAMAM saturated with ionic silver.

The release observed between 10 and 20 hours is explained by the interaction between Ag^+ and dendrimer molecules which form coordinated or electrostatic bonds.[16] If the Ag^+ contained in AgSD had no interaction with the dendrimer monolayers, all the released silver should be derived from AgSD. Silver constitutes ~30.20 wt% of AgSD, and provides the theoretical amount to be released from AgSD[15] and experimental correlation was sought on this basis.

Figure 4a shows the silver release obtained for uncoated AgSD, and the results in Figure 4b were collected from PAMAM-coated AgSD. Figure 4c shows AgSD nanoparticles that were coated with PAMAM, however with additional Ag^+ added to saturate the dendrimer monolayers with ionic silver, followed by rinsing to eliminate any free silver. It can be seen in Figure 4a and c that the predicted amount of released SDZ and silver correlated with the experimentally determined quantities.

Since the uncoated AgSD contains no dendrimer molecules to interact with silver, the result in Figure 4a was expected. The results in Figure 3c indicate that the experimental and theoretical amount of SDZ and silver released corresponded, thus saturating the dendrimer monolayers with additional silver prevented the silver, liberated from AgSD, from interacting with the dendrimers.

Figure 4b shows that a greater amount of SDZ was released than predicted. This discrepancy arose from the interaction of Ag^+ with the dendrimers, which screened some of the charge in the LbL dendrimers. A more globular structure of the dendrimers resulted and the layers became more permeable due to relaxation of the dense multivalent grip with more space between adjacent dendrimer and/or polyelectrolyte layers for diffusion of SDZ.

The amount of released Ag^+, based on AgSD released, was experimentally lower than anticipated, since the prediction was based on the amount of AgSD and SDZ in solution. The Ag^+ from the free SDZ was complexed with the dendrimer molecules and not observed. Thus, AgSD clusters broke from the surface of the encapsulated nanoparticles and diffused through the LbL dendrimer layers whilst some Ag^+ dissociated from AgSD which aggregated within the dendrimers in the monolayers, releasing only SDZ. Since the solubility of SDZ (74 μg/mL) is 22 times higher than AgSD (3.4 μg/mL)[15,31], the increase in release of AgSD observed for the PAMAM-coated nanoparticles (Figure 3b) between 10 and 20 hours resulted from SDZ released due to charge screening by Ag^+, driving the release equilibrium positively.

The decrease in release from 20 to 30 hours resulted from depletion of the AgSD core since 91.5% SDZ released within 30 hours. The light-yellow suspension of PAMAM coated AgSD nanoparticles turned black towards the end of the release experiment (Figure 5a) with black spots observed on the surface of the AgSD nanoparticles (Figure 5b). These black spots indicated the presence of metallic silver nanoparticles that formed upon reduction of the silver ions which came in close contact with the dendrimer molecules in ambient ultraviolet light.[16,32]

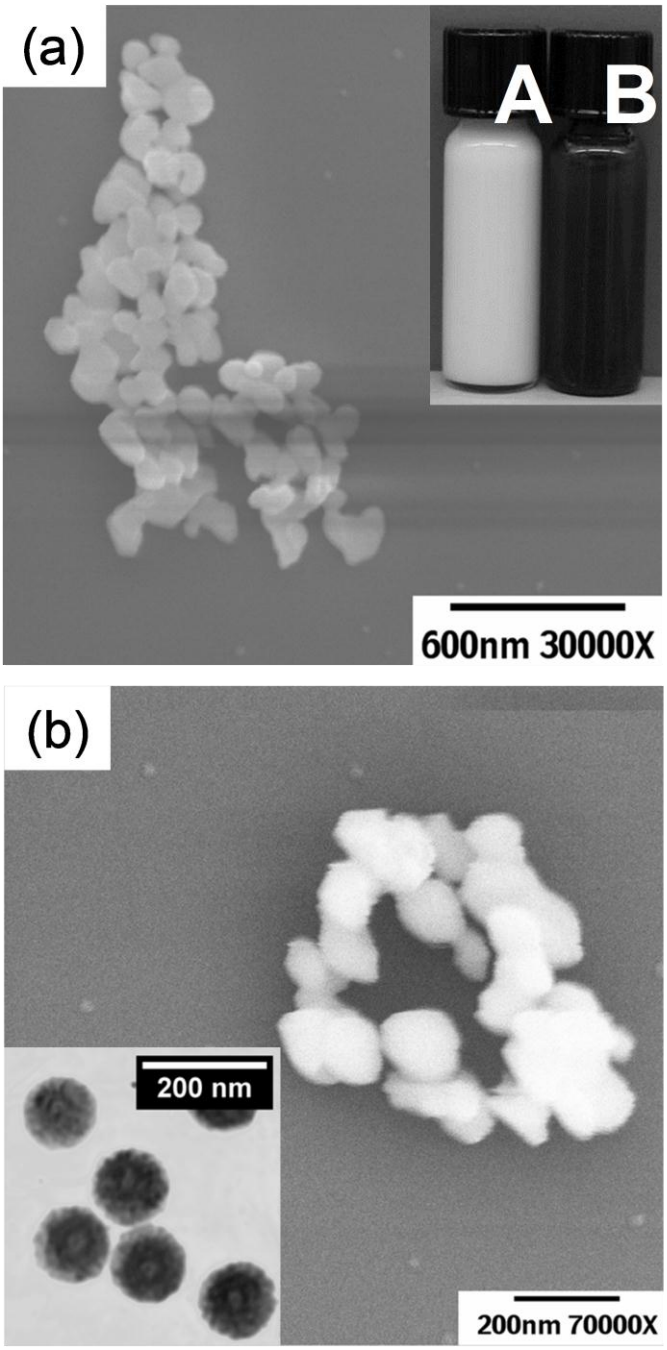

Figure 5. SEM images of (a) the AgSD nanoparticles; inserts shows (A) a fresh suspension of PAMAM-coated AgSD nanoparticles, and (B) the black suspension after dissolution. (b) SEM image of PAMAM-coated AgSD nanoparticles containing silver in the coating and an insert of a TEM micrograph showing the reduced silver nanoparticles on the surface of the AgSD.

Effect of added silver on drug release kinetics

To determine if the formation of the silver nanoparticles in the dendrimer monolayer influenced the release of SDZ from the coated nanoparticles, PAMAM-coated AgSD nanoparticles were prepared and ionic silver ($AgNO_3$) was added. This increased the likelihood of interaction between the dendrimers and the drug-bound Ag^+ from AgSD and a zero-order release pattern observed at 0.67 mg/h - twice the

rate from the PAMAM-coated nanoparticles was observed when silver was added. Any disruptions in the electrostatic forces in polyelectrolyte monolayers would markedly compromise the integrity of the multilayered LbL construct, increasing drug release.[34] It is possible that the dendrimer monolayers are weakened by the electrostatic interactions between silver and dendrimers weakening layer integrity, increasing the release compared to the unmodified PAMAM coating (Figure 3). Maximum SDZ release (~96%) from these saturated, coated nanoparticles was observed after 30 hours and was the largest quantity of SDZ released compared to the other particles.

Drug release from topical formulations of PAMAM-coated AgSD nanoparticles

Silver sulfadiazine is generally prescribed as a 1% (w/w) cream formulation to treat burn wound infections.[4,35] A cream containing 1% (w/w) PAMAM coated AgSD nanoparticles (based on AgSD) was compared to a commercial product containing only 1% AgSD. Addtionally, three different AgSD cream formulations (1% w/w AgSD), including micronized AgSD, PAMAM-coated AgSD nanoparticles and PAMAM coated AgSD nanoparticles saturated with Ag^{+}, were evaluated. Figure 6 depicts the release patterns of SDZ from creams that were generally comparable to the native (not formulated) nanoparticle release pattern (Figure 3) which implied that the same release mechanism was present in all systems.

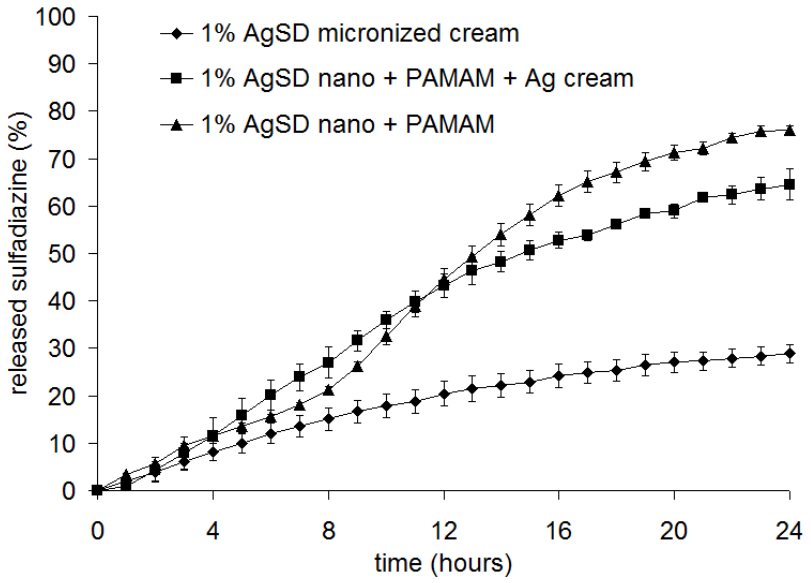

Figure 6. The release of sulfadiazine from different 1% (w/w) AgSD cream formulations.

However, the release rates of SDZ from the creams were markedly slower compared to the solution due to the higher viscosity of the creams. The cream formulated with micronized AgSD (commercial equivalent) released 28.9% of its SDZ content. However, the creams formulated with PAMAM-coated

AgSD nanoparticles, one of which was saturated with silver, released 76.0% and 64.5% respectively, equating a ~2.5 fold increase in SDZ release.

Antimicrobial efficacy

Table 1 and 2 as well as Figure 7 show the effect of the heightened release of SDZ from the topical dendrimer formulations against the most commonly-found burn wound bacteria[1,39] including ATCC *Staphylococcus aureus* 29213 and 25923, *Staphylococcus epidermidis* 12228, *Escherichia coli* 29212 and 25922, and *Pseudomonas aeruginosa* 27853 (supplementary material).

Dendrimers[8,12] and silver nanoparticles have inherent antibacterial properties[8,36,37,38], therefore three additional control creams containing only PAMAM or silver nanopowder and PAMAM with silver nanoparticles were formulated in equivalent quantities to amount of the substances in the AgSD creams. These control creams and the cream containing micronized AgSD demonstrated the smallest zones of inhibition.

Table 1

Antibacterial activity of the ingredients and their combinations (n=2)

Bacterial strains	Zone of inhibition (mm)			
	PAMAM	Ag	Ag + PAMAM	(AgSD) + (Ag PAMAM)
Staphylococcus aureus ATCC 29213	5.4±0.2	6.4±0.3	9.7±0.4	13.8±0.3
Staphylococcus aureus ATCC 25923	4.4±0.4	5.0±0.2	11.8±0.4	18.1±0.4
Staphylococcus epidermidis ATCC 12228	4.0 ± 0.2	4.8 ± 0.6	14.5 ± 0.4	23.9 ± 0.4
Escherichia coli ATCC 29212	4.5 ± 0.4	5.2 ± 0.4	8.2 ± 0.7	12.2 ± 0.5
Escherichia coli ATCC 25922	2.6 ± 0.5	4.2 ± 0.1	5.6 ± 0.8	10.9 ± 0.3
Pseudomonas aeruginosa ATCC 27853	4.1 ± 0.4	4.3 ± 0.1	10.9 ± 0.6	17.5 ± 0.4

Table 2

Antibacterial activity of AgSD cream formulations (n=2)

Bacterial strains	Zone of inhibition (mm)		
	AgSD micro	AgSD nano + PAMAM	Ag + nano+PAMAM + Ag
Staphylococcus aureus ATCC 29213	4.1 ± 0.2	35.6 ± 0.4	33.5 ± 0.5
Staphylococcus aureus ATCC 25923	6.3 ± 0.4	36.1 ± 0.3	34.2 ± 0.6
Staphylococcus epidermidis ATCC 12228	9.4 ± 0.4	45.2 ± 0.6	39.5 ± 0.4
Escherichia coli ATCC 29212	4.0 ± 0.5	19.4 ± 0.6	19.0 ± 0.3
Escherichia coli ATCC 25922	5.3 ± 0.3	24.0 ± 0.7	20.7 ± 0.7
Pseudomonas aeruginosa ATCC 27853	6.6 ± 0.2	17.9 ± 0.5	26.4 ± 0.4

Therefore, PAMAM dendrimers and the silver nanoparticles were less, or equally as effective at bacterial inhibition as the cream containing micronized AgSD. However, the zones of inhibition were largest for the creams comprising of the dendrimer-coated AgSD nanoparticles and with dendrimer-coats saturated with silver. No significant difference for the inhibitory effects of the different coated nanoparticles was illustrated; however the zone of inhibition of the coated AgSD nanoparticles was between 2 and 7 times greater (gram positive bacteria) and between 2 and 5 times greater (gram negative bacteria) than that of the micronized AgSD cream. No significant difference between the AgSD nanoparticles with and without silver nanoparticles in the dendrimer coating was demonstrated which suggested a limited contribution for the metallic silver to the antibacterial effect of the AgSD. Again it was suggested that the Ag^{+} was probably complexed to the dendrimers and not available for an antibacterial effect. Therefore, it was primarily SDZ and the dendrimers that resulted in the antibacterial effects.

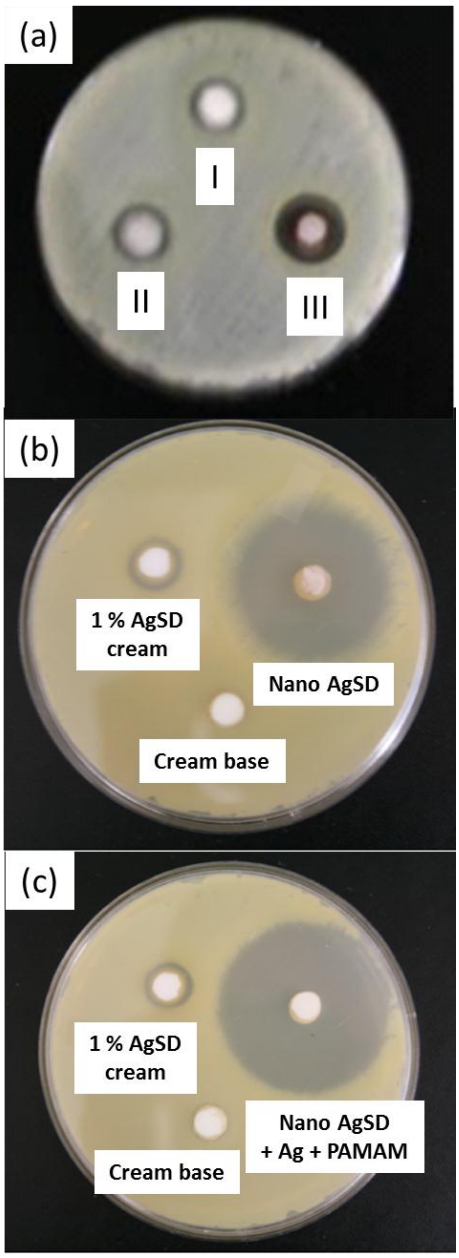

Figure 7. Photos of agar plates inoculated with *Staphylococcus aureus* (ATCC 2913), illustrating the inhibition zones for (a) cream formulations containing either PAMAM dendrimers (I), silver nanopowder (II) or a combination of PAMAM dendrimers and Ag nanopowder (III), (b) for the cream base, commercially available 1 % AgSD cream and a cream containing 1 % nano AgSD and (c) for the commercially available 1 % AgSD cream and a cream containing a PAMAM-coated 1 % AgSD nanoparticle formulation with Ag nanoparticles in the coating.

Dendrimers are able to cause cell lysis and increase membrane permeability to ultimately result in an antibacterial effect.[8,12] The antibacterial effect of AgSD resulted from both ionic silver that binds bacterial DNA, and the sulfadiazine moiety which precludes PABA assimilation in DNA, which ultimately increases the cell permeability to ionic silver.[5,40] The enhanced antibacterial effect of the AgSD nanoparticles resulted from both the increased amount of SDZ released from the nanoparticles, as well as the antibacterial effect of the PAMAM dendrimers, and perhaps to a lesser extent due to Ag nanoparticles in the coating.

Discussion

A novel application for PAMAM dendrimers was illustrated for a bottom-up approach to synthesize uncoated and multilayer-coated silver-containing antibiotic nanoparticles. Our approach illustrated several purposes for the utilized PAMAM dendrimers used here.

First, the dendrimers served as a solubility enhancer for a poorly water-soluble antibiotic, silver sulfadiazine. The increase in solubility of the antibiotic was illustrated by the fact that more sulfadiazine was observed in release studies for dendrimer-coated particles than for uncoated particles.

Second, by complexation of the dendrimers with ionic silver and sulfadiazine, a reactions system could be produced which resulted in a very efficient process to produce silver sulfadiazine (supplemental material). This process optimization coincided with the characterization of the formed complexes to select the best silver-complexed and sulfadiazine-complexed dendrimer reagents that were subsequently processed via microfluidization.

Third, the PAMAM dendrimers could impart significant colloidal stability to the produced nanoparticles if these were coated with dendrimers of different generation and type after production. It was illustrated that the LbL coating process stabilized these particles at the nanoscopic level at approximately 240 nm with an insignificant contribution to particle size growth due to coating.

Due to the colloidal and size stability introduced by the LbL coats on the nanoparticles, a much more efficient release of the antibiotic was seen due to the fact that surface crystallization, therefore particle growth, was impeded even over prolonged periods of time. This effectively increased the surface that was available to the release medium with resultant higher concentrations of the drug in solution.

Fourth, the results suggested that ionic silver could screen some of the charge in the multilayer-coated nanoparticles through interaction with the charged dendrimer layers. At first glance, one might assume that this phenomenon would preclude any beneficial antibacterial effects of silver in the antibiotic. However, it was revealed that the release equilibrium of sulfadiazine from the silver sulfadiazine could indeed be driven positively with significantly higher release values found for the coated nanoparticles in comparison to all the other tested systems. The screening effect or filtering of silver ions by the dendrimers could liberate more sulfadiazine that does not occur in systems devoid of dendrimer coats which are not capable of forming complexes with the silver ions or in particles of larger size.

As far as the antibacterial properties of the dendrimers were concerned, these showed some antibacterial effects although not as significant as when they contained the sulfonamide. However, this illustrated yet another beneficial property of the PAMAM dendrimers in addition to their use as excipient or reagent in the synthesis of the nanoparticles.

A well-known problem in modern day hospitalization is the occurrence of nosocomial or hospital-acquired infections caused by multiresistant pathogens. As stated, burn wound patients will have a compromised primary defense system due to the destruction of the skin barrier and easily acquire infections. In several cases, many of these patients will be hospitalized which puts them at even greater risk to not only acquire infections, but also virtually untreatable nosocomial infections.

Since systemic administration of antibiotics is ineffective in the treatment of these infections due to poor permeation of drug into these wounds, topical treatment is quintessential to curb infections, complications and even death. Several useful applications of antibiotic nanoparticles have been illustrated in bacterial susceptibility tests which evaluated commonly-found burn wound bacteria including *Pseudomonas*, *Staphylococcus* and *Escherichia* species. However these nanoparticles were incubated directly in these cultures without formulating them into topical dosage forms.

In this study, topical formulations of coated and uncoated nanoparticles were indeed formulated and evaluated to determine if the formulation did not hamper the effect of the antibiotic. Here, topical creams containing the synthesized antibiotic nanoparticles, demonstrated significantly higher release efficiencies compared to microparticulate commercial products. This enhanced release was seen even though the viscous environment of the cream stunted the release to some extent compared to solutions. Therefore, our formulations can be seen as very efficient. The PAMAM-coated, stabile silver sulfadiazine particles in the creams subsequently also resulted in markedly larger zones of inhibition in the burn wound bacterial cultures.

To conclude, one of the first accounts of the efficacy of a dosage form containing antibiotic nanoparticles was illustrated and characterized. This illustrated that nanotechnology-based dosage forms can be realized and create a realistic clinical platform for the treatment of burn wound infections. The PAMAM dendrimers used in this study proved crucial to the success of this dosage form and future applications of these molecules can be envisaged to create bottom-up processes to create effective nanomedicines.

References

1. Kooistra-Smid M, Nieuwenhuis M, Van Belkum A, Verbrugh H. The role of nasal carriage in *Staphylococcus areus* burn wound colonization. FEMS Immunol Med Microbiol 2009;57:1-13.
2. Alexander JW. Pathophysiologic events related to thermal injury of skin. J Trauma 1990;30:S70-5.

3. Erol S, Altoparlak U, Akcay MN, Celebi F, Parlak M. Changes of microbial flora and wound colonization in burned patients. Burns 2004;30:357-361.

4. Fox CL. Silver sulfadiazine – a new topical therapy for *Pseudomonas* in burns. AMA Arch Surg 1968;96:184-8.

5. Fox CL, Modak SM. Mechanism of silver sulfadiazine action on burn wound infections. Antimicrob Agents Chemother 1974;5:582-8.

6. Tomalia DA, Naylor AM, Goddard WA, III. Starburst dendrimers: molecular-level control of size, shape, surface chemistry, topology, and flexibility from atoms to macroscopic matter. Angew Chem Intl Eng Ed 1990;29:138-175.

7. Bielinska A, Kukowska-Latallo JF, Johnson J, Tomalia DA, Baker JR. Regulation of *in vitro* gene expression using antisense oligonucleotides or antisense expression plasmids transfected using starburst PAMAM dendrimers. Nucleic Acids Res 1996;24:2176-82.

8. Calabretta MK, Kumar A, McDermott AM, Cai C. Antibacterial activities of poly(amidoamine) dendrimers terminated with amino and poly(ethylene glycol) groups. Biomacromolecules 2007;8:1807-11.

9. Svenson S, Tomalia DA. Dendrimers in biomedical applications – reflections on the field. Adv Drug Delivery Rev 2005;57:2106-29.

10. Devarakonda B, Hill RA, Liebenberg W, Brits M, De Villiers MM. Comparison of the aqueous solubilization of practically insoluble niclosamide by polyamidoamine (PAMAM) dendrimers and cyclodextrins. Int J Pharm 2005;304:193-209.

11. Menjoge AR, Kannan RM, Tomalia DA. Dendrimer-based drug and imaging conjugates: design considerations for nanomedical applications. Drug Discovery Today 2010; 15:171-85.

12. Devarakonda B, Judefeind A, Chigurupati S, Thomas S, Shah GV, Otto DP, De Villiers, MM. The effect of polyamidoamine denrimers on the in vitro cytotoxicity of paclitaxel in cultured prostate cancer (PC-3M) cells. J Biomed Nanotechnol 2007;3:384-93.

13. Ma M, Cheng Y, Xu Z, Xu P, Qu H, Fang Y, Xu T, Wen L. Evaluation of polyamidoamine (PAMAM) dendrimers as drug carriers of anti-bacterial drugs using sulfamethoxazole (SMZ) as a model drug. Eur J Med Chem 2007;42:93-8.

14. Shaffer C. Nanomedicine transforms drug delivery. Drug Discovery Today 2005;10:1581-2.

15. Bult A, Plug CM. Silver Sulfadiazine: In: Analytical Profiles of Drug Substances, Volume 13, Florey, K. Ed.; Academic Press: New York, 1984, 553-71.

16. Kéki S, Török J, Deák G, Daróczi L, Zsuga MJ. Silver nanoparticles by PAMAM-assisted photochemical reduction of Ag(+). Colloid Interface Sci 2000;229:550-3.

17. Prieto MJ, Bacigalupe D, Pardini O, Amalvy JI, Venturini C, Morilla MJ, Romeo EL. Nanomolar cationic dendrimeric sulfadiazine as potential antitoxoplasmic agent. Int J Pharm 2006,326:160-8.

18. Jin L, Yang SP, Wu HX, Huang WW, Tian QW. Preparation and characterization of silver nanoparticles with dendrimers as templates. J Appl Polym Sci 2008;108:4023-8.

19. Wang BB, Zhang X, Jia XR, Li ZC, Ji Y, Yang L, Wie Y. Fluorescence and aggregation beahvior of poly(amidoamine) dendrimers peripherally modified with aromatic chromophores: the effect of dendritic architectures. J Am Chem Soc 2004;126:15180-94.

20. Jasmine, M.J, Kavitha, M, Prasad E. Effect of solvent-controlled aggregation on the intrinsic emission properties of PAMAM dendrimers. J Luminescence 2009;129:506-13.

21. Topp A, Bauer BJ, Prosa TJ, Scherrenberg R, Amis EJ. Size change of dendrimers in concentrated solution. Macromolecules 1999;32:8923-31.

22. Carbone P, Müller-Plathe F. Molecular dynamics simulations of polyaminoamide (PAMAM) dendrimer aggregates: molecular shape, hydrogen bonds and local dynamics. Soft Matter 2009;5:2638-47.

23. Nesamony J, Kolling WM. IPM/DOSS/water microemulsions as reactors for silver sulfadiazine nanocrystal synthesis. J Pharm Sci 2005;94(6):1310-20.

24. Wu T, Sun Y, Li N, De Villiers MM, Yu L. Inhibiting surface crystallization of amorphous indomethacin by nanocoating. Langmuir 2007;23:5148-53.

25. Strydom SJ, Otto DP, Liebenberg W, Lvov YM, De Villiers MM. Preparation and characterization of directly compactible layer-by-layer nanocoated cellulose. Int J Pharm 2011;404:57-66.

26. Khopade AJ, Caruso F. Electrostatically assembled polyelectrolyte/dendrimer multilayer films as ultrathin nanoreservoirs. Nano Letters 2002;2:415-8.

27. Ai H, Jones SA, De Villiers MM, Lvov YM. Nano-encapsulation of furosemide microcrystals for controlled drug release. J Controlled Release 2003;86:59-68.

28. Tsukruk VV, Rinderspacher F, Bliznyuk VN. Self-assembled films from dendrimers. Langmuir 1997;13:2171-6.

29. Khopade, A.J.; Caruso, F. Investigation of the factors influencing the formation of dendrimer/polyanion multilayer films. Langmuir 2002;18:7669-76.

30. Vergnaud JM. Controlled Drug Release of Oral Dosage Forms; Ellis Horwood: New York, 1993, p. 346.

31. Stober, H.; DeWitte, W. Sulfadiazine: In: Analytical Profiles of Drug Substances, Volume 11, Florey, K. Ed.; Academic Press: New York, 1984, 523-51.

32. Liu Z, Wang X, Wu H, Li C. Silver nanocomposite layer-by-layer films based on assembled polyelectrolyte/dendrimer. J Colloid Interface Sci 2005;287:604-11.

33. Li L, Cao X, Yu F, Yao Z, Xie Y. G1 dendrimers-mediated evolution of silver nanostructures from nanoparticles to solid spheres. J Colloid Interface Sci 2003;261:366-71.

34. Shutava T, Prouty M, Kommireddy D, Lvov Y. pH responsive decomposable layer-by-layer nanofilms and capsules on the basis of tannic acid. Macromolecules 2005;38:2850-8.

35. Fraser JF, Bodman J, Sturgess R, Faoagali J, Kimble RM. An in vitro study of the anti-microbial efficacy of a 1% silver sulphadiazine and 0.2% chlorhexidine digluconate cream, 1% silver sulphadiazine cream and a silver coated dressing. Burns 2004;30:35-41.

36. Balogh L, Swanson DR, Tomalia DA, Hagnauer GL, McManus AT. Dendrimer-silver complexes and nanocomposites as antimicrobial agents. Nano Letters 2001;1:18-21.

37. Morones JR, Elechiguerra JL, Camacho A, Holt K, Kouri JB, Ramíres JT, Yacaman MJ. The bacterial effects of silver nanoparticles. Nanotechnol 2005;16:2346-53.

38. Kim JS, Kuk E, Yu KN, Kim JH, Park SJ, Lee HJ et al. Antimicrobial effects of silver nanoparticles. Nanomed Nanotechnol Biol Med 2007;3:95-101.

39. Busch NA, Zanzot EM, Loiselle PM, Carter EA, Allaire, JE, Yarmush ML, Warren HS. A model of infected burn wounds using *Escherichia coli* O18:K1:H7 for the study of gram-negative bacteremia and sepsis. Infect Immun 2000;68:3349-51.

40. Richards RME, Xing DKL. Evaluation of synergistic effects of combinations of antibacterials having relevance on burn wound infections. Int J Pharm 1991;75:81-7.

Supplementary Material

Poly(amidoamine) Dendrimer-Mediated Synthesis and Stabilization of Silver Sulfonamide Nanoparticles with Increased Antibacterial Activity

Schalk J. Strydom, MSc[a,b], Warren E. Rose, PharmD[a], Daniel P. Otto, PhD[c], Wilna Liebenberg, DSc[b], and Melgardt M. de Villiers, PhD[a,*]

[a]School of Pharmacy, University of Wisconsin-Madison, Madison, Wisconsin 53705-2222

[b]Unit for Drug Research and Development, Faculty of Health Sciences, North-West University, Potchefstroom, 2520, South Africa

[c]Catalysis and Synthesis Research Group, Chemical Resource Beneficiation Focus Area, Faculty of Natural Sciences, North-West University, Potchefstroom, 2520, South Africa

Materials

The following materials were purchased: micronized silver sulfadiazine USP (with an average particle size of 5.8 μm) and sodium sulfadiazine USP (Spectrum Chemicals & Laboratory Products, Gardena, CA), silver nanopowder (average particle size of less than 100 nm), silver nitrate and ethylene diamine core poly(amidoamine) (PAMAM) dendrimers, G1.0-PAMAM-NH_2, G3.5-PAMAM-COOH, G4.0-PAMAM-NH_2, G4.5-PAMAM-COOH and G.5.0-PAMAM-NH_2(Sigma-Aldrich, St. Louis, MO.). Hydrophilic ointment (Aquaphilic®) was obtained from Medco Lab Inc. (Sioux City, IA). milli-Q water with a resistivity of 18.2 MΩ.cm was used throughout this study. All other reagents were of analytical grade.

Methods

Experimental procedures

Preparation of sulfadiazine nanoparticles

For silver-dendrimer complexation experiments, the method of Keki et al. was followed.[1] The complex formation between sulfadiazine and the dendrimers was carried out according to the method of Prieto et al.[2] A bottom-up synthesis process was used to produce nanosuspensions of silver sulfadiazine because it allows the formation and stabilization of nanosuspensions without the need for size reduction. This method is based on the observation that when equimolar aqueous solutions of G4.0- and G5.0-PAMAM-NH_2/Ag complexes and G3.5- and G4.5-PAMAM-COOH/SDZ complexes are mixed, silver sulfadiazine (357.14 g/mol) was produced and was precipitated from these solutions because of its low solubility product ($K_{SP} \sim 8 \times 10^{-12}$ at pH 7 and 25ºC).

This method was refined and scaled-up by using a modified Microfluidizer (model 110-Y, Microfluidics, Newton, MA, USA) process. In the modified process the two separate reactant solutions, 0.001 M G4.0-PAMAM-NH_2 complexed with silver and 0.001 M G4.5-PAMAM-COOH complexed with sulfadiazine, were pumped into a 2 mL reaction chamber. The microfluidizer contains an air-powered intensifier pump designed to supply the desired pressure at a constant rate to the product stream coming from the reaction chamber. As the pump travels through its pressure stroke, it drives the product at constant pressure through precisely defined fixed-geometry microchannels within an interaction chamber. As a result, the product stream accelerates to high velocities, creating shear rates within the product stream, which ensures uniform particle size and deagglomeration (extrusion) of the silver sulfadiazine nanoparticles produced after synthesis.

Crystallization experiments were conducted at 138 MPa (20,000 psi) process pressure. The interaction chamber that was used had a minimum channel dimension of 87 µm. After the initial synthesis process the silver sulfadiazine nanosuspensions were passed an additional two times through the microfluidizer. Then the dispersions were centrifuged to separate the solids from the dendrimer solvent mixtures. The solids were then rinsed with water, filtered, and either air dried or dried in a vacuum oven. Figure 1 illustrates the microfluidization methodology used here.

In order to prepare AgSD nanoparticles with a uniform size on a large scale, 30 mL each of the G4.0-PAMAM-NH_2/Ag and G4.5-PAMAM-COOH/SDZ solutions were processed three times through a microfluidizer.

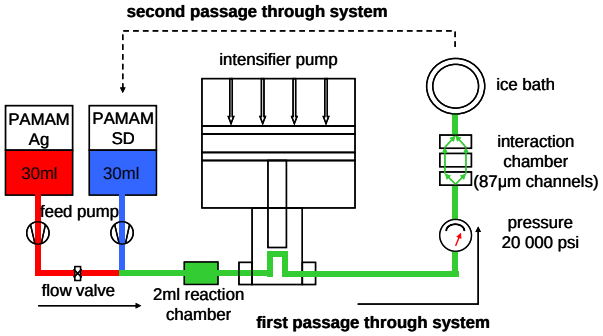

Figure 1. A schematic illustration of the microfluidizer used for preparing the AgSD nanoparticles.

This resulted in the average synthesis of 0.652 g of nanoparticles consisting of 99.16% AgSD, determined by HPLC analysis, yielding 88.7% product.

LbL coating of nanoparticles: QCM-D

Prior to polyion multilayer formation on SDZ nano crystals, the coating procedure was elaborated on gold electrode resonators of a 9-MHz quartz crystal microbalance (USI-Systems Inc., Fukuoka, Japan). The resonators were immersed in a polyion solution for 15 min, removed, and dried. The added mass and the coating thickness (ΔL) was calculated from the frequency shift (ΔF), according to the Sauerbrey equation, using a special scaling. For the instrument used in this study, the calibration was ΔL (nm) = 0.017 ΔF (Hz).

LbL coating of nanoparticles: zeta potential measurements

To ensure the reversal of charge after each polyion coating, the zeta-potential of the suspended particles were measured and the reported results represents the mean of 10 measurements determined with a Zeta-plus photon correlation spectroscopy and microelectrophoresis instrument (Brookhaven Instruments, Holtsville, NY, USA). All measurements were performed in air-equilibrated 1 mM KCl solution.

LbL coating method

The electrostatic layer-by-layer method was used to coat the silver sulfadiazine nanoparticles by the layer-by-layer self-assembly technique. The bare, negatively charged particles (1 mL of a 10 wt % dispersion) were incubated with 10 mL of positively charged electrolyte solution (1 mg/mL containing 0.154 M NaCl) for 5 min, followed by centrifugation (Eppendorf 5804R centrifuge at 1,000 g). Recovered coated nanoparticles were washed twice and then redispersed in 1 mL of water before further assembly. 1 mL of a negatively charge electrolyte solution (1 mg/mL containing 0.154 M NaCl) was then added to the particle dispersion, 5 min was allowed for adsorption, and another centrifugation and two wash cycles were performed. The adsorption steps were repeated to build multilayers on the silver sulfadiazine nanoparticles. Figure 2, illustrates the process.

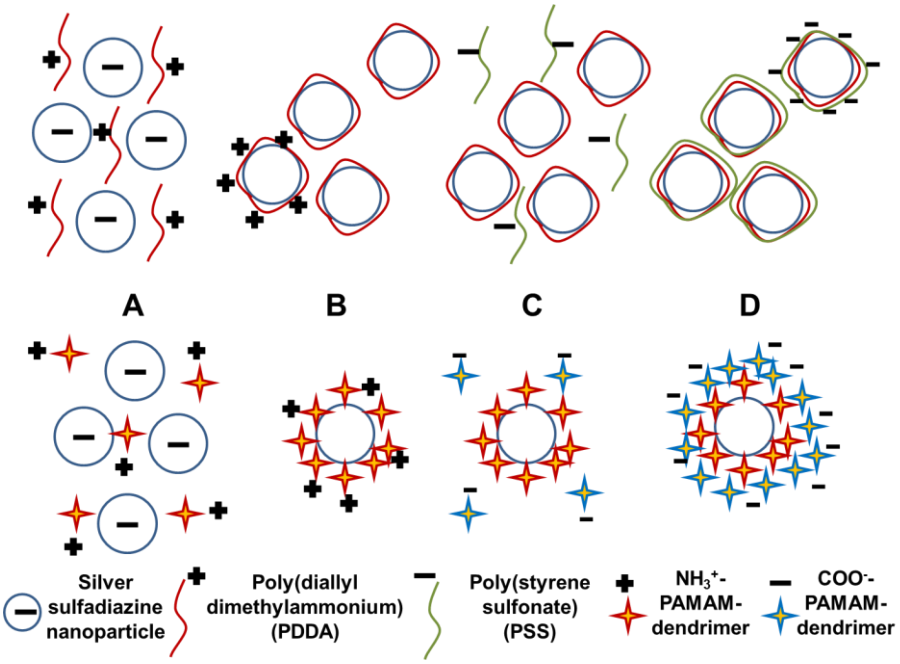

Figure 2. The layer-by-layer coating process is illustrated for the recovered, pristine AgSD nanoparticles that were synthesized with G4.0-PAMAM-NH_2/Ag and G4.5-PAMAM-COOH/SDZ reactants. The negatively charged, pristine nanoparticles are suspended in NaCl buffer containing (A, top) the polycation, PDDA or (A, bottom) a dendrimer solution containing the positively charged NH_2-terminated PAMAM dendrimer. Adsorption of the polyions takes place to form either polycation-coated (B, top) or NH_2-PAMAM-dendrimer-coated nanoparticles (B, bottom) to produce particles with an excess positive charge. The coated particles are washed to remove unbound polyions preceding coating of the positive nanoparticles with (C, top) the polyanion, PSS or the negatively charged COOH-terminated-dendrimer (C, bottom) and the nanoparticles now assume a net negative charge as seen in (D) after washing off the unbound polyions. Therefore, the dendrimers used to coat were fresh solutions

of the dendrimers and not the same as those used for manufacturing the nanoparticles. The charge reversal is reflected as polarity changes in the zeta potential measurements.

Release of silver sulfadiazine from nanoparticles

In vitro release of silver sulfadiazine was measured by a dialysis technique. The dialysis technique made use of Slide-A-Lyzer dialysis cassette (3 to 12 mL capacity) with low-binding regenerated cellulose (MWCO = 10,000 g/mol). Nanoparticles were suspended in the dissolution medium at a concentration equivalent to 2 mg/ml SDZ. Samples were taken from the solutions (10 mL equivalent to 20 mg silver sulfadiazine) and transferred immediately to the dialysis cassettes. The cassettes were promptly placed in 500 mL glass-jacketed beakers containing 400 mL of the dissolution medium maintained at 32ºC. The dissolution medium consisted of a solution of 100 mM acetate buffer, pH 6.0. The outer phase, receptor medium, was stirred continuously with a magnetic stirrer and sampling (10 mL) was made at specific time intervals followed by replenishment with 10 mL fresh, heated buffer. The dialysis apparatus was completely covered with aluminum foil to prevent photochemical degradation of silver sulfadiazine.

Release of silver sulfadiazine nanoparticles from a cream base

The enhancer cell used in this study consisted of a metal load ring, a cap, a membrane and a drug reservoir. The ointment was placed in the drug reservoir (2 cm diameter) on top of the membrane. The membrane used in this study a cellulose acetate with a pore size of 0.45 μm soaked in 15% oleic acid in isopropyl myristate. A metal load ring was used to keep the membrane and the washer in place during the cap application. Finally, the bottom screw was tightened to bring the ointment, or semisolid preparation, in complete contact with the membrane certain that no entrapped air is present at the interface of the ointment and the membrane.

A USP Six Spindle Dissolution Tester (Vanderkamp 600, Van Kel Industries, NJ, USA) with modified flask assemblies substituting of 200 mL for the standard 900 mL flasks and smaller-sized paddles, were used to measure drug release from the enhancer cell assembly. The paddles were rotated at 100 rpm. The dissolution medium consisted of a solution of 100 mM acetate buffer, pH 6.0 and the temperature was controlled at a constant of 32°C and exact volume samples were withdrawn at 1 hour intervals from each vessel up to 24 hours. The volume withdrawn was replaced with an identical volume of fresh medium.

A correction factor was applied in the calculations to account for the drug loss during sampling. For each sample a set of six diffusions were run to obtain cumulative release profiles.

Antibacterial activity of cream with nanoparticles

A modified agar well dilution technique compared the inhibitory zone for antibacterial activity of AgSD, AgSD-dendrimer, and nanoparticle AgSD -dendrimer creams against common organisms associated with burn infections (ATCC *Staphylococcus aureus* 29213 and 25923, *Staphylococcus epidermidis* 12228, *Escherichia coli* 29212 and 25922, and *Pseudomonas aeruginosa* 27853).

The bacteria were incubated for 18 to 24 hours at 37ºC on Mueller-Hinton agar (MHA). The resulting colonies were suspended in normal saline to a turbidity measurement consistent with a 0.5 McFarland standard. An inoculum of ~10^6 cfu/mL was obtained by spreading 200 μL of the organism suspension onto freshly prepared MHA plates.

Three agar wells were created in each plate using a 6 mm diameter tube to remove the agar. The wells were filled with 200 μL of cream, allowed to settle at room temperature for 1 hour and incubated for 18 to 24 hours at 37ºC. The three different cream types were evaluated in the same plate for each organism to ensure accurate comparisons in antibiotic activity. The resulting zone of inhibition was measured in millimeters with vernier calipers and compared to the control AgSD cream. All antibacterial experiments were performed in duplicate for reproducibility.

Analytical procedures

Particle sizing

Light scattering experiments were performed to measure the size of the nanoparticles using a NICOMP 380 submicron particle sizer (Particle Sizing Systems, Santa Barbara, CA, USA) equipped with a He-Ne laser (45 mW, 644 nm wavelength), an avalanche photodiode detector (APD) optimized for wavelength, and a goniometer. All DLS experiments were performed at 25ºC. The experiments were run in the auto-mode of the instrument, and the digital correlator analyzed the intensity of scattered light collected at an angle of 90°. The viscosity of the dispersions was taken as the same as that of the dispersion medium (water). Samples were withdrawn for DLS analysis at predetermined times after mixing of the reagent dendrimer complexes. Since the data obtained in initial part of the synthesis method are bimodal, a NICOMP analysis method that is based on a proprietary extension of the CONTIN technique, involving the discrete Laplace transformation inversion of the acquired autocorrelation data, was used. The particle size of larger sized particles, >1 μm, was measured with a Malvern Mastersizer X (Malvern, Worcestershire, UK) using a 100 mm Fourier transformation lens at 25 °C. For this method, all samples were diluted with demineralized particle-free water to an adequate obscuration prior to size measurement.

Transmission electron microscopy

Transmission electron microscopy (TEM) analysis was performed on a JEOL JEM 1200 EXII TEM (JEOL USA, Inc., Peabody, MA, USA). A Tietz camera was used to obtain digital images. All images were acquired at a tension of 80 kV and current density of 20 pA/cm^2. High-resolution TEM (HRTEM) images were obtained using a Tecnai G2 S-Twin electron microscope operated at 200 kV (FEI, Hillsboro, Oregon, USA).

Specimens were prepared by mounting a drop of an aqueous suspension of nanoparticles on a carbon coated copper grids followed by evaporation under vacuum at room temperature.

X-ray powder diffraction

X-ray powder diffraction (XRPD) patterns were recorded using a Bruker D8 Advanced diffractometer (Bruker, Germany), and the data were analyzed using the Eva software package. The instrumental setup was as follows: voltage, 40 kV; current, 40 mA; radiation source, Cu; divergence slit of 1 mm; anti-scatter slit, 0.1 mm; detector slit, 0.1 mm; scan range, from 2° to 40° 2θ, scan speed, 0.4° 2θ/min with a step size of 0.02° 2θ and a step time of 3.0 seconds.

Raman analyses

For Raman microscopy analysis, the powder samples were placed on a glass microscope slide and was analyzed using a Thermo Scientific DXR Raman microscope (Waltham, MA) with a diode pump solid state (DPSS) laser, with an excitation wavelength of 532 nm and 10 mW laser power.

HPLC assay of silver sulfadiazine

Silver sulfadiazine was analyzed using a high performance liquid chromatograph (AS 1000 auto sampler and P2000 pump, Thermo Separation Products, Waltham, MA) equipped with a multiple wavelength UV detector (UV 3000 detector) set at a wavelength of detection λ_{max} of254 nm. Chromatographic separation was performed using a C_{18} column (Econosil, 5 µm particles, 250 × 4.6 mm, Alltech, Deerfield II).

The mobile phase consisted of a solution of water, acetonitrile, and phosphoric acid (900:99:1) filtered through a 0.45 µm membrane filter (Gelman Sciences Inc., Ann Arbor, MI, US) and degassed in an ultrasonic bath for 15 min before use. The flow rate was 1 ml/min, injection volume 20 µL and all analyses were conducted at ambient temperature (~23 °C).

All solutions were protected from light. Solutions of stock reference standards were prepared daily. Silver sulfadiazine (100 µg/mL) was dissolved in the mobile phase. These solutions were diluted further with the mobile phase to prepare calibration standards ranging 0 to 60 µg/mL.

Quantitation was based on linear regression analysis of analyte peak area versus analyte concentration in µg/mL. Least squares linear regression analysis of the data gave slope, intercept, and correlation coefficient data. The HPLC method used in this study were evaluated for precision, accuracy, selectivity, linearity, robustness and system suitability. Samples were quantified using peak areas of the analyte.

Atomic absorption spectroscopy assay of elemental silver

The silver content of the suitably diluted samples was analyzed by flame atomic absorption spectrometer and the concentration was determined using standard solutions of silver in a background matrix. A Perkin Elmer model 5100 PC Zeeman atomic absorption spectrophotometer, HGA-600 Graphite Furnace, Model AS-60 Autosampler, Perkin Elmer 5100 ZL Zeeman furnace module, Perkin Elmer furnace cooling system, Perkin Elmer Model 0057-0759 EDL power supply, and computer software furnished with a silver hollow cathode lamp and air-acetylene flame, was used for the analysis.

The operating conditions were: wavelength, 328.1 nm; spectral bandwidth 0.7 nm; lamp current 10 mA. Pyrolytically-coated graphite tubes with L'vov platforms (Perkin-Elmer) were used. For the silver standard, a standard solution of silver for atomic absorption spectroscopy (BDH Chemicals), which contained $AgNO_3$ equivalent to 1 mg Ag (9.270 µmol) per mL was used.

Calibration curves for silver were linear across the range of 0 to 7 µg/mL. Working standards were prepared by diluting the stock standard with the release medium. Since silver nitrate solutions are light sensitive and have the tendency to plate silver out on the container walls, they were stored in amber bottles.

Titration of silver and sulfadiazine with PAMAM dendrimer complexes

For silver dendrimer complexation experiments, silver nitrate was selected because of its good solubility both in water and in methanol. Briefly, 10 mL aqueous solutions of the PAMAM dendrimers (1×10^{-5} M) were titrated with $AgNO_3$ solution (1×10^{-4} M) and monitored by UV-VIS spectroscopy. Absorbance of the solutions was recorded at λ_{max} 380 nm using a Multispec-1510 spectrophotometer (Shimadzu, Japan).

The UV-method was calibrated and complied with generally accepted specifications for linearity, precision, accuracy, repeatability, and recovery.

Complex formation between sulfadiazine and the dendrimers was carried out as described.[2] In short, the dendrimers were combined with SDZ in methanolic solution and the mixtures were incubated for 12 h at 25ºC. The methanol was evaporated and the resultant solid residues were dissolved in 0.1 ml of Tris buffer 10 mM pH 7.5 plus NaCl 0.9% p/v (Tris buffer) at room temperature. The solutions were

centrifuged at 10,000×g for 5 min, in order to separate soluble complexes from the non-complexed insoluble free SDZ. The amount of SDZ in the complexes was quantified by HPLC after dilution in the mobile phase. Solubility profiles were constructed by adding excess amounts of SDZ was added to dendrimer solutions ranging from 0 to 3×10^{-3} M.

These profiles revealed two sections of the curve for which linear regression equations of the sloped and horizontal portions were calculated. The saturation point was indicated by interpolation of these equations to produce the point of intersection, equivalent to the amount of monovalent silver ions bound to one dendrimer molecule.

Results

Nanoparticle complexation in the microfluidizer

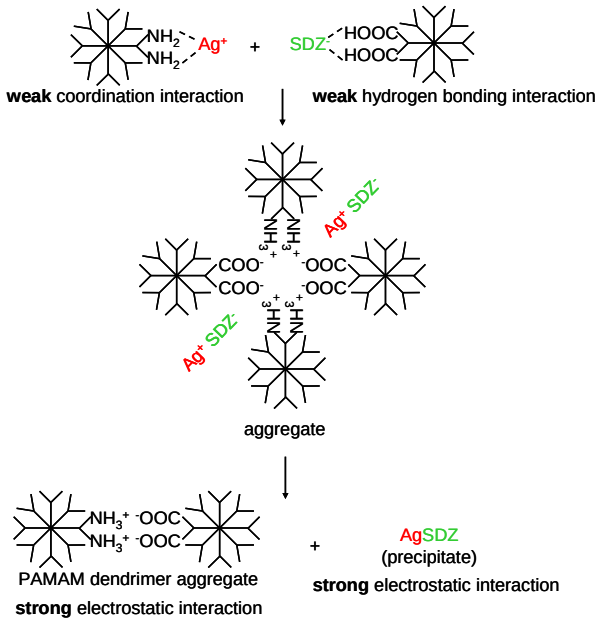

Figure 3. An illustration of the reaction between the Ag and SDZ dendrimer complexes, and the dendrimer aggregates that form during the preparation of the AgSD nanoparticles (the reaction scheme shown occurs in the 2 mL reaction chamber of the microfluidizer).

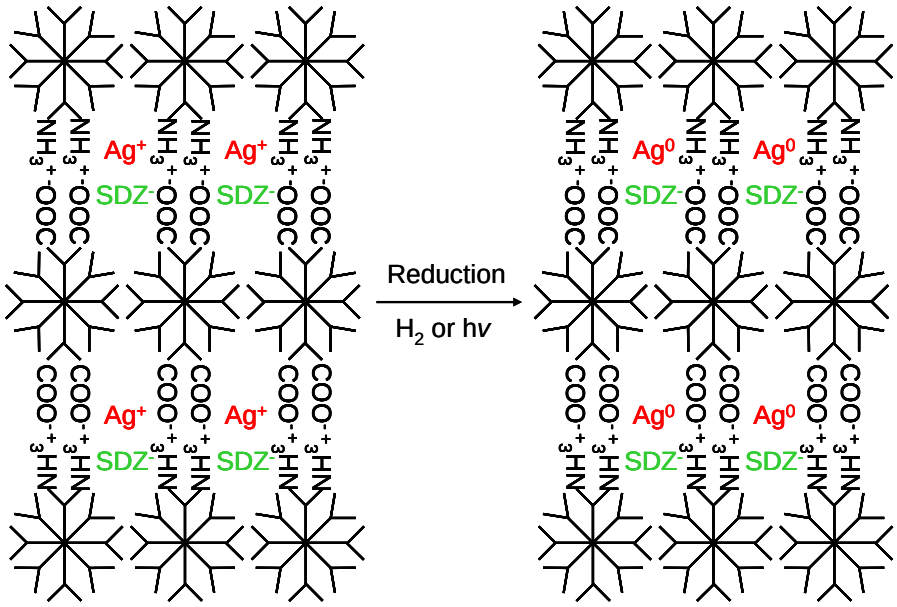

Figure 4. A schematic representation of the mechanism by which silver nanoparticles are synthesized in the dendrimer monolayers during dissolution of AgSD from the nanoparticles.[1,3]

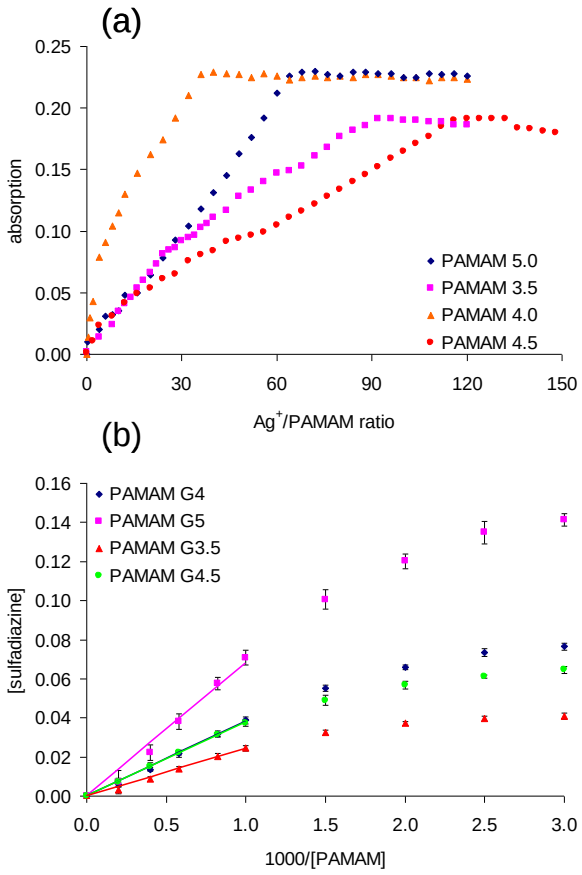

Figure 5. The results from (a) the titrations of silver nitrate ($AgNO_3$) and the various PAMAM dendrimer solutions and (b) the complexation between sulfadiazine (SDZ) and the dendrimers, that were used for determining the amount of silver ions that complexes with each dendrimer and the loading capacity for the different dendrimer molecules respectively.

Particle sizing

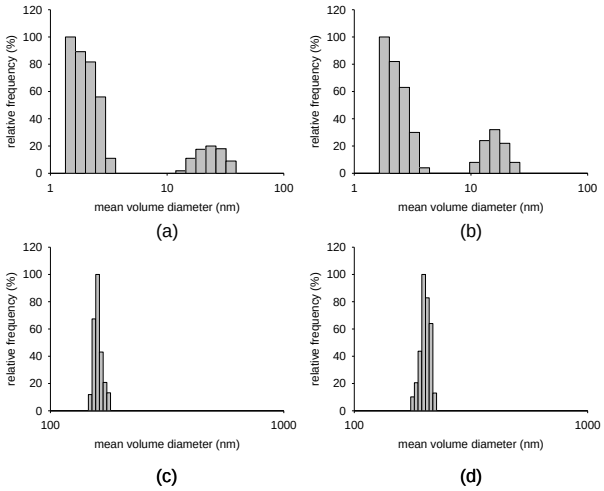

Figure 6. Particle size analyses of the dendrimer solutions, indicating the size of the dendrimer complexes that form in solution, as well as the distribution of aggregates formed by mixing dendrimers with different terminal functional groups of 0.1 M (a) G4.0-PAMAM-NH_2, (b) G4.5-PAMAM-COOH and (c) G4.0-PAMAM-NH_2 combined with G4.5-PAMAM-COOH, whereas (d) is the results from a 1 mM solution of both G4.0-PAMAM-NH_2 and G4.5-PAMAM-COOH.

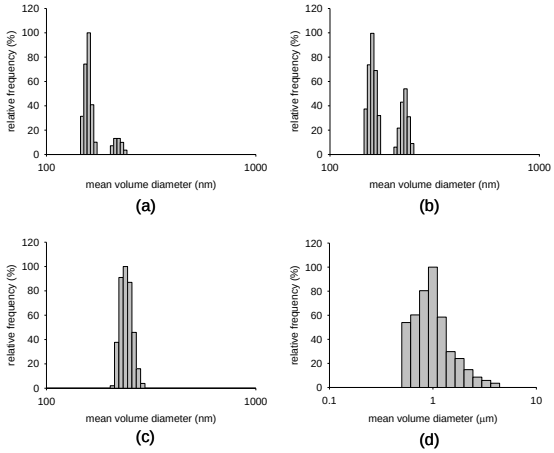

Figure 7. The results from particle size analyses of the AgSD nanoparticles that were processed (a) once, (b) twice and (c) three times through the microfluidizer and (d) AgSD nanoparticles were triple-processed followed by suspension in water for 4 hours.

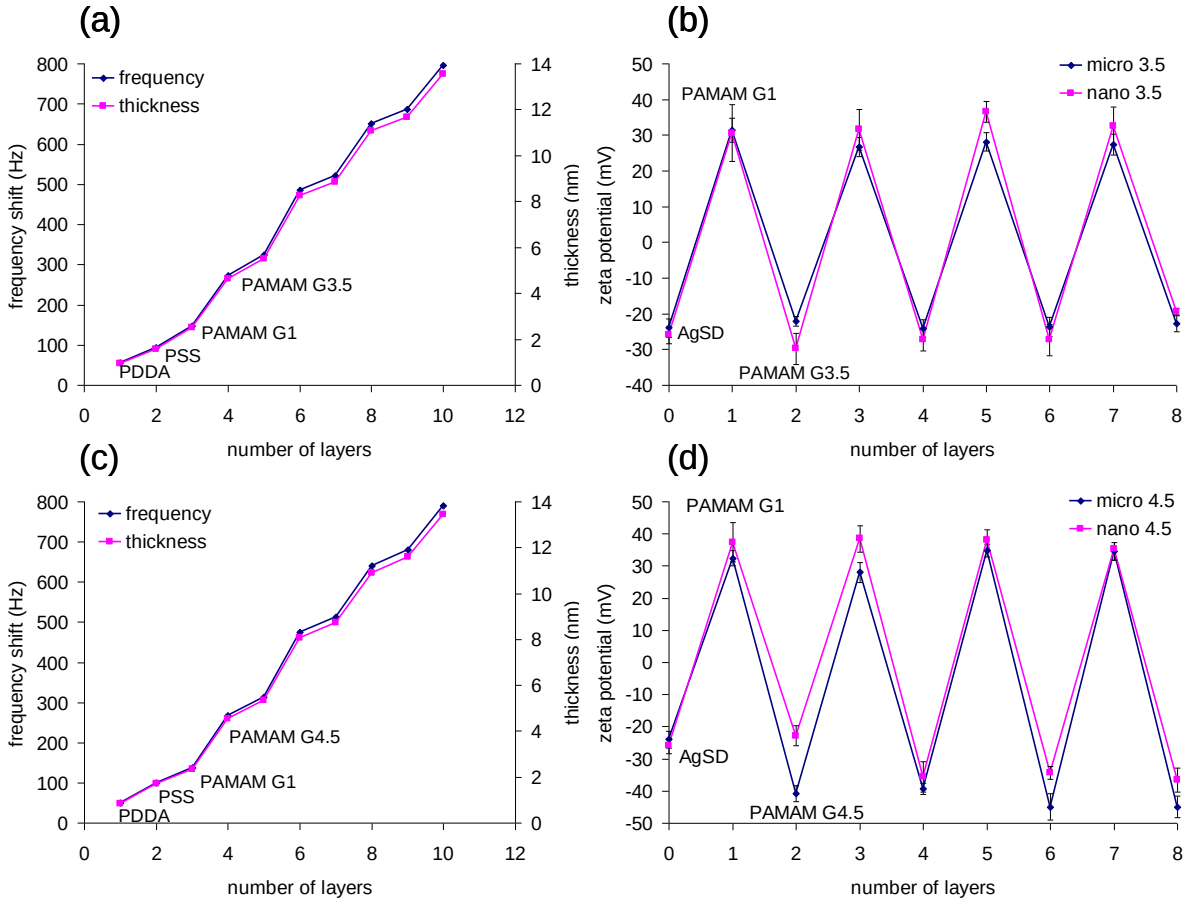

Figure 8. QCM-D (a), (c) and zeta potential measurements (b), (d) indicating the formation of the LbL coating on nano- and micronized AgSD, consisting of G1.0-PAMAM-NH_2 and either G3.5- or G4.5-PAMAM-COOH dendrimers.

XRPD

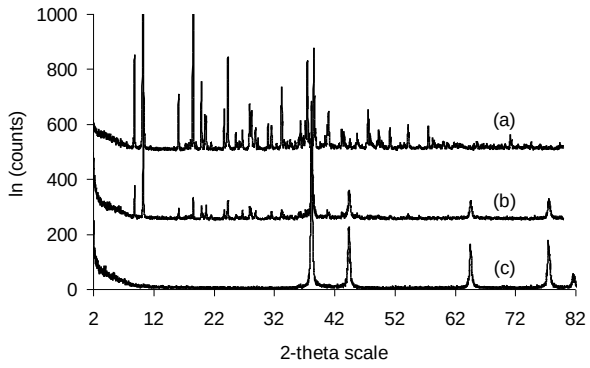

Figure 9. XRPD analyses of (a) micronized AgSD, (b) PAMAM coated AgSD with additional added silver and (c) silver nanopowder.

Raman analysis

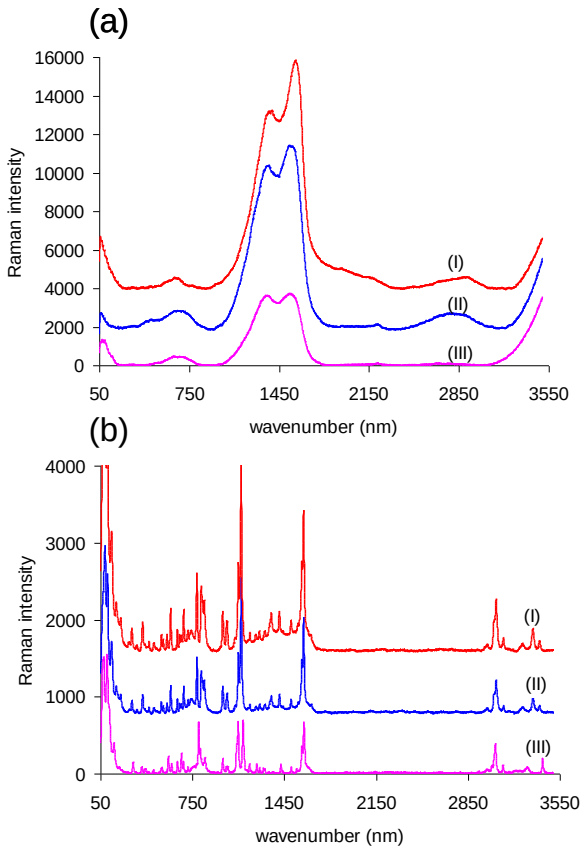

Figure 10. Raman spectra of (a) (I) silver nanopowder, (II) PAMAM coated AgSD with added silver nitrate and (III) a solution of G4.5-PAMAM-COOH to which silver nitrate has been added and (b) (I) AgSD nanoparticles, (II) micronized AgSD and (III) sodium sulfadiazine.

References

41. Kéki S, Török J, Deák G, Daróczi L, Zsuga MJ. Silver nanoparticles by PAMAM-assisted photochemical reduction of Ag(+). Colloid Interface Sci 2000;229:550-3.

42. Prieto MJ, Bacigalupe D, Pardini O, Amalvy JI, Venturini C, Morilla MJ, Romeo EL. Nanomolar cationic dendrimeric sulfadiazine as potential antitoxoplasmic agent. Int J Pharm 2006,326:160-8.

43. Shutava T, Prouty M, Kommireddy D, Lvov Y. pH responsive decomposable layer-by-layer nanofilms and capsules on the basis of tannic acid. Macromolecules 2005;38:2850-8.

CHAPTER 4

This chapter was submitted to the journal Powder technology.

STRYDOM, S.J., OTTO, D.P., AUCAMP, M., STIEGER, N., LIEBENBERG, W. & DE VILLIERS, M.M. 2014. Self-assembled macromolecular nanocoatings to stabilize and control drug release from nanoparticles. Powder Technology, 256:470-476.

IMPACT FACTOR: 2.024

INSTRUCTIONS TO AUTHORS (SUMMARY)

POWDER TECHNOLOGY - An International Journal on the Science and Technology of Wet and Dry Particulate Systems

DESCRIPTION

Powder Technology is an International Journal on the Science and Technology of **Wet** and **Dry Particulate Systems**. *Powder Technology* publishes papers on all aspects of the formation of **particles** and their characterisation and on the study of systems containing **particulate solids**. No limitation is imposed on the size of the particles, which may range from nanometre scale, as in pigments or aerosols, to that of mined or quarried materials. The following list of topics is not intended to be comprehensive, but rather to indicate typical subjects which fall within the scope of the journal's interests: Formation and synthesis of particles by precipitation and other methods. Modification of particles by agglomeration, coating, comminution and attrition. Characterisation of the size, shape, surface area, pore structure and strength of particles and agglomerates (including the origins and effects of inter particle forces). Packing, failure, flow and permeability of assemblies of particles. Particle particle interactions and suspension rheology. Handling and processing operations such as slurry flow, fluidization, pneumatic conveying. Interactions between particles and their environment, including delivery of particulate products to the body. Applications of particle technology in production of pharmaceuticals, chemicals, foods, pigments, structural, and functional materials and in environmental and energy related matters. Contact and other information: Please feel free to contact us for any comments, questions or feedback. In addition, we are always interested in any publication proposals for books, electronic products, new journals and co-operation for existing journals. It is now possible to submit your paper online and benefit from the considerably shorter time required to reach an editorial decision

about publication. For all further information, please go directly to http://www.elsevier.com/authors.

AUDIENCE

Chemical engineers, food technologists, physicists, powder metallurgists, materials scientists, pharmaceutical scientists

•**Normal length research papers** - these should be complete & authoritative accounts of work which has a special significance and must be presented clearly and concisely.
•**Review articles** - these will normally be commissioned by one of the Editors. Prospective authors of a review article should consult with one of the Editors to check the suitability of their topic & material before submitting their review.
•**Short communications** - will be accepted for the early communication of important and original advances. Such accounts may be of a preliminary nature but should always be complete and should not exceed the equivalent of 3000 words, including figures and tables.
•The journal also publishes **Letters to the editors** (commenting on work published in the journal) and **Book reviews**.

Article structure

Subdivision - numbered sections

Divide your article into clearly defined and numbered sections. Subsections should be numbered 1.1 (then 1.1.1, 1.1.2, ...), 1.2, etc. (the abstract is not included in section numbering). Use this numbering also for internal cross-referencing: do not just refer to 'the text'. Any subsection may be given a brief heading. Each heading should appear on its own separate line.

Introduction

State the objectives of the work and provide an adequate background, avoiding a detailed literature survey or a summary of the results.

Material and methods

Provide sufficient detail to allow the work to be reproduced. Methods already published should be indicated by a reference: only relevant modifications should be described.

Theory/calculation

A Theory section should extend, not repeat, the background to the article already dealt with in the Introduction and lay the foundation for further work. In contrast, a Calculation section represents a practical development from a theoretical basis.

Results

Results should be clear and concise.

Discussion

This should explore the significance of the results of the work, not repeat them. A combined Results and Discussion section is often appropriate. Avoid extensive citations and discussion of published literature.

Conclusions

The main conclusions of the study may be presented in a short Conclusions section, which may stand alone or form a subsection of a Discussion or Results and Discussion section.

Appendices

If there is more than one appendix, they should be identified as A, B, etc. Formulae and equations in appendices should be given separate numbering: Eq. (A.1), Eq. (A.2), etc.; in a subsequent appendix, Eq. (B.1) and so on. Similarly for tables and figures: Table A.1; Fig. A.1, etc.

Essential title page information

• **Title**

Concise and informative. Titles are often used in information-retrieval systems. Avoid abbreviations and formulae where possible.

Author names and affiliations

Where the family name may be ambiguous (e.g., a double name), please indicate this clearly. Present the authors' affiliation addresses (where the actual work was done) below the names. Indicate all affiliations with a lower-case superscript letter immediately after the author's name and in front of the appropriate address. Provide the full postal address of each affiliation, including the country name and, if available, the e-mail address of each author.

Corresponding author

Clearly indicate who will handle correspondence at all stages of refereeing and publication, also post-publication. Ensure that phone numbers (with country and area code) are provided in addition to the e-mail address and the complete postal address. Contact details must be kept up to date by the corresponding author.

Present/permanent address

If an author has moved since the work described in the article was done, or was visiting at the time, a 'Present address' (or 'Permanent address') may be indicated as a footnote to that author's name. The address at which the author actually did the work must be retained as the main, affiliation address. Superscript Arabic numerals are used for such footnotes.

Abstract

A concise and factual abstract is required. The abstract should state briefly the purpose of the research, the principal results and major conclusions. An abstract is often presented separately from the article, so it must be able to stand alone. For this reason, References should be avoided, but if essential, then cite the author(s) and year(s). Also, non-standard or uncommon abbreviations should be avoided, but if essential they must be defined at their first mention in the abstract itself.

Graphical abstract

A Graphical abstract is mandatory for this journal. It should summarize the contents of the paper in a concise, pictorial form designed to capture the attention of a wide readership online. Authors must provide images that clearly represent the work described in the paper. Graphical abstracts should be submitted as a separate file in the online submission system. Maximum image size: 400 × 600 pixels (h × w, recommended size 200 × 500 pixels). Preferred file types: TIFF, EPS or MS Office files. See http://www.elsevier.com/graphicalabstracts for examples.

Highlights

Highlights are mandatory for this journal. They consist of a short collection of bullet points that convey the core findings of the article and should be submitted in a separate file in the online submission system. Please use 'Highlights' in the file name and include 3 to 5 bullet points (maximum 85 characters, including spaces, per bullet point). See http://www.elsevier.com/highlights for examples.

Keywords

Immediately after the abstract, provide a maximum of 6 keywords, using British spelling and avoiding general and plural terms and multiple concepts (avoid, for example, 'and', 'of'). Be sparing with abbreviations: only abbreviations firmly established in the field may be eligible. These keywords will be used for indexing purposes.

Abbreviations

Define abbreviations that are not standard in this field in a footnote to be placed on the first page of the article. Such abbreviations that are unavoidable in the abstract must be defined at their first mention there, as well as in the footnote. Ensure consistency of abbreviations throughout the article.

Acknowledgements

Collate acknowledgements in a separate section at the end of the article before the references and do not, therefore, include them on the title page, as a footnote to the title or otherwise. List here those individuals who provided help during the research (e.g., providing language help, writing assistance or proof reading the article, etc.).

Figure captions

Ensure that each illustration has a caption. Supply captions separately, not attached to the figure. A caption should comprise a brief title (**not** on the figure itself) and a description of the illustration. Keep text in the illustrations themselves to a minimum but explain all symbols and abbreviations used.

Tables

Number tables consecutively in accordance with their appearance in the text. Place footnotes to tables below the table body and indicate them with superscript lowercase letters. Avoid vertical rules. Be sparing in the use of tables and ensure that the data presented in tables do not duplicate results described elsewhere in the article.

References

Citation in text

Please ensure that every reference cited in the text is also present in the reference list (and vice versa). Any references cited in the abstract must be given in full. Unpublished results and personal communications are not recommended in the reference list, but may be

mentioned in the text. If these references are included in the reference list they should follow the standard reference style of the journal and should include a substitution of the publication date with either 'Unpublished results' or 'Personal communication'. Citation of a reference as 'in press' implies that the item has been accepted for publication.

Web references

As a minimum, the full URL should be given and the date when the reference was last accessed. Any further information, if known (DOI, author names, dates, reference to a source publication, etc.), should also be given. Web references can be listed separately (e.g., after the reference list) under a different heading if desired, or can be included in the reference list.

References in a special issue

Please ensure that the words 'this issue' are added to any references in the list (and any citations in the text) to other articles in the same Special Issue.

Reference style

Text: Indicate references by number(s) in square brackets in line with the text. The actual authors can be referred to, but the reference number(s) must always be given. Example: '..... as demonstrated [3,6]. Barnaby and Jones [8] obtained a different result ....' *List:* Number the references (numbers in square brackets) in the list in the order in which they appear in the text.

Examples: Reference to a journal publication: [1] J. van der Geer, J.A.J. Hanraads, R.A. Lupton, The art of writing a scientific article, J. Sci. Commun. 163 (2010) 51–59. Reference to a book: [2] W. Strunk Jr., E.B. White, The Elements of Style, fourth ed., Longman, New York, 2000. Reference to a chapter in an edited book: [3] G.R. Mettam, L.B. Adams, How to prepare an electronic version of your article, in: B.S. Jones, R.Z. Smith (Eds.), Introduction to the Electronic Age, E-Publishing Inc., New York, 2009, pp. 281–304.

Powder technology

Self-assembled Macromolecular Nanocoatings to Stabilize and Control Drug Release from Nanoparticles (2014)

Schalk J. Strydom[1,2], Daniel P. Otto[3], Nicole Stieger[1,2], Marique E. Aucamp[1,2], Wilna Liebenberg[2], and Melgardt M. de Villiers[1,]*

[1]School of Pharmacy, University of Wisconsin-Madison, WI, USA.

[2]Centre of Excellence for Pharmaceutical Sciences, North-West University, Potchefstroom, South Africa.

[3]Research Focus Area for Chemical Resource Beneficiation, Catalysis and Synthesis Research Group, North-West University, Potchefstroom, South Africa.

*Corresponding author: MM de Villiers, School of Pharmacy, UW-Madison, WI. mmdevilliers@pharmacy.wisc.edu

Abstract

A layer-by-layer (LbL) nanocoat (< 25 nm thick) of two polyelectrolytes, chitosan and chondroitin sulfate, were self-assembled step-wise onto drug nanoparticles that were prepared by a solvent-evaporation emulsification method using eucalyptol as the oil phase. Four poorly water-soluble model drugs, furosemide, isoxyl, rifampin and paclitaxel were chosen to prepare these particles. Zeta potential, particle size measurements, and microscopic inspection of the coated particles, were used to confirm the successful addition of each polyelectrolyte layer and the stability of the nanoparticles. This manufacturing process produced stable drug nanoparticles with volume mean diameters below 250 nm. Dissolution tests confirmed that although the nanocoat reduced the dissolution of nanoparticles proportional to the coat thickness, they still dissolved much faster than commercially available micronized powders of the drugs. In addition, increasing the layer thickness (still less than 50 nm thick) by adding more LbL bilayers produced sustained release nanoparticles. Ultimately, the LbL nanocoating stabilized these small particles against crystal growth and aggregation in suspension and resulted in nearly perfect controlled drug release.

Keywords: poorly water soluble; nanoparticle, layer-by-layer; self-assembly; stability; controlled release

Text Graphical Abstract

Nanocoating through LbL-self-assembly using minute quantities of polyelectrolytes provides control of drug release and physical stability of nanoparticles. This improves the pharmaceutical performance of poorly water-soluble drugs.

1. Introduction

Powder agglomeration can significantly deter efficient mixing, dispersion and fluidization of particles into a medium of choice. Physical stability of small particles is significantly compounded since their large surface free energy can only be dissipated by agglomeration [1]. In the case of nanocrystals, a special phase definition states that the stable seed size will be where the interfacial free energy will be a minimum for a specific phase volume, otherwise known as Wulff's theorem [2]. In the case of drug nanoparticles, these are not necessarily presented as single phase, homogeneously sized particles. Most often these small particles incorporate an array of inhomogeneous particles of various size and shape distributions which will result in the well-known Ostwald-ripening effect [3]. Due to this ripening effect, particles with wide size distributions will continue to grow and redissolve to finally reach a thermodynamically stable size as predicted by Wulff's theorem.

The need for drug nanoparticles arose from the fact that approximately 95% of all new drugs have poor pharmacokinetic properties such as low water solubility and bioavailability [4]. The well-established and current dissolution theory argues that an optimum, small particle size will result in the highest rate of dissolution and solubility [5-7] and therefore proposes that these insoluble drugs would demonstrate significant improvements in their technological behaviour if they were deagglomerized and if a small particle size, possibly in the nanoscale range, could be assured [8].

It is quite apparent that size reduction of these insoluble drugs would induce physical instability of the particles that will compromise any advantages that size reduction would have imparted. Therefore, several stabilization mechanisms were introduced to maintain the benefit of particle size reduction on release rate and solubility of drugs. Some examples include the encapsulation of poorly water-soluble drugs such as paclitaxel [9], furosemide [10] and nifedipine [11, 12] in PAMAM dendrimers, interactive powder mixing which deposited minute particles of griseofulvin on a larger carrier particle [13], dispersion of poorly water-soluble drugs in highly soluble polymers such as poly(vinylpyrrolidone) [14], and poly(ethylene glycol) [15]. Perhaps the most robust and easiest method to ensure small particle stability, also in is the layer-by-layer (LbL) self-assembly nanocoating technique [16]. The successive deposition of minute quantities of polyelectrolytes of alternating polarities has been shown to create a highly stable nanoshell around dexamethasone microparticles [17]. Additional successful applications of LbL coating were illustrated for the

inhibition of surface crystallization of amorphous indomethacin [18], nanoencapsulation of furosemide microcrystals to control drug release [19], to improve the photostability and pharmacokinetic profile of nifedipine [20] and the stabilization of dexamethasone nanoparticles [21].

In this study, several poorly water soluble drugs with diverse surface properties were subject to a LbL nanocoating procedure to investigate whether any beneficial properties could be imparted to these troublesome drugs.

2. Materials and methods

2.1 Materials

Chitosan (CHI) of molecular weight, 15 000 g/mol was purchased from Polysciences, Inc, (Warrington, PA, USA). Chondroitin sulfate sodium salt (CS, MW ~ 50,000 g/mol) from bovine trachea, cationic poly(dimethyldiallyl ammonium chloride) (PDDA, MW ~ 150,000 g/mol), anionic sodium poly(styrenesulfonate) (PSS, MW ~ 70,000 g/mol), fluorescein isothiocyanate (FITC), USP grade furosemide and nifedipine, eucalyptol FCC grade, and analytical grade organic solvents were purchased from Sigma Aldrich Chemicals (St. Louis, MO, USA). Isoxyl and paclitaxel were supplied by Cayman Chemicals (Sapphire, Redfern, NSW, Australia). Ultrapure water used for all experiments and cleaning steps was obtained from a Barnstead Nanopure Diamond RO system having a specific resistance of greater than 18 MΩ/cm. Except for CHI, the polyelectrolyte (PE) solutions were prepared in 0.1 M phosphate buffered saline solution (PBS, pH 7.40) consisting of 1.1 mM potassium phosphate monobasic, 3 mM sodium phosphate dibasic heptahydrate, and 0.15 M NaCl. CHI was dissolved in 0.01 M acetic acid solution.

The synthesis of FITC-labeled CHI was based on the reaction between the isothiocyanate group of FITC and the primary amino group of chitosan as reported in the literature [22,23]. Briefly, 20 mg FITC was dissolved in 20 ml anhydrous methanol and added to 20 ml 1% w/v CHI in 0.01 M acetic acid solution. After 3 h under light occlusion at ambient temperature, the FITC-labeled chitosan (FITC-CHI) was precipitated by raising the pH to 10.0 with 0.5 M NaOH. The unreacted FITC was removed by washing with distilled water and centrifugation (10 000 rpm for 5 minutes) until no fluorescence was detected in the supernatant.

2.2 Preparation of nanoparticles

Nanoparticles of the drugs were prepared by a modified solvent-evaporation emulsification method as previously reported in the literature [21]. Briefly, 30 mg/mL solutions of the drugs

in acetone were emulsified with twice the volume of eucalyptol for 30 minutes under vigorous agitation and low temperature (ice bath with 2000 rpm stirrer, IKA Eurostar PWR, Wilmington, NC, USA). Prepared emulsions were then further processed using a microfluidizer (model 110-Y, Microfluidics, Newton, MA, USA) [24]. The drug particles were collected by centrifugation at 5 000 RPM for 10 minutes and resuspended in 0.1 M PBS. The nanoparticles were again collected by centrifugation at 5 000 RPM for 10 minutes. This process was repeated several times to remove all the eucalyptol. The nanoparticle powders were dried and stored in a refrigerator for future use.

2.3 Layer-by-layer absorption of polyelectrolytes

Except for CHI that was dissolved in 0.01 M acetic acid, the pH of the PE solutions was maintained at 7.40. The LbL assembly procedure was as follows: 1.0 mL of a 20 mg/mL of the PE solution was mixed with 1 ml of 30 mg/mL drug nanoparticles, followed by 5 minute incubation under gentle shaking [16]. After a layer was added, three washing cycles of centrifugation, removal of the supernatant, and re-suspension in 1.5 mL of pH 7.20 buffer solution were performed to ensure the removal of unbound PE. The centrifugation was performed at 5 000 RPM for 5 to 10 minutes. The process was continued by alternating the polycationic and polyanionic layers until the desired number of layers was attained. The first PE layer was either PDDA or PSS dependent on the ζ –potential of the uncoated drug nanoparticles (furosemide + 22 mV, paclitaxel – 39 mV, isoxyl + 35 mV and nifedipine -32 mV).

2.4 Characterization of nanoparticles

2.4.1 Quartz crystal microbalance analysis

Prior to PE multilayer formation on the nanoparticles, the coating procedure was elaborated on gold electrode resonators of 5 MHz quartz crystal microbalance (QCM200, Stanford Research Systems, Sunnyvale, CA, USA). The resonators were immersed in a polyion solution for 15 minutes, removed, and dried. The added mass and the coating thickness (ΔL) can be calculated from the frequency shift (ΔF), according to the Sauerbrey equation [25], using a scaling factor. For the instrument used in this study, the scaling factor was ΔL (nm) = - 0.022 ΔF (Hz). These experimental self-assembly conditions were then applied to the LbL shell assembly on the nanocrystals. In addition, after each PE coating on the nanoparticles, the ζ-potential of the particles suspended in water was measured using a ZetaSizer Nano ZS (Malvern, Westborough, MA, USA).

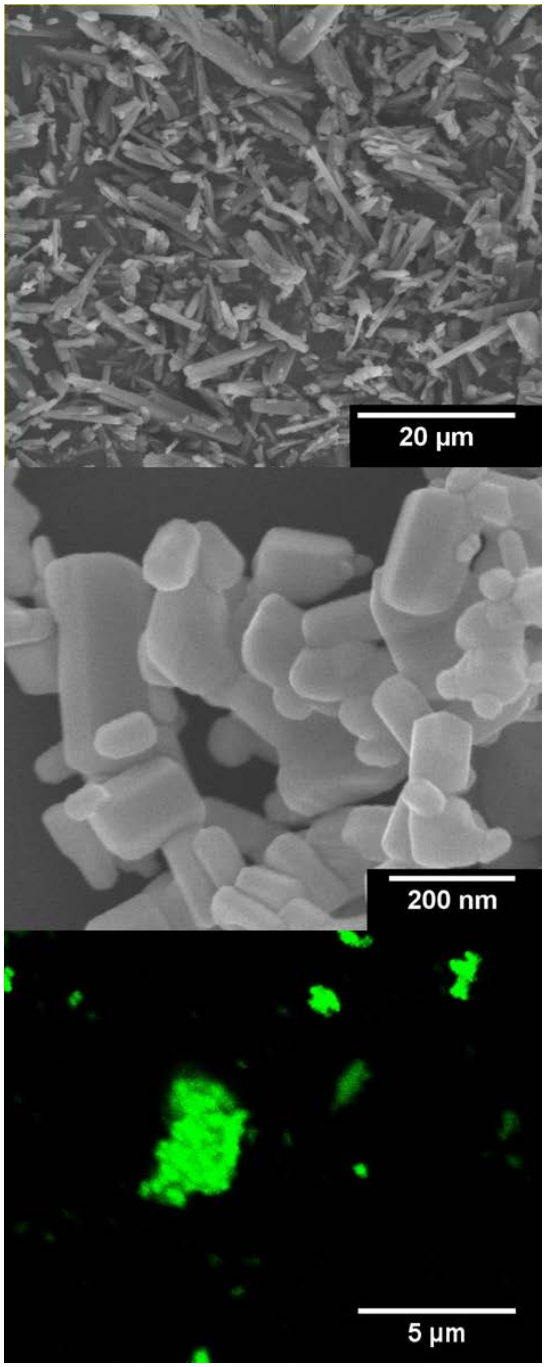

Figure 1. SEM photomicrographs of furosemide microparticles (top), coated nanoparticles (middle) and nanoparticles LbL coated with FITC labeled chitosan (bottom). Particles were coated with 4 layers of PE's (see Fig. 7).

2.4.2 Electron microscopy and confocal scanning laser microscopy

Scanning electron microscopy (SEM) studies were performed on samples that were affixed on carbon-taped stubs and thinly coated with Au/Pd. Both a Hitachi S570 and a Hitachi S-900 FESEM was used to photograph the samples (Hitachi High Technologies, Dallas, TX, USA). All micrographs were recorded with a crystal emission of 10 keV. Additional SEM

micrograph analysis was conducted with automated image analysis routines available in ImageJ 1.47 imaging analysis software [26]. Confocal laser scanning microscopy (model DMI RE2; Leica, Allendale, NJ, USA) and fluorescent spectrometry (Photon Technology International, Lawrenceville, NJ, USA) were used to visualize the LbL coating. For fluorescence, the drug nanoparticles were coated with FITC labeled CHI.

2.4.3 Particle sizing and zeta potential

The particle size distributions of the centrifuged nanoparticles, before and after LbL coating, were measured with the ZetaSizer Nano ZS. Material index of refraction for PE coated particles was set to 1.46 and PBS solution (saturated or unsaturated with drug) was set to 1.33. A volume of 1.5 mL of the drug particle suspension was pipetted into a disposable cuvette. Acquisition was performed at room temperature and volume mean diameters D[4,3] calculated.

2.5 Dissolution and release studies

The *in vitro* dissolution rates of the drug nanoparticles were determined by a dialysis method under sink conditions [27,28]. Dialysis cassettes (Slide-A-Lyzer, 10 000 MWC, Pierce, Rockford, IL, USA) containing 3 mL of drug solution or suspension was placed in 80 ml beakers containing 50 mL of the dissolution medium. Release studies were conducted at 37 ºC in a water bath under stirring (100 RPM). At fixed intervals, 2 mL of the dissolution medium was withdrawn and the amount of drug released measured using HPLC. After each withdrawal the volume removed was replaced with 2 mL fresh dissolution medium. All experiments were repeated 6 times. Drug solutions in methanol (2 mg/mL) and suspensions prepared from the micron-sized particles were used as controls. For furosemide (pH 5.80 phosphate buffer) and nifedipine (simulated gastric fluid TS without pepsin and sodium lauryl sulfate), the dissolution media specified by the USP was used [27]. The dissolution medium for isoxyl and paclitaxel was PBS buffer pH 6.80. The HPLC analysis methods specified in the USP for furosemide, nifedipine and paclitaxel were used to determine the amount of drug released as a function of time. Isoxyl was analyzed by HPLC using a C18 column (Hypersil™ 5 µm ODS, Phenomenex, USA), UV detection at 270 nm and 70% acetonitrile in 20 mM ammonium acetate buffer as the mobile phase [28]. All drug samples were analyzed with a Shimadzu Prominence HPLC system (Kyoto, Japan), consisting of a LC-20 AT pump, a SIL-20 AC HT autosampler and a SPD-M20A diode array detector.

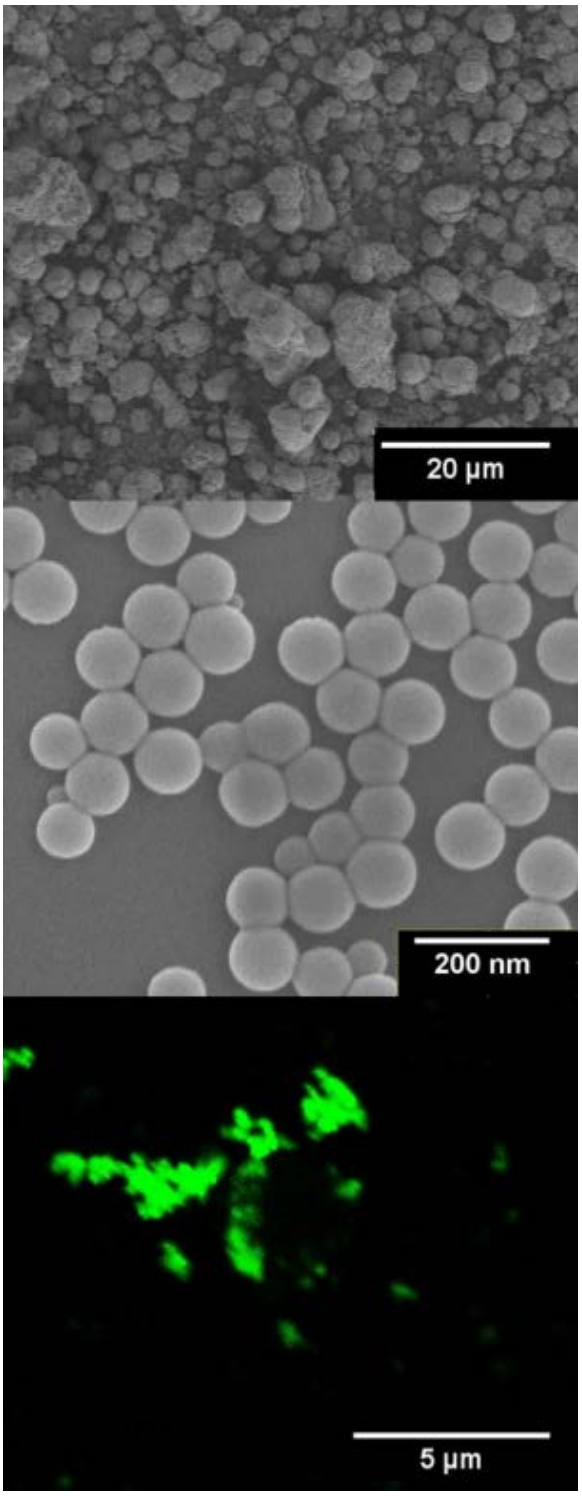

Figure 2. SEM photomicrographs of paclitaxel microparticles (top), coated nanoparticles (middle) and nanoparticles LbL coated with FITC labeled chitosan (bottom). Particles were coated with 5 layers of PE's (See Fig. 7).

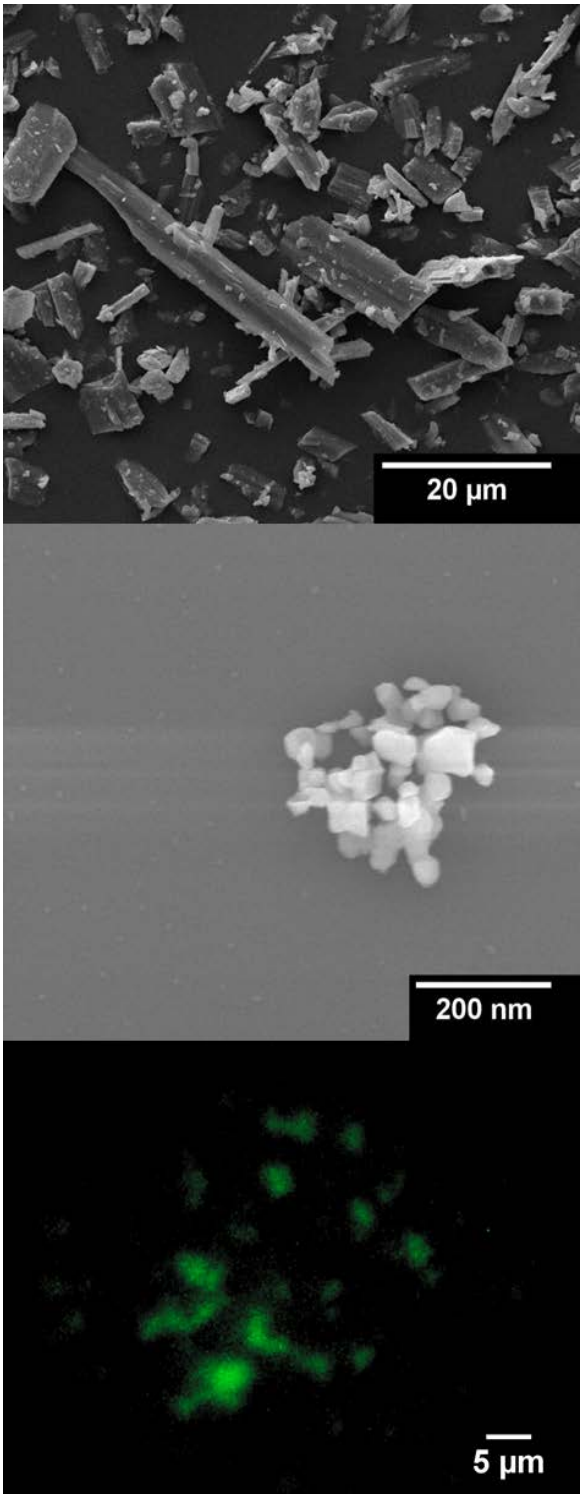

Figure 3. SEM photomicrographs of isoxyl microparticles (top), coated nanoparticles (middle) and nanoparticles LbL coated with FITC labeled chitosan (bottom). Particles were coated with 4 layers of PE's (see Fig. 7).

3. Results and discussion

The goal of this study was to improve the dissolution rate of water-insoluble and practically insoluble drugs by reducing the particle size to below 500 nm, since a significant increase in available surface area could be affected compared to unprocessed drug particles. The drugs chosen were furosemide, nifedipine, isoxyl and paclitaxel. The aqueous solubility of furosemide ranges from 10 µg/ml at pH 2.00 to 22 mg/ml at pH 8.00 [10]. The aqueous solubility of nifedipine has been measured at 5-6 µg/mL in the pH range of 4.00-13.0 [12]. The reported aqueous solubilities of paclitaxel and isoxyl are 3-4 µg/ml [9] and 3-6 µg/ml respectively [28]. In this study drug nanoparticles were prepared using a modified solvent-evaporation emulsification method described above. SEM photomicrographs of the micron-sized raw materials and the prepared nanoparticles are shown in Figures 1-4.

Using the particle shape characterization guidelines from the USP the micronized furosemide crystals (D[4,3] = 14±4 µm) can be described as partially split, acicular and columnar particles with sharp ends (Figure 1). In contrast the furosemide nanoparticles were plate like with rounded edges and smooth surfaces. The paclitaxel microparticles (D[4,3] = 12±4 µm) looked like milled equant spherical aggregates with rough surfaces (Figure 2) while the paclitaxel nanoparticles were equant spheres with smooth surfaces. The isoxyl crystals (D[4,3] = 21±6 µm) was a mixture of drusy columnar and lath-like particles with cracked surfaces (Figure 3). Processing produced very small equant nearly spherical isoxyl particles with smooth surfaces. The nifedipine microparticles (D[4,3] = 19±5 µm) were lamellar, flake and plate like particles sometimes aggregated with sharp edges and cracked surfaces (Figure 4).

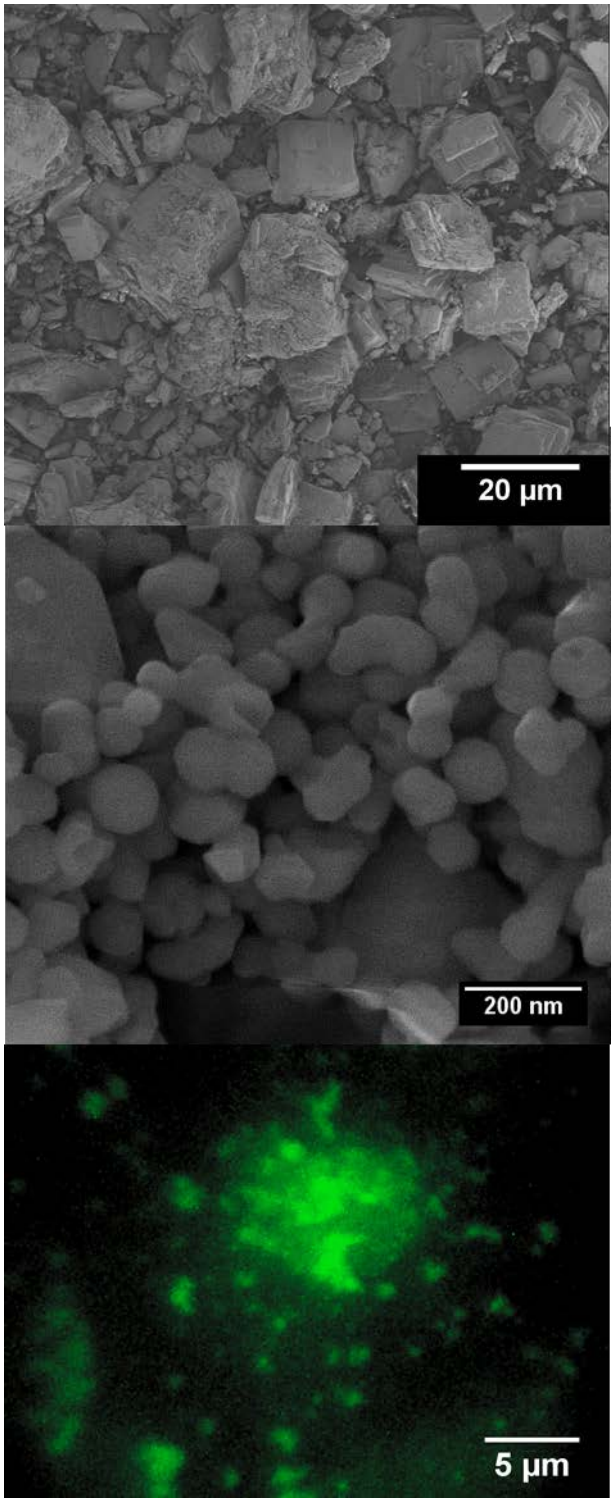

Figure 4. SEM photomicrographs of nifedipine microparticles (top), coated nanoparticles (middle) and nanoparticles LbL coated with FITC labeled chitosan (bottom). Particles were coated with 5 layers of PE's (see Fig. 7).

The nifedipine nanoparticles were small spheres or larger plate-like particles with smooth surfaces and rounded edges. The mean volume particle diameter of the nanoparticles recovered after preparation were 174±31 nm for furosemide, 110±31 nm for nifedipine, 65±19 nm for isoxyl, and 156±22 nm for paclitaxel (Figure 5).

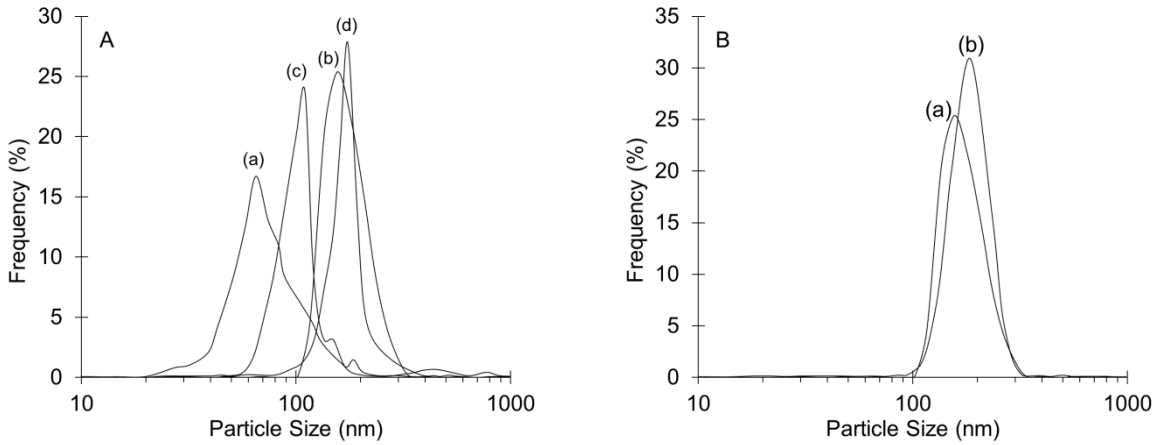

Figure 5. (A) Volume particle size distributions of freshly prepared drug nanoparticles (a) isoxyl, (b) paclitaxel, (c) nifedipine and (d) furosemide. (B) Volume size distribution of (a) uncoated and (b) LbL coated paclitaxel nanoparticles.

One challenge associated with very small drug particles are their stability in suspension. Very small particles tend to aggregate in suspension [1] or, due to their higher solubility; nanoparticles may grow orders of magnitude in size due to Ostwald ripening [2,5-7]. As shown in Figure 6(a) the uncoated particles grew larger when suspended in water. Within 24 hours the particles doubled in size, except for the nifedipine particles which showed a mean volume particle size in the micron range after 5 days. To prevent growth and to increase the stability of the particles prepared in this study, particles were coated with polyelectrolytes using layer-by-layer self-assembly [16]. The coating process was first confirmed by QCM, Figure 7(a). Briefly, the coating conditions employed during QCM experiments were also applied to drug nanoparticle coating. From these results the predicted thickness of the layers on the particles were also estimated using the Sauerbrey equation.

The actual coating of the nanoparticles was confirmed by measuring the successive reversal of the polarity of the particle zeta potential after coating. Initially, the ζ-potential of the pure particles was measured, Figure 7(b), followed by measuring the coated particles after application of the PE coats. During the coating process, the particles were also coated with

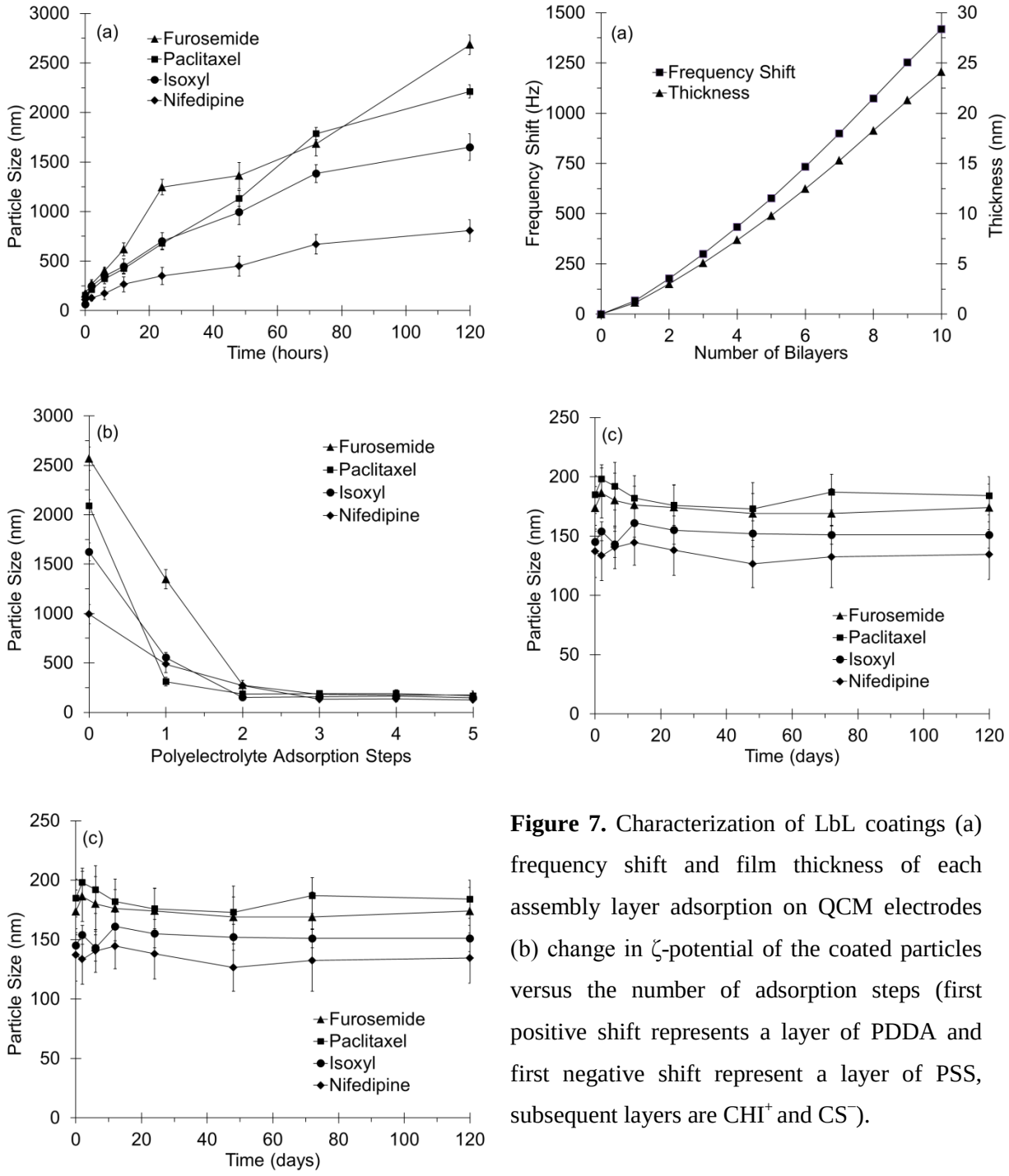

Figure 7. Characterization of LbL coatings (a) frequency shift and film thickness of each assembly layer adsorption on QCM electrodes (b) change in ζ-potential of the coated particles versus the number of adsorption steps (first positive shift represents a layer of PDDA and first negative shift represent a layer of PSS, subsequent layers are CHI^{+} and CS^{-}).

Figure 6. The effect of LbL coating on the long-term stability of nanoparticles suspended for 120 hours: (a) time dependent growth and aggregation of uncoated particles when suspended in water; (b) effect of number of LbL layers on the reduction in particle growth and aggregation of drug particles suspended in saturated aqueous solutions of the drugs; (c) long term stability of LbL coated (2-4 layers) particles suspended in a saturated solution of the drug in water for 120 days. Suspensions were kept in a water bath at 25±1.5°C. (Saturated aqueous solutions of the drugs were prepared by adding an excess amount of drug powder to ultrapure water, putting the suspensions in a shaking water bath for 24 hours at 25±1.5°C and filtering the solutions through 0.2 μm filters).

FITC-labeled CHI. In Figures 1-4 the fluorescence of the particles coated with the FITC-CHI also confirmed the deposition of a thin layer of CHI. Together QCM data, ζ-potential measurements and fluorescence microscopic evaluation, proved the successful LbL coating process in the application to drug nanoparticles. The process also illustrated its versatility in coating diverse nanoparticulate drug substrates with significantly different solubility, particle size and shape, and surface properties. In Figure 6(b) the effect of coating on the particle size of the drug particles are shown. The results represent the mean volume particle sizes of uncoated particles and those coated with up to 15 polyelectrolyte double layers suspended in saturated drug solutions for 120 hours. For the four drugs, coating with only 3 polyelectrolyte layers showed no change in the particle size measured before and after suspension during a lapse of 120 hours. These results show that LbL coating stunted particle growth and that it required only a few layers of electrolyte to produce very stable particles in suspension. These results agree with those reported for larger amorphous indomethacin particles [18].

Due to the potential *in vivo* toxicity associated with positively charged particles, it was decided to only assess the drug release of particles that demonstrated a negative zeta potential. For furosemide and isoxyl, 3 PE layers (Figure 5a) were required to render a negative zeta potential (thickness ~ 5 nm measured by QCM) to stabilize the particles. Nifedipine and paclitaxel (Figure 5a) both required 4 layers (thickness ~ 8 nm measured by QCM) to produce a negative zeta potential. These coats increased the diameters of the particles, Figure 5b. After coating, the mean volume particle diameters were 186±15 nm for furosemide, 136±21 nm for nifedipine, 151±10 nm for isoxyl, and 185±16 nm for paclitaxel. However, the long-term suspension stability of these particles was satisfactory since an insignificant increase in particle size was observed up to 120 days and the particles of all the drugs remained smaller than 200 nm (Figure 6c). In Figure 8, the release profiles of the LbL-coated, negatively charged drug particles in biorelevant dissolution mediums are shown. None of the coated drug particles released the drug as fast as from a drug solution; however drug release was significantly faster than from micronized commercially available drug powders. Since the surface area through which diffusion occurred was known for the dialysis cassettes, the intrinsic dissolution rates (IDR) were calculated using the release data shown in Figure 8. Calculated IDR values are listed in Table 1. Evaluation of these values shows that optimized coatings used for stable, negatively charged nanoparticles decreased the IDR approximately 1.1-1.3 times compared to the drug solutions. In contrast, drug release from these LbL-coated particles was 1.8 times faster for furosemide, 3.9 times faster for paclitaxel,

2.4 times faster for isoxyl and 3.3 times faster for nifedipine when compared to the IDR of micronized commercially available powders.

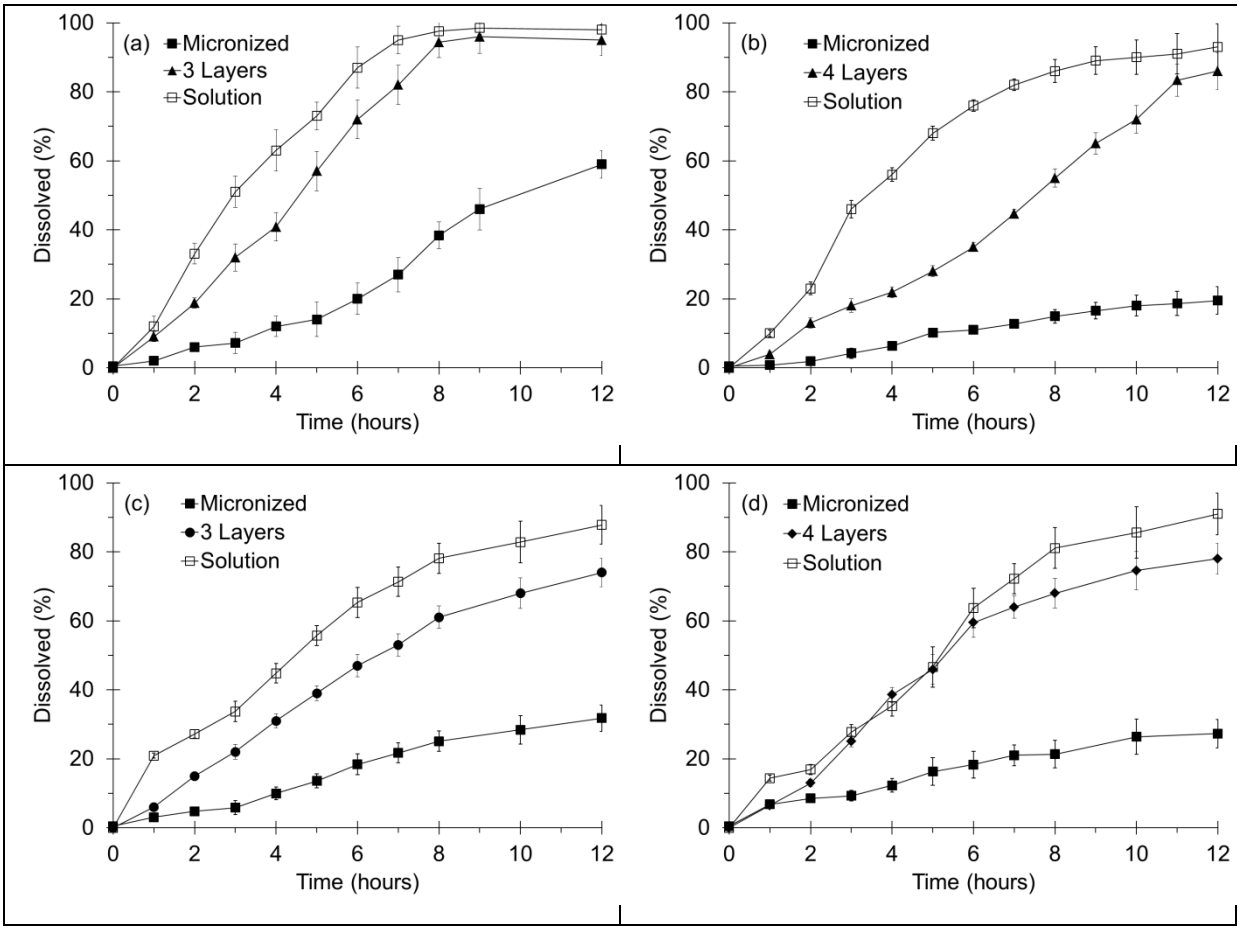

Figure 8. Drug release profiles for (a) furosemide, (b) paclitaxel, (c) isoxyl and (d) nifedipine after coating with the minimum number of polyelectrolyte layers that stabilized the nanoparticles against growth while maintaining a negative surface charge. For reference purposes the release profiles from drug solutions in methanol and aqueous suspensions of micronized drug particles are also shown.

The effect of the number of polyelectrolyte bilayers on drug release was also measured and the IDR calculated from these curves are listed in Table 1. The drug release rates, IDR, of all the drugs decreased almost linearly ($R^2 > 0.92$) with an increase in the number of bilayers up to a thickness < 50 nm. From the linear relationships it was estimated that a drug with 9-11 bilayer coatings would produce particles < 250 nm with a release rate similar to uncoated drug powder with average mean volume particle sizes > 12 μm. These results show the potential preparation of sustained release drug nanoparticles coated by the LbL method. For all the drugs, virtually no drug release was observed for the 15 bilayer-coated particles for up to 12 hours. The release rates from the coated particles were also 7 times slower for furosemide, 15 times slower for paclitaxel, 24 times slower for isoxyl and 10 times slower for

nifedipine compared to the micronized suspensions. The magnitude in the decrease of the release rate depended on the aqueous solubility of the drugs. The effect was less for more soluble drugs, furosemide and nifedipine, compared to the less soluble drugs, paclitaxel and isoxyl.

Table 1. IDR rates for drug solutions, micronized powder suspensions and LbL coated drug nanoparticles measured from dialysis cassettes. IDR rate shown in italics represent the minimum number of polyelectrolyte layers necessary to stabilize the particle against growth in suspension.

	IDR (mg/hr/cm^2)			
	Furosemide	Paclitaxel	Isoxyl	Nifedipine
Solution	0.0440	0.0270	0.0309	0.0283
Micronized	0.0177	0.0061	0.0098	0.0076
1 bilayer	0.0345	0.0259	0.0258	0.0264
1.5 bilayer	*0.0324*		*0.0240*	
2 bilayers		*0.0242*		*0.0248*
5 bilayers	0.0251	0.0149	0.0145	0.0158
10 bilayers	0.0171	0.0061	0.0076	0.0072
15 bilayers	0.0025	0.0004	0.0004	0.0007

4. Conclusion

The robust nature of LbL self-assembly was illustrated in this study by successfully depositing PE nanocoats on poorly water-soluble drugs with markedly different surface characteristics. Additionally, a common challenge associated with small particles, namely their physical stability against particle growth, could be surmounted efficiently by coating. The coated nanoparticles demonstrated long-term stability against particle growth over the test period of 120 days which suggests a sufficient period for storage of the particles prior to dosage form formulation and most probably stability of the dosage form, should the PE coats remain intact.

Another advantage of the LbL coating procedure was demonstrated in the release pattern of the chosen drugs. It is well-known from dissolution theory that a reduction in particle size will result in higher rates of dissolution. The size reduction of the particles compared to the commercially available raw materials, did indeed demonstrate this effect as seen from the

IDR values measured for various drug compositions. Although the coated nanoparticles showed a lower IDR than the uncoated particles, their IDR was still superior to the raw materials. The ultimate advantage illustrated for the nanocoated drug particles was however realized in the observation of nearly perfect zero-order controlled release patterns. Considering the ease of application of the coatings through LbL-self-assembly, the minute quantities of PE deposited and the advantageous effects of the coat on release and physical stability of drug nanoparticles, the LbL coating method can only be advocated to improve the performance of poorly water-soluble drugs.

Acknowledgements

We are grateful to the University of Wisconsin (USA) and the North-West University (South Africa) for research support. SJS was supported by a grant from AstraZeneca.

References

[1] M.M. de Villiers, J.G. van der Watt, The measurement of mixture homogeneity and dissolution to predict the degree of drug agglomerate breakdown achieved through powder mixing, Pharmaceutical Research, 11 (1994) 1557-1561.

[2] G. Wulff, On the question of the rate of growth and dissolution of crystal surfaces. Zeitschrift für Kristallographie und Mineralogie, 34 (1901) 449-530.

[3] V.F: Smolden, D.O. Kildsig, Vapor pressure of and solubility of small particles, American Journal of Pharmaceutical Education, 31 (1967) 512-514.

[4] D.J. Brayden, Controlled release technologies for drug delivery, Drug Discovery Today, 8 (2003) 976-978.

[5] A.A. Noyes, W.R. Whitney, The rate of solution of solid substances in their own solutions, Journal of the American Chemical Society, 19 (1897) 930-934.

[6] A.P. Tinke, K. Vanhoutte, R. de Maesschalck, S. Verheyen, H.A. de Winterm, A new approach in the prediction of the dissolution behavior of suspended particles by means of their particle size distribution, Journal of Pharmaceutical and Biomedical Analysis, 39 (2005), 900-907.

[7] M. Mosharraf, C. Nyström, Effect of particle size and shape on the surface specific dissolution rate of micronized practically insoluble drugs, International Journal of Pharmaceutics, 122 (1995) 35-47.

[8] D.P. Otto, M.M. de Villiers, Why is the nanosclae special (or not)? Fundamental properties and how it relates to the design of nano-enabled drug delivery systems, Nanotechnology Reviews, 2 (2013) 171-199.

[9] B. Devarakonda, A. Judefeind, S. Chigurupati, S. Thomas, G.V. Shah, D.P. Otto, M.M. de Villiers, The effect of polyamidoamine (PAMAM) dendrimers on the in vitro cytotoxicity of paclitaxel in cultured prostate cancer (PC-3M) cells, Journal of Biomedical Nanotechnology, 3 (2007) 384–393.

[10] B. Devarakonda, D.P. Otto, A. Judefeind, R.A. Hill, M.M. de Villiers, Effect of pH on the solubility and release of furosemide from polyamidoamine (PAMAM) dendrimer complexes, International Journal of Pharmaceutics, 345 (2007) 142-153.

[11] B. Devarakonda, R.A. Hill, M.M. de Villiers, The effect of PAMAM dendrimer generation size and surface functional group on the aqueous solubility of nifedipine, International Journal of Pharmaceutics, 284 (2004) 133-140.

[12] B. Devarakonda, N. Li, M.M. de Villiers, Effect of polyamidoamine (PAMAM) dendrimers on the in vitro release of water insoluble nifedipine from aqueous gels. AAPS PharmSciTech, 6(3): Article 63, E504-E512.

[13] H. Ibrahim, E. Sallam, M. Takkieddin, M. Abu Shamat, Dissolution characteristics of interactive powder mixtures. Part one: effect of solubility and particle size of excipients, Drug Development and Industrial Pharmacy, 14 (1988) 1249-1276.

[14] D.E. Alonzo, Y. Gao, D. Zhou, H. Mo., G.G.Z. Zhang, L.S. Taylor, Dissolution and precipitation behaviour of amorphous solid dispersions, Journal of Pharmaceutical Sciences, 100 (2011) 3316-3331.

[15] Y. Özkan, N. Doğanay, N. Dikmen, A. Işmer, Enhanced release of solid dispersions of etodolac in polyethylene glycol, Farmaco, 55 (2000) 433-438.

[16] M.M. de Villiers, D.P. Otto, S.J. Strydom, Y.M. Lvov, Introduction to nanocoatings produced by layer-by-layer (LbL) self-assembly, Advanced drug delivery reviews, 63 (2011) 701-715.

[17] N. Pargaonkar, Y.M. Lvov, N. Li, J.H. Steenekamp, M.M. de Villiers, Controlled release of dexamethasone from microcapsules produced by polyelectrolyte layer-by-layer nanoassembly, Pharmaceutical research, 22 (2005) 826-835.

[18] T. Wu, Y. Sun, N.Li, M.M. de Villiers, L.Yu, Inhibiting surface crystallization of amorphous indomethacin by nanocoating, Langmuir, 23 (2007) 5148-5153.

[19] H. Ai, S.A. Jones, M.M. de Villiers, Y.M. Lvov, Nano-encapsulation of furosemide microcrystals for controlled drug release, Journal of controlled release, 86 (2003) 59-68.

[20] N. Li, D.S. Kommireddy, Y. Lvov, W. Liebenberg, L.R. Tiedt, M.M. de Villiers, Nanoparticle multilayers: surface modification of photosensitive drug microparticles for increased stability and in vitro bioavailability, Journal of nanoscience and nanotechnology, 6 (2006) 3252-3260.

[21] A.S. Zahr, M.M. de Villiers, M.V. Pishko, Encapsulation of drug nanoparticles in self-assembled macromolecular nanoshells, Langmuir, 21 (2005) 403-410.

[22] C.P. Wan, C.S. Park, B.H.S. Kau, A rapid and simple microfluorometric phagocytosis assay, Journal of Immunological Methods, 162 (1993) 1-7.

[23] S. Sahlin, J. Hed, I. Rundquist, Differentiation between attached and ingested complexes by a fluorescence quenching cytofluorometric assay, Journal of Immunological Methods, 60 (1983) 115-124.

[24] S.J. Strydom, W.E. Rose, D.P. Otto, W. Liebenberg, M.M. de Villiers, Poly(amidoamine) dendrimer-mediated synthesis and stabilization of silver sulfonamide nanoparticles with increased antibacterial activity, Nanomedicine: Nanotechnology, Biology, Medicine, 9 (2013) 85-93.

[25] G. Sauerbrey, The use of quartz oscillators for weighing thin layers for microweighing, Zeitschrift für Physik, 155 (1959) 206-222.

[26] W.S. Rasband, ImageJ, U.S. National Institutes of Health, Bethesda, Maryland, USA, http://imagej.nih.gov/ij/

[27] United States Pharmacopeia, USP 36–NF 31, United States Pharmacopeial Convention, Rockville, MD, USA (2013).

[28] J. Li, S.A. Bourne, M.M. de Villiers, A.M. Crider, M.R. Caira, Polymorphism of the antitubercular isoxyl, Crystal Growth and Design, 11 2011 4950-4957.

CHAPTER 5

Concluding remarks

Layer-by-layer (LbL) is a self-assembly technique that has garnered popularity in the field of controlled drug delivery. As demonstrated throughout this study, LbL is a technique whereby oppositely charged polymers are sequentially added onto the surface of a drug or pharmaceutical excipient (either crystalline or amorphous) to form a multilayer. This multilayer is formed through a combination of interactions between the alternating polymer layers, including electrostatic attraction, hydrogen bonding, hydrophobic interactions and (in some cases) covalent bonding. The multilayer that is formed can be tailored to achieve specific physicochemical and/or drug-release properties, and this is dependent on the substrates that are selected to form the multilayers. Substrates which have been utilised in the literature include synthetic polymers (dendrimers), natural polymers (DNA, RNA, peptides and polysaccharides), macromolecules (micelles and liposomes) and nano-particles.

This study is comprised of three separate LbL studies. The first study sought to investigate the impact of LbL nanocoatings on the powder flow and compactibility of cellulose microfibers. LbL multilayers were produced using various combinations of either poly(styrenesulfonate) (PSS), polyvinylpyrrolidone (PVP), poly(dimethyldiallyl ammonium chloride) (PDDA), chitosan or gelatin. The powder flow properties and tableting indices of compacts compressed from these nanocoated cellulose microfibers were similar or better than that of directly compactible microcrystalline cellulose (MCC) powders. Cellulose microfibers coated with four PSS/PVP bilayers had the best compaction properties while still producing tablets that were able to absorb water and disintegrate. This technique thus turned non-flowing, non-compacting cellulose into powders with positive tabletting properties which can be used in direct compression during the tabletting process.

In the second study, silver sulfadiazine (AgSD) nanoparticles were synthesized using poly(amidoamine) (PAMAM) dendrimer complexes, in order to improve the aqueous solubility and topical antibiotic effect of AgSD (commonly used in the treatment of burn wounds). The AgSD nanoparticles were shown to be highly soluble, and LbL coatings of various PAMAM dendrimers were used to stabilize these nanoparticles against crystal

growth. Additionally, silver nanoparticles were incorporated in the dendrimer shells which augmented the AgSD release. Formulation of the nanoparticles in a cream base provided a topical drug delivery platform with enhanced antibacterial properties against burn wound infections.

The third study involved the step-wise LbL self-assembly of nanocoats (< 25 nm thick) of chitosan and chondroitin sulfate onto drug nanoparticles. Furosemide, isoxyl, rifampin and paclitaxel were chosen to prepare these nanoparticles due to their poor aqueous solubility properties. Although the nanocoatings reduced the dissolution of the coated nanoparticles, it still dissolved faster than the commercially available micronized powders of the drugs. This reduction in dissolution was also shown to be proportional to the thickness of the nanocoating. In addition, LbL nanocoating was shown to stabilize the small particles against crystal growth and aggregation in suspension, and sustained release nanoparticles were produced by increasing the layer thickness. This study proved that LbL coating can improve the performance of poorly water soluble drugs.

Overall, this study has shown that LbL nanocoatings produced by self-assembly of poly-electrolytes is a relatively simple and inexpensive experimental technique that can be applied to a variety of drugs and excipients. The resultant nanocoating that is formed has a variety of applications in the field of drug-delivery research, including manipulation of the physicochemical properties of the coated particles and modification of the release profile of the drug from the coated particles.

ANNEXURE

List of other publications authored or co-authored.

STRYDOM, S.J., LIEBENBERG, W., YU, L & DE VILLIERS, M.M. 2009. The effect of temperature and moisture on the amorphous-to-crystalline transformation of stavudine. International journal of Pharmaceutics, 379(1):72-81.

DE VILLIERS, M.M., CAIRA, M.R., LI, J., ***STRYDOM, S.J.***, BOURNE, S. & LIEBENBERG, W. 2011. Crystallization of toxic glycol solvates of rifampin from glycerin and propylene glycol contaminated with ethylene glycol or diethylene glycol. Molecular Pharmaceutics, 8:877-888.

AUCAMP, M., LIEBENBERG, W., ***STRYDOM, S.J.***, VAN TONDER, E.C. & DE VILLIERS, M.M. 2012. Physicochemical properties of amorphous roxithromycin prepared by quench cooling of the melt or desolvation of a chloroform solvate. AAPS PharmSci Tech, 13(2):467-476.